

การกำหนดขนาด ตำแหน่ง และการทำงานของระบบกักเก็บพลังงานแบตเตอรี่ที่เหมาะสม
เพื่อลดปัญหาแรงดันไฟฟ้าในการไฟฟ้าฝ่ายจำหน่ายที่มีโซลาร์รูฟท็อปปริมาณมาก



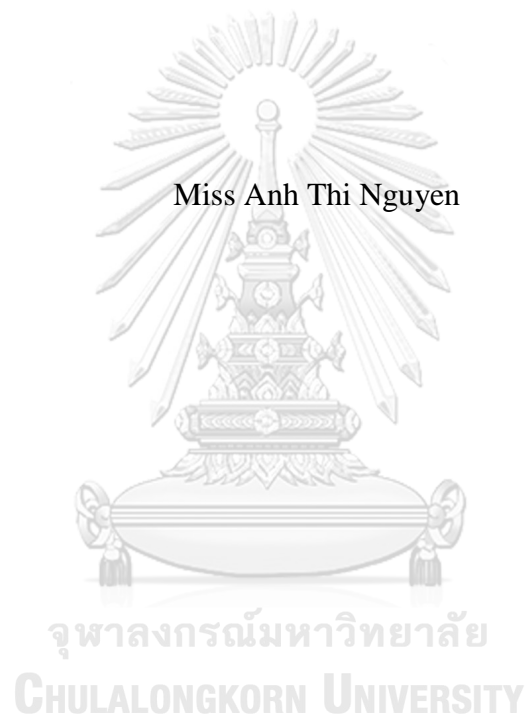
นางสาวอ้น ทิ เห่งย่น

บทคัดย่อและแฟ้มข้อมูลฉบับเต็มของวิทยานิพนธ์ตั้งแต่ปีการศึกษา 2554 ที่ให้บริการในคลังปัญญาจุฬาฯ (CUIR)
เป็นแฟ้มข้อมูลของนิสิตเจ้าของวิทยานิพนธ์ ที่ส่งผ่านทางบัณฑิตวิทยาลัย

The abstract and full text of theses from the academic year 2011 in Chulalongkorn University Intellectual Repository (CUIR)
are the thesis authors' files submitted through the University Graduate School.

วิทยานิพนธ์นี้เป็นส่วนหนึ่งของการศึกษาตามหลักสูตรปริญญาวิศวกรรมศาสตรดุษฎีบัณฑิต
สาขาวิชาวิศวกรรมไฟฟ้า ภาควิชาวิศวกรรมไฟฟ้า
คณะวิศวกรรมศาสตร์ จุฬาลงกรณ์มหาวิทยาลัย
ปีการศึกษา 2560
ลิขสิทธิ์ของจุฬาลงกรณ์มหาวิทยาลัย

OPTIMAL SIZING, SITING, AND SCHEDULING OF BESS FOR MITIGATING
VOLTAGE PROBLEM IN DISTRIBUTION UTILITIES WITH HIGH
PENETRATION OF PV ROOFTOPS



A Dissertation Submitted in Partial Fulfillment of the Requirements
for the Degree of Doctor of Philosophy Program in Electrical Engineering
Department of Electrical Engineering
Faculty of Engineering
Chulalongkorn University
Academic Year 2017
Copyright of Chulalongkorn University

Thesis Title OPTIMAL SIZING, SITING, AND
 SCHEDULING OF BESS FOR
 MITIGATINGVOLTAGE PROBLEM IN
 DISTRIBUTION UTILITIES WITH
 HIGHPENETRATION OF PV ROOFTOPS

By Miss Anh Thi Nguyen

Field of Study Electrical Engineering

Thesis Advisor Assistant Professor Surachai Chaitusaney, Ph.D.

Accepted by the Faculty of Engineering, Chulalongkorn University in
Partial Fulfillment of the Requirements for the Doctoral Degree

..... Dean of the Faculty of Engineering
(Associate Professor Supot Teachavorasinskun, Ph.D.)

THESIS COMMITTEE

..... Chairman
(Associate Professor Thavatchai Tayjanant, Ph.D.)

..... Thesis Advisor
(Assistant Professor Surachai Chaitusaney, Ph.D.)

..... Examiner
(Associate Professor Kulyos Audomvongseree, Ph.D.)

..... Examiner
(Pisitpol Chirapongsananurak, Ph.D.)

..... External Examiner
(Pradit Fuangfoo, Ph.D.)

CHULALONGKORN UNIVERSITY

5871430021 : MAJOR ELECTRICAL ENGINEERING

KEYWORDS: AGING DEGRADATION OF BATTERY / LV NETWORK / PV ROOFTOPS / SCHEDULING OF BESS / SITING OF BESS / SIZING OF BESS / VOLTAGE MANAGEMENT

ANH THI NGUYEN: OPTIMAL SIZING, SITING, AND SCHEDULING OF BESS FOR MITIGATING VOLTAGE PROBLEM IN DISTRIBUTION UTILITIES WITH HIGH PENETRATION OF PV ROOFTOPS. ADVISOR: ASST. PROF. SURACHAI CHAITUSANEY, Ph.D., 93 pp.

For ambition of reducing CO₂ emission and reliance on fossil fuels, solar power generation has been received special supports and deployed rapidly in many distribution networks. However, with a high presence of solar power generation, power grid control is no longer simple as conventional one due to natural variation of solar power and large space dispersion of solar power systems. The negative impacts comprise power system stability, electric power quality involving frequency and voltage criteria and other potential issues. Among these impacts, voltage problem is most obvious. Many solutions have been proposed to solve the voltage problem whereas battery energy storage system (BESS) exhibits technically dominant capability in comparison with other ones. However, the price of the battery is, currently, still high, strategies to minimize the operation cost are necessary.

This dissertation investigates the BESS, the selected solution for mitigating voltage problem in LV network caused by high penetration of PV rooftops. Two optimal strategies of BESS are proposed to help utilities minimize their operation cost. These strategies cover sitting and sizing of BESSs which is used for long-term planning and scheduling of the installed BESSs for operation planning. Cost evaluations consider aging degradation of the BESS and some additional cost such as O&M cost and so forth. The effectiveness of the proposed methods is demonstrated on a simplified network of Metropolitan Electricity Authority (MEA), Thailand, using Matlab 2016a and Matpower 6.0.

Department: Electrical Engineering Student's Signature

Field of Study: Electrical Engineering Advisor's Signature

Academic Year: 2017

ACKNOWLEDGEMENTS

From bottom of my heart, I would like to express my deep thankfulness to my advisor Assist. Prof. Dr. Surachai Chaitusaney and co-advisor Prof. Akihiko Yokoyama for their experienced guidance and inspiring advice which help me overcome academic challenges throughout my Ph.D. study. I would say that without those supports I could not have this achievement.

I would like to give my special thanks to ASEAN University Network/ Southeast Asia Engineering Education Development Network (AUN/SEED-Net) Program of Japan International Cooperation Agency (JICA) for the full scholarship and Collaborative Research Fund during my research in Chulalongkorn University, Thailand and The University of Tokyo, Japan.

I would like to extend my thankfulness to the staffs of Department of Electrical Engineering, Chulalongkorn University as well as my friends in Power System Research Laboratory and Yokoyama Laboratory who have directly shared study life and supported me during this time. They are a part of my unforgettable memory.

Lastly, I am wholly indebted my family, especially my parents, my husband and my sons who have been always beside me, giving unconditioned supports and loves. They are my love and motivation of my life.

CONTENTS

	Page
THAI ABSTRACT	iv
ENGLISH ABSTRACT.....	v
ACKNOWLEDGEMENTS.....	vi
CONTENTS.....	vii
LIST OF TABLES	x
LIST OF FIGURES	xi
LIST OF ABBREVIATIONS.....	xiii
CHAPTER 1 INTRODUCTION.....	1
1.1 Problem Statement.....	1
1.2 Objective.....	4
1.3 Scope of Research Work and Limitations	4
1.4 Steps of Study.....	4
1.5 Expected Benefits from Dissertation.....	5
1.6 Structure of Dissertation.....	5
CHAPTER 2 VOLTAGE PROBLEMS AND SOLUTIONS FOR LV NETWORK WITH HIGH PENETRATION OF PV ROOFTOPS.....	7
2.1 Effect of high penetration of PV rooftops in LV network.....	7
2.1.1 Voltage violation by PV generation.....	7
2.1.2 Voltage criteria applied in LV network.....	9
2.2 Solutions for voltage problem in LV network.....	11
2.2.1 Reference voltage regulated at MV/LV transformer.....	12
2.2.2 Network reinforcement.....	13
2.2.3 PV inverter	15
2.3.4 Battery energy storage system.....	16
2.3.5 Other solution and conclusion.....	17
CHAPTER 3 BESS, SOLUTION FOR VOLTAGE MANAGEMENT IN FUTURE LV NETWORK.....	18
3.1 BESS integration to power network	18

	Page
3.1.1 Functional principle of grid-interconnected BESS	18
3.1.2 Requirement of BESS for voltage management.....	21
3.2 Battery modeling for economic assessment of BESS project	30
3.2.1 Basic battery concepts	31
3.2.2 Battery modeling and lifetime estimation methods.....	39
CHAPTER 4 COST MINIMIZATION METHODS OF BESS FOR VOLTAGE MANAGEMENT IN LV NETWORK	45
4.1 Cost minimization of BESS.....	46
4.1.1 Objective function	46
4.1.2 Constraints.....	48
4.2 Siting and sizing strategy of BESSs	50
4.2.1 Objective function	51
4.2.2 Constraints.....	51
4.3 Scheduling of the installed BESSs	53
4.3.1 Objective function	53
4.3.2 Constraints.....	54
CHAPTER 5 SIMULATION NETWORK	56
5.1 Network configuration.....	56
5.2 Load and PV generation profiles	59
5.3 Technical and economic parameters for BESS simulation.....	61
CHAPTER 6 APPLICATION OF THE PROPOSED METHODS	64
6.1 Cost minimization of BESS – An economically analytic tool of BESS.....	64
6.1.1 Case study for basic cost minimization of BESS	64
6.1.2 Effect of the installation sites on the cost and size of the BESS	67
6.2 Strategy of siting and sizing of BESSs	68
6.2.1 Case-study for siting and sizing strategies of BESS	68
6.2.2 Effect of PV rooftop dispersion on siting and sizing of BESSs.....	71
6.3 Operation planning and cost evaluation of BESSs	72
6.3.1 Operation planning of the BESSs.....	73

	Page
6.3.2 Cost evaluation of the BESSs.....	76
CHAPTER 7 CONCLUSION	78
7.1 Dissertation summary and conclusion	78
7.2 Recommendation for research development	80
REFERENCES	81
APPENDIX A Newton Raphson method for load flow calculation.....	87
APPENDIX B Matlab simulation result.....	91
VITA.....	93



LIST OF TABLES

	Page
Table 2.1 International standards for PV integration in LV network	9
Table 2.2 Grid code applied in EU countries for PV integration in LV network	10
Table 2.3 PEA (Provincial Electricity Authority) grid code.....	10
Table 2.4 MEA (Metropolitan Electricity Authority) grid code.....	11
Table 3.1 Technical review of LA, NiCd and NiMH battery [30]	23
Table 3.2 Application of Li-ion battery in power systems [31].....	24
Table 3.3 Technical review of Li-ion, NaS and NaNiCl battery [30].....	26
Table 4.1 Operating conditions of BESSs	52
Table 4.2 Operating conditions of the installed BESSs represented for BESS at node k.....	54
Table 5.1 Network parameters in per unit with $S_{base} = 100MVA$, $U_b = 380V$	57
Table 5.2 Loads and PV generations of Case A	58
Table 5.3 Loads and PV generations of Case B.....	58
Table 5.4 Typical load profiles for one-month cost evaluation application of BESS .	60
Table 5.5 Initial assumptions for simulations of BESSs using LA technology.....	62
Table 5.6 Technical and economic characteristics of battery technologies.....	63
Table 6.1 Simulation result for Case B with BESS installed at node 23.....	66
Table 6.2 Simulation results for Case A and Case B.....	70
Table 6.3 Optimal strategies of BESSs.....	72
Table 6.4 Parameters of the BESSs installed in Case B.	73
Table B.1 Cost evaluation of the BESSs with different battery technologies	91

LIST OF FIGURES

	Page
Figure 1.1 PV installation in the world [1]	1
Figure 2.1 Network with voltage problem due to the high penetration of PV rooftops	8
Figure 2.2 Equivalent circuit of simply network	8
Figure 2.3 Solutions for the voltage problem	11
Figure 2.4 Typical design of distribution system in Germany [27]	12
Figure 2.5 Effect of sending voltage on network voltages	13
Figure 2.6 Effectiveness of network reinforcement on voltage profile [27].....	14
Figure 2.7 Effectiveness of voltage regulation solutions.....	14
Figure 2.8 Voltage support curves of PV inverter	16
Figure 3.1 Functional principle of grid-interconnected BESS.....	19
Figure 3.2 Operation principle of storage battery SCADA [30].....	20
Figure 3.3 Considered aspects of battery selection.....	27
Figure 3.4 Framework of the IEC 61850 [33]	29
Figure 3.5 Examples of setting modes of converters for voltage support [33].....	30
Figure 3.6 Charging process of typical lead acid battery.....	33
Figure 3.7 Degradation of battery capacity [37]	35
Figure 3.8 Effects of discharge rates and ambient temperatures on discharged capacity [38].....	36
Figure 3.9 Charge/discharge profiles [37]	37
Figure 3.10 Effect of the temperature on battery lifetime [39].....	38
Figure 3.11 Relationship between number of cycles and DOD [15].....	38
Figure 3.12 Effect of charge/discharge rates on the lifetime of a battery [39]	39
Figure 3.13 Battery modeling classification	40
Figure 3.14 Ah curve calculated from data sheet [41].....	41
Figure 3.15 Capacity loss due to aging degradation [43]	43
Figure 4.1 Contents of the proposed methods	45

Figure 4.2 Convention of power flows in the network	46
Figure 5.1 Configurations of the simulated network	56
Figure 5.2 Load and PV generation profiles of the worst case.....	59
Figure 5.3 Load and PV generation profiles for one-month cost evaluation of BESS.....	61
Figure 6.1 Case B with BESS installed at node 23.....	64
Figure 6.2 Voltages of the network with and without BESS support.....	65
Figure 6.3 Capacity degradation of the BESS	67
Figure 6.4 Required cost and size of BESS depending on installation sites.....	68
Figure 6.5 Case A and Case B with considered locations for BESSs installation.....	69
Figure 6.6 Scenarios of PV rooftop dispersions of Case A	71
Figure 6.7 Network for operation planning simulation of the BESSs	73
Figure 6.8 Voltage profiles of the network for the forecasted day	74
Figure 6.9 Charge/discharge schedules of the BESSs for the forecasted day	74
Figure 6.10 Usable capacity of the BESSs for the forecasted day.....	75
Figure 6.11 Capacity degradation of the BESSs for the forecasted day	75
Figure 6.12 Case study for one-month cost evaluation of the BESSs	76
Figure 6.13 Cost of the BESSs according to battery technologies	77

LIST OF ABBREVIATIONS

Abbreviations

ac	Alternating current
ANSI	American National Standards Institute
BESS	Battery Energy Storage System
BMS	Battery Management System
DC	Demand Controller
dc	Direct current
DER	Distributed Energy Resource
DOD	Depth Of Discharge
EOL	end-of-life
EVs	Electric Vehicles
IEC	International Electrotechnical Commission
IEEE	Institute of Electrical and Electronics Engineers
LA	Lead Acid
LDCs	Line Drop Compensators
Li-ion	Lithium ion
LV	Low Voltage
MEA	Metropolitan Electricity Authority
NaNiCl	Sodium Nickel Chloride
NaS	Sodium Sulphur
NiCd	Nickel Cadmium
NiMH	Nickel Metal Hydride
OLTC	On-Load Tap Changer
PEA	Provincial Electricity Authority
PHEVs	Plug-in Hybrid Electric Vehicles
PLC	Programmable Logic Control
PV	Photovoltaic
SCADA	Supervisory Control And Data Acquisition
SOC	State Of Charge

SOH	State of Health
TEPCO	Tokyo Electric Power Company
UPS	Uninterrupted Power Supply
VRLA	Valve-regulated Lead-Acid
ZEBRA	Zero Emission Battery Research

Constant Parameters

C_0	Cost per unit investment capacity of the BESS (\$/kWh)
D	Operation duration (day)
N	Number of considered locations for BESS installation in the network
OM	Annual O&M rate of the BESS
r	Annual interest rate
SOC_{min} , SOC_{max}	Minimum and maximum states of charge those the BESS is allowed to operate
T	Number of time intervals in considered duration D
T_c	Minimum charge time
T_d	Minimum discharge time
V_{min} , V_{max}	Minimum and maximum acceptable voltages (pu)
Z	Linear aging coefficient
β	Additional cost per unit investment capacity of the BESS and duration (\$/kWh.day)
Δt	Time interval (h)
η	Efficiency of BESS for charge and discharge processes
λ	Cost per unit capacity loss of the BESS (\$/kWh)

Indices

(t)	Time index indicating t^{th} time interval
Σ	Notation indicates total value
k	Index indicates node k of the network

max	Notation indicates maximum value
min	Notation indicates minimum value

Sets

N^k	Set of considered locations for BESS installation
Ω^k	Set of the installed BESSs

Variables

a^k	Optimal contribution-percentage of BESS at node k
$C_{B,nom}$	Nominal capacity of the BESS (kWh)
$C_{B,nom}^k$	Nominal capacity of the BESS at node k
$C_{B,nom}^{\Sigma}$	Total nominal capacity of the BESSs (kWh)
C_{int}^k	Initial capacity of the BESS at node k (kWh)
$C_{(t)}$	Capacity of BESS in t^{th} time interval (kWh)
$C_{(t)}^k$	Capacity of the BESS at node k in t^{th} time interval (kWh)
$C_{(t)}^{\Sigma}$	Capacity of total BESSs in t^{th} time interval (kWh)
$E_{(t)}$	Available energy in the BESS in t^{th} time interval (kWh)
$E_{(t)}^k$	Available energy of the BESS at node k in t^{th} time interval (kWh)
$E_{(t)}^{\Sigma}$	Available energy of total BESSs in t^{th} time interval (kWh)
$P_{c(t)}$	Charge power of the BESS in t^{th} time interval (kW)
$P_{c(t)}^k$	Charge power of the BESS at node k in t^{th} time interval (kW)
$P_{c(t)}^{\Sigma}$	Total charge power of the BESSs in t^{th} time interval (kW)
$P_{d(t)}$	Discharge power of the BESS in t^{th} time interval (kW)
$P_{d(t)}^k$	Discharge power of the BESS at node k in t^{th} time interval (kW)
$P_{d(t)}^{\Sigma}$	Total discharge power of the BESSs in t^{th} time interval (kW)
$SOC_{(t)}$	State of charge of the BESS in t^{th} time interval
$SOC_{(t)}^k$	State of charge of the BESS at node k in t^{th} time interval
$SOC_{(t)}^{\Sigma}$	State of charge of total BESSs in t^{th} time interval
$V_{(t)}^k$	Voltage at node k and in t^{th} time interval (pu)

$\Delta C_{(t)}$	Capacity loss in t^{th} time interval (kWh)
$\Delta C_{(t)}^{\Sigma}$	Capacity loss of total BESSs in t^{th} time interval (kWh)
$\Delta C_{(t)}^k$	Capacity loss of the BESS at node k in t^{th} time interval (kWh)



CHAPTER 1

INTRODUCTION

The introduction begins with the problem statement which specifies the problem to be solved in this dissertation. After that, objective, scope of research work and limitation, steps of study, and expected benefits are described. Finally, the structure of dissertation is presented.

1.1 Problem Statement

Lying on the acts toward sustainable energy development through using clean energy resources in conjunction with reducing reliance on fossil fuels and carbon dioxide emission, solar power generation has been receiving necessary supports to deploy widely around the world. The development of solar generation can be seen with the number of PV installation in the world depicted in Figure 1.1. The leader countries in this area are Germany, China, Japan, United States and Italy [1]. Thanks to such incentive supports of the governments in many countries through a feed-in tariff for solar generation, low-carbon power generation technology based on solar energy has had an amazing jump in cost reduction over the past decade. Price of Photovoltaic (PV) generation has been reduced significantly from 16\$/Wp in the 1990s in Europe to 1.55\$/Wp recorded in Germany in 2013 [2].

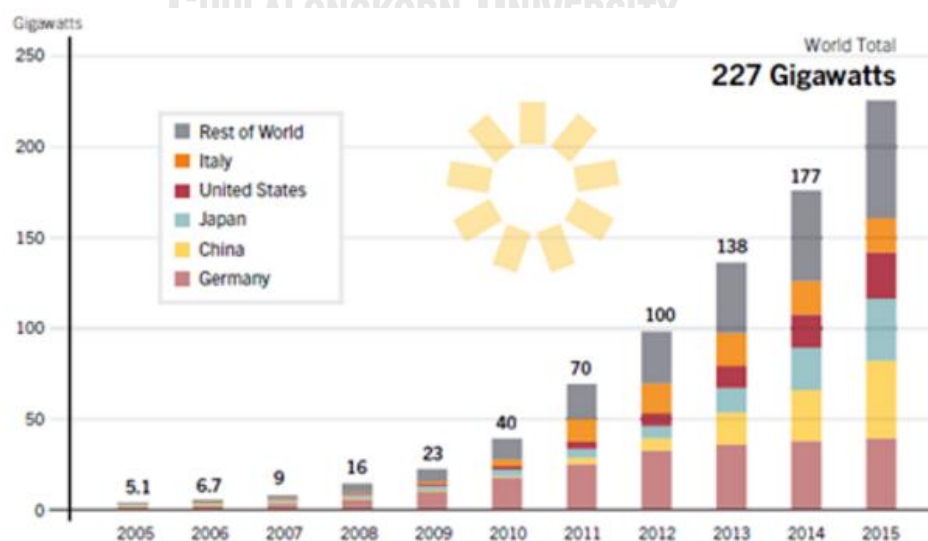


Figure 1.1 PV installation in the world [1]

Together with that development, topic related to solar power generation has been becoming a research interest of many researchers. The potential impacts of solar power integration on the grid were also specified [2-4]. Specifically, as the penetration of solar generation is still low, solar power generators may help network operate more reliably and economically due to frequency and voltage support, loss reduction and delayed power network upgrade. However, on the other hand, when solar penetration is high, the challenges bring back to the network with potential issues such as voltage rise and voltage fluctuation, reverse power flow, overloading for conductors, and other issues [2-4].

Regarding voltage problem, many solutions have been proposed in the literature which can be implemented either by utilities or customers. The methods at customers site are mainly based on a local control such as $\cos\phi(P)$, $Q(U)$ and $P(U)$ function of PV inverters [5, 6], demand response, time-shift support by energy storage system. All of them need additional investment from customers. This may interfere PV deployment in the low voltage network. In addition, overvoltage rates are significantly different according to locations [6], leading to different stresses on different customers. Hence, an effective and fair policy is necessary for applying these methods in practice. On the other side, the methods provided by utilities seem simpler. The most important consideration is effectiveness coupled with the cost of the solution. The proposed solutions were investigated in the literature including network reinforcement, active control with OLTC (On-Load Tap Changer) enhancement at MV/LV transformer, operating coordination of some voltage regulator devices such as PV inverters, OLTC and LDCs (Line Drop Compensators) [7-9]. Another promising solution that uses battery energy storage system (BESS) was also investigated in references [10-14]. In comparison, while network reinforcement seems to be an ineffective-cost solution due to the short and rare occurrence of overvoltage, OLTC alone may not adapt to the complexity of LV network. Coordination of customers' devices faces the same obstacle of policy. On the contrary, BESS can bring the necessary flexibility to power system in general and LV network in particular in order to effectively deal with high penetration to solar power generation in near future.

From that point of view, this research investigates both technical and economic aspects of the battery energy storage system owned by utilities for voltage management

in LV network. The motivations for this research come from the dominant capability of BESS that can actively manage power flow within the network, overcome various problems regarding unbalance between generation and load, including overvoltage caused by high penetration of PV rooftops. It is assessed as a solution for the future smart grid. Another reason is increasing use of BESS for renewable integration, resulting in the expectation of cost reduction in near future [15]. In addition, the effectiveness of overvoltage prevention by BESS for LV network has been proved in many research works [10-14]. Voltage control can be operated through decentralized control, centralized control or combination two methods [13, 14]. While decentralized scheme does not need exchanged information among distributed energy storage systems, the system may operate more reliably and require less investment in comparison with the centralized scheme. On the contrary, thank to communication network, optimum operation can be achieved by centralized control. Advantages and disadvantage of each method were demonstrated in reference [14]. Besides, BESS coordinated with other devices such as PV inverters in case they are not sufficient for voltage regulation were also investigated in the literature. It is obvious that technical effectiveness of BESS solution for overvoltage problem has been confirmed. However, no economic measurement of BESS as a single solution that utilities are owners has been done. Whereas, it has been more commonly formulated in various objective functions of the customer (e.g. minimizing electricity bill [16], daily expenditure [17] or maximizing self-consumption [18]). The reasons for that might come from its high cost and complexity of aging modeling of BESS. Currently, precise estimation of BESS lifetime that influences economic criteria is still a challenge. Consequently, cost of BESS may be calculated simply based on fixed number of charge/discharge cycles with regard or regardless of DOD (Depth Of Discharge) [14, 17]. In fact, DOD of BESS frequently varies across working cycles. Therefore, this dissertation utilizes the aging model inherited from references [16, 19, 20]. The model does not only overcome the weak point of the previous models but also represent dynamic conversion of battery parameters.

Fully aware of a gap in the literature, this dissertation primarily formulates minimum cost of a BESS owned by utilities to deal with voltage problem based on aging degradation cost with the model inherited from references [16, 19, 20] and some

additional costs. After that, the formulation is developed for long-term planning and operation planning. For long-term planning, the optimum sites and sizes of BESSs are specified while for operation planning, the optimum schedule of each BESS is suggested based on one-day load and PV generation forecasts.

1.2 Objective

The main objective of the dissertation is to minimize the cost of BESS which is implemented in the LV network with high penetration of PV rooftops in order to maintain network voltages within acceptable limits.

1.3 Scope of Research Work and Limitations

Cost minimization of BESSs is formulated based on aging degradation model in references [16, 19, 20] and some additional costs which are specified in the proposed formulations. The strategies are developed for practical applications that include sizing, siting and scheduling of BESS in order to obtain their minimum cost. In the meanwhile, network voltages are managed within the desired range. Scope and limitation of the proposed formulation and strategies are specified as follows:

1. The proposed methods are primarily applied to low voltage network and simulated for balanced systems.
2. Cost of BESS is investigated for purpose of voltage regulation only. Accompanying benefits such as load shaving, arbitrage of BESS and so forth are not taken into account in this dissertation.
3. Aging degradation model in this research is a linear model of capacity loss during operation of BESS. Although, this model can describe aging degradation of BESS dynamically for a quite precise estimating cost of BESS but not precise enough for real-time control application.

1.4 Steps of Study

1. Reviewing on PV development and potential issues
2. Studying grid codes for PV integration into the distribution network

3. Reviewing solutions for overvoltage prevention applied in LV network with PV integration

4. Studying battery characteristics and its models

5. Studying optimal operation of battery and methods for cost calculation

6. Reviewing standards for BESS integration in power grid

7. Formulating minimum cost of BESS for voltage management

8. Developing the optimization problem for a strategy of sizing and siting of BESS.

9. Developing the optimization problem for a strategy of scheduling of the installed BESSs within the network

10. Simulating the proposed methods on the test systems

1.5 Expected Benefits from Dissertation

The main contributions of the dissertation are three proposed formulations described in Chapter 4 which can be used in the following practical applications:

1. Utilities can utilize the second formulation to select locations and sizes of BESS in their network to minimize the cost for purpose of voltage regulation.

2. With pre-specified size and site of BESSs, schedules of charge and discharge are produced as a guide for operation planning by the third formulation based on one-day load and PV generation forecasts. Cost of BESSs is also estimated.

3. Besides, all three proposed formulations are capable to be used as a quantitative tools to analyze the effect of influential factors on the cost of BESS. The influential factors are such as:

- BESS locations
- Dispersion of PV rooftops or loads
- Climate ...

1.6 Structure of Dissertation

The rest of the dissertation is presented as follows. In the next chapter, voltage problem caused by high penetration of PV rooftops in LV network is described and solutions for that problem are discussed. Chapter 3 takes consideration on BESS, an

effective and flexible solution for the power system in general and voltage problem in LV network in particular. Integration of BESS to the power network and BESS modeling for economic assessment are the main content of this chapter. In Chapter 4, the proposed methods for cost minimization of BESS which is used for voltage management in LV network are presented. Two main strategies are sitting and sizing of BESSs and then scheduling of BESSs. Network and input data for the simulations are described in Chapter 5. Chapter 6 presents simulations and applications of the proposed methods, simultaneously discusses simulated results. Chapter 7 is the conclusion with a summary of the dissertation and its future development.



CHAPTER 2

VOLTAGE PROBLEMS AND SOLUTIONS FOR LV NETWORK WITH HIGH PENETRATION OF PV ROOFTOPS

There is no consistent definition of “penetration” of solar power generation and how high is. From the review of the authors in reference [21], penetration of solar power generation was defined variously among researchers. Some of them simply defined as the ratio of houses with PV installation and total houses while others defined by peak PV generation over peak load demand. Many other definitions were also pointed out. The authors also revealed and specified that PV penetration limit is not a fixed number for every network. It depends on the characteristic of a network, dispersion of loads and PV generations and load and PV generation profiles. Therefore, PV penetration limit can be a very small number or quite a big number. However, the concept of high PV penetration can be understood as follows: In the network, PV generation power exceeds load demand causing reversed power flow at MV/LV transformer. That network is considered as high PV penetration. This chapter discusses the effect of high penetration of PV rooftops in LV network with a deep description of voltage problem. Simultaneously, solutions proposed in the literature for this problem are also discussed.

2.1 Effect of high penetration of PV rooftops in LV network

Many research works have addressed potential impacts of high PV penetration on the grid [2-4]. They are voltage rise and voltage fluctuation, reverse power flow, unintended islanding, network congestion and other potential issues. Whereas, voltage violation is one of the constraints that limit the penetration of PV mostly. As a result, this section analyzes voltage violation in low voltage networks caused by high penetration of PV rooftops and simultaneously reviews some voltage criteria applied in the world.

2.1.1 Voltage violation by PV generation

Since the significant presence of PV rooftops, power flows in the low voltage network are no longer in one way. They change dynamically in both directions to

balance between load demand and power supply. Power flows coupled with voltage problem are illustrated in Figure 2.1.

Reversed power flows occur during high PV generation when generated powers exceed demands at nodes with high penetration of PV rooftops, causing voltage rise at those nodes. To understand voltage problem more clearly, an equivalent circuit of a simple network of two nodes are analyzed in Figure 2.2 with the influenced factors specified in the approximated formulas (2.1) and (2.2) [5, 14].

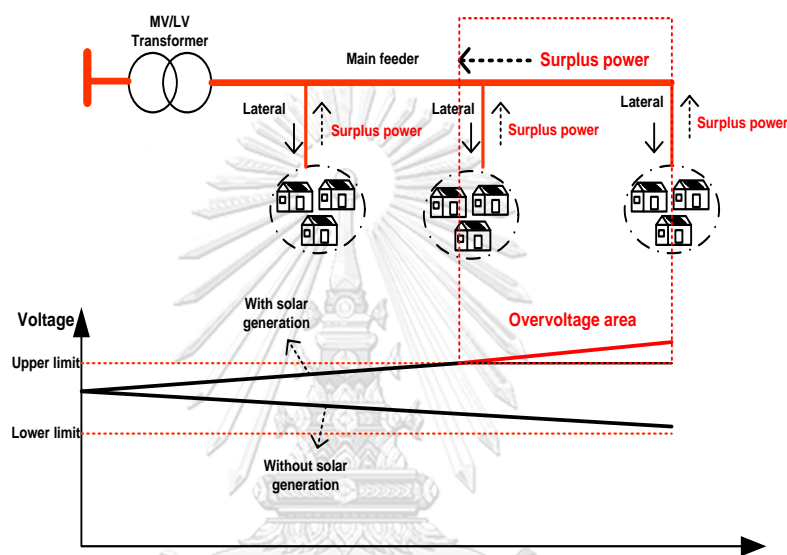


Figure 2.1 Network with voltage problem due to the high penetration of PV rooftops

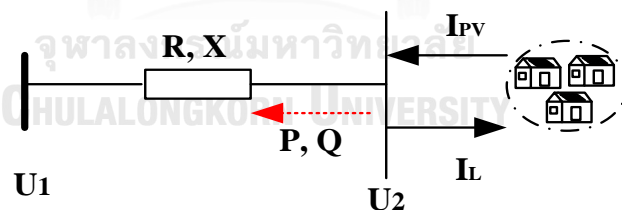


Figure 2.2 Equivalent circuit of simply network

Different voltage between two nodes

$$\Delta U = \frac{P.R + Q.X}{U_n} \quad (2.1)$$

The voltage at node 2

$$U_2 \approx U_1 + \frac{P.R + Q.X}{U_n} \quad (2.2)$$

Where

P, Q are active and reactive power flows (W), (VAr)

R, X are resistance and reactance of conductor (Ω)

U_1, U_2 are voltages at node 1 and node 2 (V)

U_n is the nominal voltage of the network (V)

It is obvious that voltage rise or voltage dip in a comparison between two nodes is defined by the sign of ΔU or direction of power flows. If the voltage at node 1 is considered as a reference, the level of voltage rise or voltage dip at node 2 is determined by the combination of the reference voltage, generated power, load demands as well as network parameters. Voltage regulation methods applied in power system are, therefore, based on controlling those influential factors. For the low voltage network with penetration of PV rooftops, power flows will change along a day in both direction and quantity, leading to a larger range of voltage change. As a result, utilities need to make more efforts to maintain node voltages of the network within acceptable limits.

2.1.2 Voltage criteria applied in LV network

Voltage is a criterion reflecting the electric quality of network due to its effect on electric devices' lifetime and performance. It, therefore, should be kept within acceptable range. Table 2.1 summarizes operational voltage range in some main international standards for PV integration in LV networks [22-24].

Table 2.1 International standards for PV integration in LV network

Standard	Operational voltage (%)	Voltage range (%)	Disconnection (sec)
IEEE 1574	$88 \leq V \leq 110$	$V < 50$	0.16
		$50 \leq V < 88$	2
		$110 < V < 120$	1
		$V \geq 120$	0.16
IEC 61727	$85 \leq V \leq 110$	$V < 50$	0.1
		$50 \leq V < 85$	2
		$110 < V < 135$	2
		$V \geq 135$	0.05
VDE - AR-N 4105	$80 \leq V < 110$	$V < 80$	0.1
		$V \geq 110$	0.1

IEEE 1547, IEC 61727 and VDE-AR- N4105 are international standards which provide a set of criteria and requirements, supporting for PV integration to the power grid. IEEE 1547, IEC 61727 standards were published by Institute of Electrical and Electronics Engineers (IEEE) and International Electrotechnical Commission (IEC) in 2003 and 2004, respectively while VDE-AR- N4105 initially was a Germany standard, published in 2011, specifying requirements for PV integration in LV network. From Table 2.1, it can be seen that voltage limitations may vary slightly across different standards. In addition, when the voltage at connection point exceeds operational range, PV generators are still connected to the network in some delayed time for purpose of light fault ride through to prevent unnecessary tripping. Table 2.2 presents standards applied in EU countries [22] while Tables 2.3 and 2.4 are voltage requirement in Thailand grid codes [25, 26].

Table 2.2 Grid code applied in EU countries for PV integration in LV network

Country	Overvoltage		Undervoltage	
	Voltage	Maximum clearance time	Voltage	Maximum clearance time
Default	230 + 15%	0.2	230 - 15%	1.5
CZ	230 + 15%	0.2	230 - 15%	0.2
DE	230 + 10%	0.2	230 - 15%	0.2
DK	230 + 10%	40	230 - 10%	10
ES	230 + 10%	-	230 - 15%	-
FR	230 + 15%	0.2	230 - 15%	0.2
GB	264	1.5	207	1.5
IT	230 + 20%	0.1	230 - 20%	0.2

Table 2.3 PEA (Provincial Electricity Authority) grid code

Base Voltage	Normal Condition (Highest Voltage)	Normal Condition (Lowest Voltage)	Severe Condition (Highest Voltage)	Severe Condition (Lowest Voltage)
380 V	418 V	342 V	418 V	342 V
220 V	240 V	200 V	240 V	200 V

Table 2.4 MEA (Metropolitan Electricity Authority) grid code

Base Voltage	Normal Condition (Highest Voltage)	Normal Condition (Lowest Voltage)	Severe Condition (Highest Voltage)	Severe Condition (Lowest Voltage)
400 V	410 V	371 V	416 V	362 V
230 V	237 V	214 V	240 V	209 V

2.2 Solutions for voltage problem in LV network

Many solutions have been proposed in the literature those are implemented either by utilities or customers' side or coordination both of them represented in Figure 2.3. Voltage control can be operated through decentralized control, centralized control or combination two methods. Besides, electricity price policy also considerably contributes to voltage violation mitigation when it directly affects the benefit of producer and electric bill of consumers.

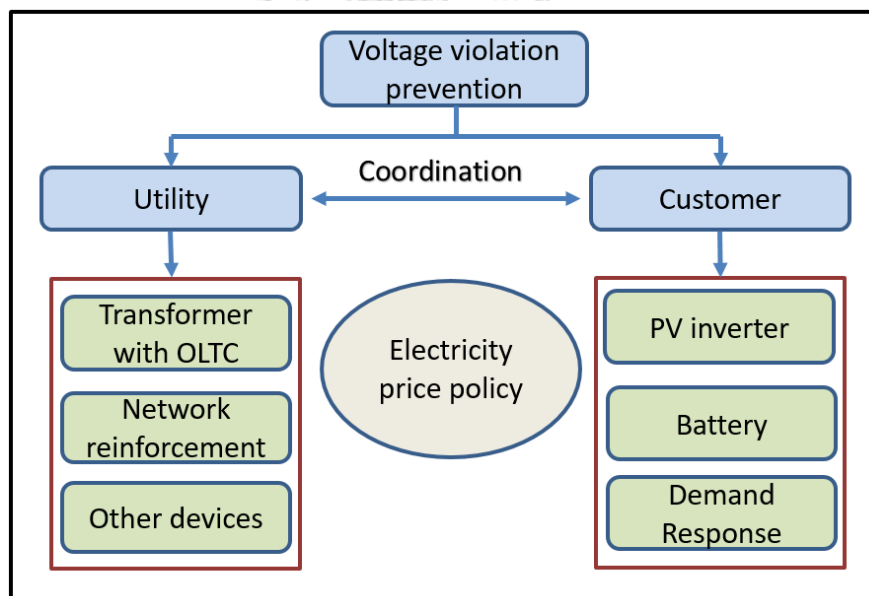


Figure 2.3 Solutions for the voltage problem

As previously specified in formulas (2.1) and (2.2), four subjects should be put in consideration to manage the voltages of the entire network within acceptable range. In this section, voltage regulation mechanisms are discussed and analyzed for each solution and its obstacles.

2.2.1 Reference voltage regulated at MV/LV transformer

Normally, a reference voltage is considered firstly by transformer tap setting change [4] due to economic effectiveness. By this means, the reference voltage which is sent from the transformer is regulated up or down to maintain all node voltages of the network within acceptable range. This is a solution influencing all network. It is a fact that this solution operates quite effectively with a simple network where the regulated room is sufficient for the change of load along a day coupled with characteristics of the network. With the presence of PV rooftops, the regulated room is lessened or even not sufficient if the density of PV rooftops is high and distributed unreasonable. Figure 2.4 illustrates a typical design of distribution in Germany [27]. According to this design, PV installations in low voltage network are limited by 3% increase in voltage with fixed tap position at MV/LV transformer. However, if sending voltage at MV/LV transformer can be controlled actively, it will allow higher voltage caused by PV generation as well as higher possible PV installations. The methods which were proposed in the literature are using OLTC at MV/LV transformer. In addition, to make OLTC operate more effectively, the feedbacks from nodes with the support of communication infrastructure were also suggested [27]. Consequently, it is very clear that more investment and operation costs are required for those control applications.

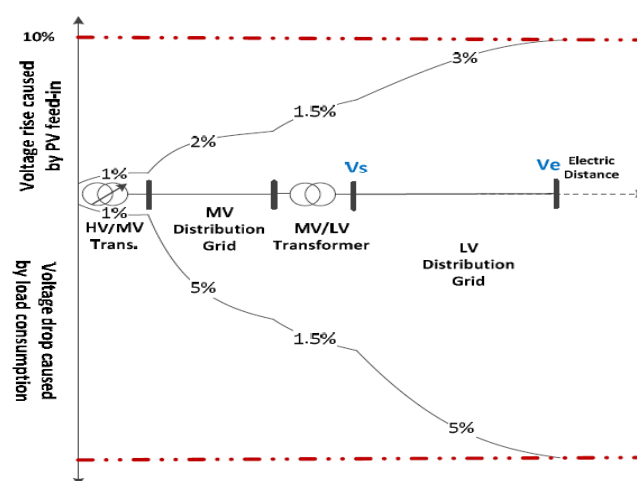


Figure 2.4 Typical design of distribution system in Germany [27]

There is another fact that sending-voltage regulation might help allow more PV installations but only some extent. Because, when penetration of PV rooftops is really

high and distributed randomly, it is more difficult for regulation such as the case depicted in Figure 2.5. Tap changer can prevent overvoltage in some areas but it might cause undervoltage on the same feeder or neighboring feeders and outage during the regulation process if offload tap changer is used. For such network, supplementary solutions are required to maintain voltages of the network within acceptable range.

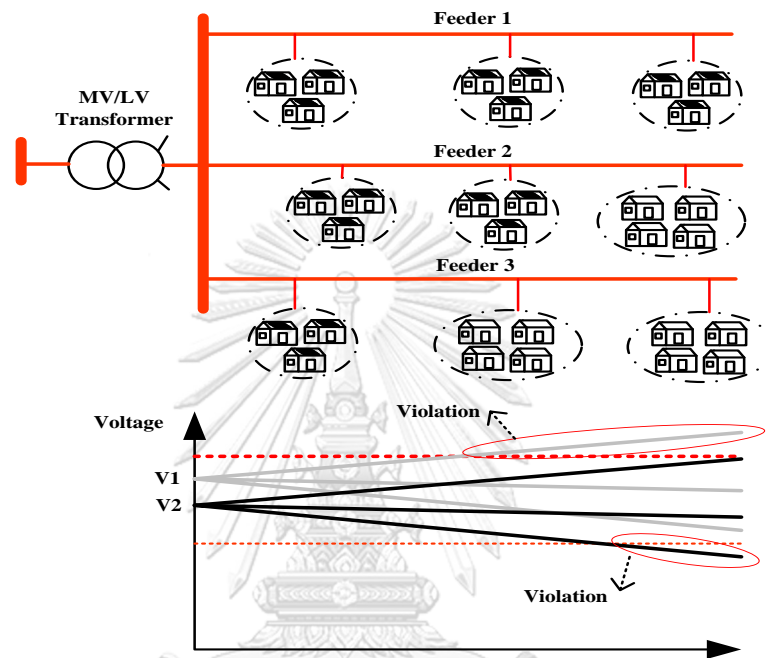


Figure 2.5 Effect of sending voltage on network voltages

Besides, another disadvantage of OLTC is that it cannot response enough quickly with a sudden change of solar irradiance. Therefore, it might confirm that OLTC is not sufficient to deal with high penetration of PV rooftops in near future.

2.2.2 Network reinforcement

Network reinforcement could be the next solution to deal with voltage problem. This solution helps reduce line impedance, resulting in larger power permission. Figure 2.6 compares real measured voltage profiles in a weak network where voltage is a barrier for PV penetration and in the reinforced network [27]. It is no doubt that this resolution is quite effective. Comparison between OLTC and network reinforcement is illustrated in Figure 2.7. Voltage curve in the reinforced network is obviously flatter. Furthermore, many reinforcement options are possible to be selected. Accordingly, utilities may make an upgrade at the transformer, change to bigger distribution lines or

simply build parallel ones. Moreover, reconfiguring network from radial becoming ring grid also contributes to increasing hosting capacity for the feeders. However, in such case, protection coordination applied in those feeders should be carefully investigated.

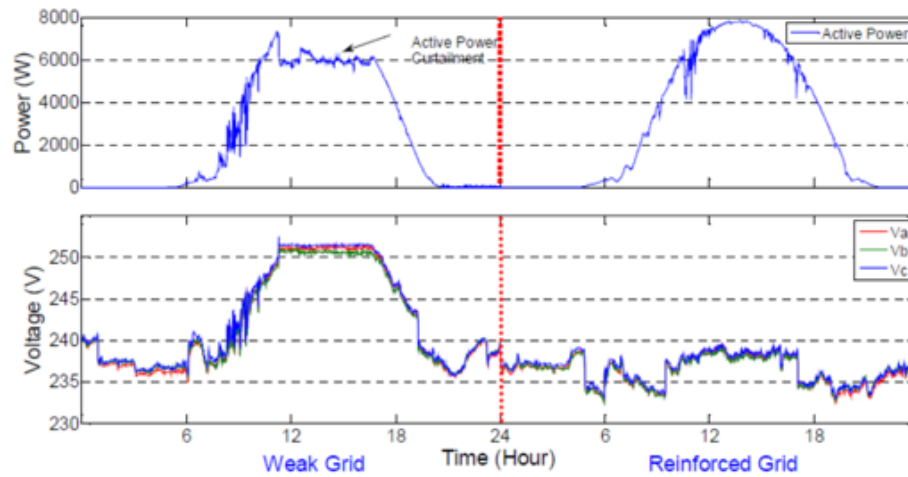


Figure 2.6 Effectiveness of network reinforcement on voltage profile [27]

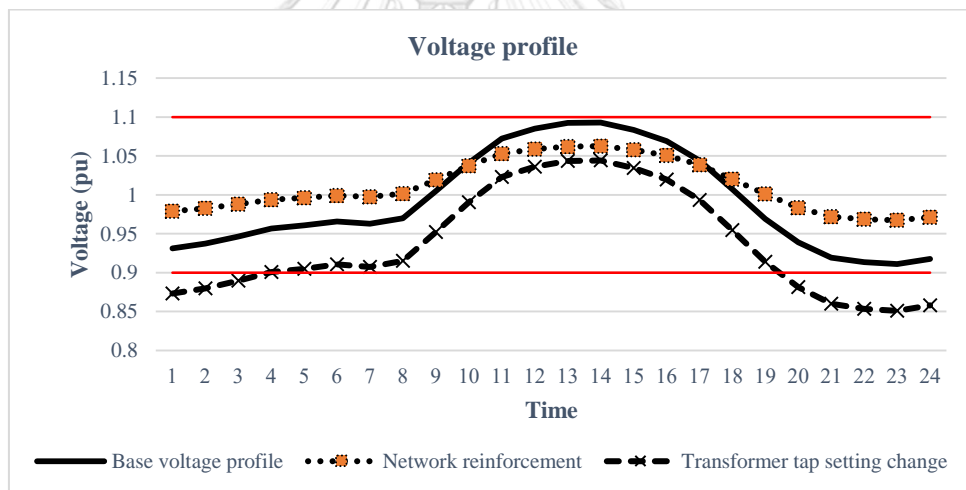


Figure 2.7 Effectiveness of voltage regulation solutions

It is a fact that network reinforcement is commonly considered to meet thermal condition than voltage violation caused by PV systems. Because the main drawback of this solution is high cost and not considered as a cost-efficient solution for voltage problem due to the rare occurrence of overvoltage caused by PV generation during a year. Moreover, this solution is not flexible for voltage regulation in the technical aspect since it does not actually take part in real-time voltage regulation.

2.2.3 PV inverter

There are plenty of research works in the literature those call support of PV inverters for voltage regulation [5, 6]. It seems reasonable when they are the cause of the problem. So, they should be responsible for that. Accordingly, utilities might force PV generators to control their outputs. However, in order to deploy in practice, PV inverters must be capable of voltage controlling and additional investment is required to customers for PV inverter improvement. This may interfere the development of PV generation if there is no more subsidy. In these research works, the proposed methods for voltage supported by PV inverters are mainly based on active power curtailment and reactive power compensation. Both of them contribute to the reduction of the numerator of the ΔU formula which is previously specified in Section 2.1.

Comparison between two methods, active power curtailment is more effective due to low X/R characteristic of LV network. This is the solution for the countries that reactive powers are not allowed to be absorbed by PV inverters stated in their grid codes. In addition, power conditioners have been designed for practical application in Japan to restrict active power output when voltage exceeds setting value [3] or simply disconnect from the electric grid when overvoltage occurs. Besides, several proposed methods are based on the capability of controlling active power output according to the voltage at the connection point. In those cases, a P(U) curve is set for that response [6]. An example of P(U) curve is illustrated in Figure 2.8. It is obvious that the main drawback of these methods is clean energy waste during the efficient operation period of PV generators. To save this energy, prosumers may install battery to store excessive energy for later use. In that case, cost- benefit should be carried out to make decision. Another drawback is that voltages are very different across different connected points. Therefore, how to fairly curtail active powers among PV inverters needs to investigate more carefully.

On the other hand, reactive power compensation resolution intends to use the remaining capacity of PV inverters when active power generation is lower than the rated capacity of PV inverter for voltage support. Control strategies can be fixed power factor ($\cos\phi$), reactive power as a function of voltage (Q(U)) or power factor as a function of active power ($\cos\phi(P)$). While this resolution is widely accepted for medium voltage grid, it faces many arguments for applying to small generator such as PV

rooftop. This is maybe because small PV generator needs to retrofit inverter for voltage support while its impact is not much. Moreover, PV inverter will consume more energy and reduce its lifetime but receive no financial benefit for its contribution.

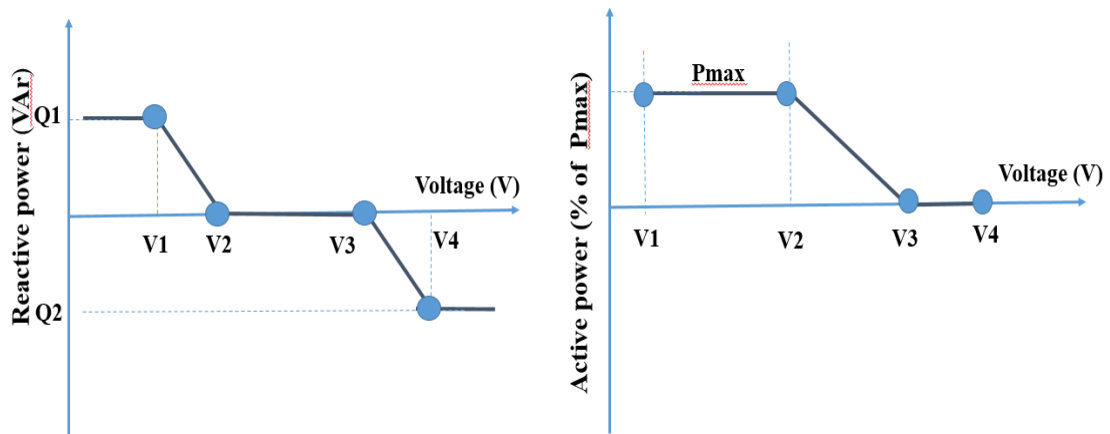


Figure 2.8 Voltage support curves of PV inverter

2.3.4 Battery energy storage system

Battery energy storage system (BESS) is receiving growing attention from researchers worldwide [10-14]. This is because it can provide needed flexibility to modern power systems while the existing devices perform limited technical capability. With the support of BESSs, various problems resulting from unbalance between load and generation can be solved easier. Particularly, BESSs can actively help control power flows within power network by controlling their charge/discharge processes, in turn preventing voltage violation as well as other problems of the power system. Principally, BESS charges the excessive power that may cause overvoltage and discharge to prevent undervoltage during peak demand. Moreover, with the capability of rapid control, BESS can compensate the fluctuation of solar power generation that OLTC and network reinforcement cannot do. However, currently, the price of the battery is still high and the deployment of solar power penetration is still in the premature stage. Other alternatives still work well. Nevertheless, when the price of the battery is lower and deployment of solar power penetration is higher in the near future, battery storage system will be preferable than other alternatives. It is also the subject to investigate in this dissertation and will be discussed further in next chapter.

2.3.5 Other solution and conclusion

Power generation and electric demand are subjects driven by electricity price policies. Therefore, appropriate policies would contribute to making coincidence between load and generation, in turn decreasing voltage problem. Policies should encourage self-consumption of prosumers and demand response of consumers.

In conclusion, it is not easy to say which one is the best solution for solving voltage problem caused by high penetration of PV rooftops in LV network. Because no universal strategy can always exhibit efficiently and economically for all cases. There are numerous influenced factors to the grid, and voltage regulators such as installed site, optimum sizing and load/generation grid patterns.



CHAPTER 3

BESS, SOLUTION FOR VOLTAGE MANAGEMENT IN FUTURE LV NETWORK

As discussed previously, BESS is the dominant solution that can bring needed flexibility to the modern power system to deal with many problems including voltage violation caused high penetration of solar power generation.

This chapter gives the description of the functional principle of grid-interconnected BESS as well as the requirement of BESS for voltage management application. Then, battery modeling for economic assessment purpose of the BESS project is also reviewed in this chapter.

3.1 BESS integration to power network

BESS applications in power system can be applied in all parts from generation to transmission system and lastly distribution part. The applications are identified as follows:

- BESS works as a reserve source
- Frequency support
- Voltage support
- Support for renewable integration
- Time shifting
- Temporary solution for urgent problems of the network such as network congestion

However, the scope of the dissertation is BESS implementing in LV network for voltage management purpose.

3.1.1 Functional principle of grid-interconnected BESS

BESS can operate independently or coordinate with others for an operation duty. For purpose of visualizing the components, operation principles are described in different management levels of BESS control schemes.

3.1.1.1 Operation principle of BESS

Battery bank and bidirectional converter are two main electrical components making up a BESS. While battery bank is the place for storing energy, the bidirectional converter is responsible for converting energy from ac to dc and vice versa of charge and discharge processes, respectively. Besides, battery management system (BMS) and demand controller (DC) are facilities which ensure safe and reliable operation of BESS components and coordinate with the grid to control charge and discharge processes of the BESS. The functional principle of grid-interconnected BESS is depicted in Figure 3.1.

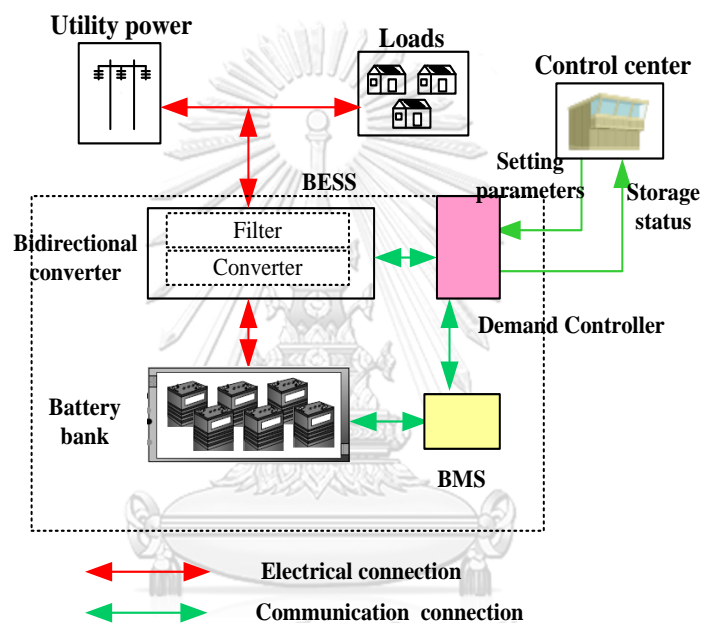


Figure 3.1 Functional principle of grid-interconnected BESS

Control signal can be set locally or remotely from the control center for a specific application via DC which is commonly based on PLC (Programmable Logic Control). Various control options have been designed in commercial products [28, 29], including:

- Scheduling of active and reactive power
- Peak Shaving
- Generation-smoothing
- Frequency regulator
- Island and advanced algorithm

In addition, required inputs, as well as control scheme implemented in DC, are determined by the optional application.

Furthermore, BMS might be designed inside demand controller but usually, battery manufacturers provide it coupled with the battery bank. BMS is responsible for battery monitoring, battery balancing, safe operating and some other functions. Communication between BMS and DC is required for safe and optimal operations of battery bank according to control strategies.

3.1.1.2 Operation principle with aggregation of many BESSs

This scenario is prepared for an expectation of battery development and popular deployment in power grid. Resolution for aggregation of many battery energy storage systems (BESSs) which is implemented both by consumers and utility is a foreseen need. In a pilot battery project of smart city implemented in Yokohama city, Japan, storage battery SCADA (Supervisory Control And Data Acquisition) which is a popular device in power system for monitoring and controlling application was proposed by a group of battery manufactures and TEPCO (Tokyo Electric Power Company) for that purpose [30]. With this resolution, many BESSs come from different manufacturers with various specifications are virtually assembled like a large capacity battery and centrally controlled. Grid operator can use the collected information not only for voltage control but also numerous utility applications such as power flow control, frequency control, load leveling and so forth. Operation principle of storage battery SCADA and BESSs are described in Figure 3.2.

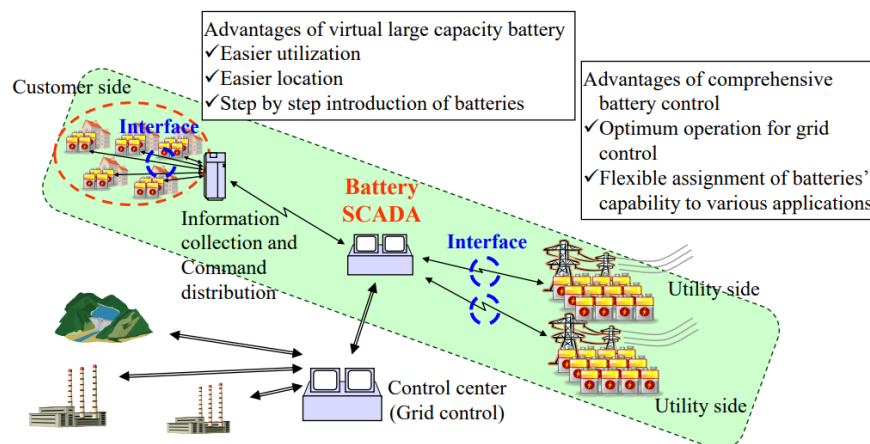


Figure 3.2 Operation principle of storage battery SCADA [30]

Information from BESSs which participate in control process is collected by storage battery SCADA. Here, the information is processed and then transmitted to the control center. It should be noted that not only utility's BESSs but also BESSs of customers are also joined in this process. Grid operator will base on this information and the collected data of the network to send commands to storage battery SCADA. From storage battery SCADA, the corresponding commands are distributed to each BESS.

3.1.2 Requirement of BESS for voltage management

Battery bank and converter are two main components of the BESS. Therefore, this subsection provides necessary information of some popular battery types in the market and notices for battery selection. After that, standards supporting for BESS integration to the grid are reviewed.

3.1.2.1 Battery technologies

Nowadays, there are various types of batteries advertised in the market. They are different by size, application, technology, and manufacturer leading to various technical characteristics, cost as well as performance. The battery types are popular in the market such as lead-acid battery (LA), Nickel-cadmium (NiCd) and nickel metal hydride battery (NiMH), Lithium-ion battery (Li-ion), Sodium-sulfur battery (NaS), and Sodium nickel chloride battery (NaNiCl). Technical characteristics of those batteries are briefly summarized in Tables 3.1 and 3.3 [30].

a. Lead-acid battery

LA battery is the most popular with wide use in both household and industrial sector. It is the oldest rechargeable battery which has been commercial since the mid-1800s. Making up the LA, positive and negative electrodes are made from lead dioxide and metallic lead, respectively. All of them are immersed in the sulphuric-acid electrolyte which has been diluted. Two typical types of LA available in the market are flooded LA and sealed valve-regulated LA (VRLA). The flooded LA is cheaper than VRLA but it requires frequent maintenance, at least one per month to add distilled water. However, in comparison with other technologies, LA still exhibits a mature, high energy efficiency and low cost. The main drawbacks of this technology are low cycle-

life, low discharge rate, and low energy density. In addition, LA uses lead, a toxic material for health which is restricted or prohibited in many jurisdictions. Since commercially distributed, typical applications LA include uninterrupted power supply (UPS), stand-alone systems with PV, support for renewable energy integration to grid and starter batteries in vehicles. Cost of stationary batteries is presently much higher than the cost of the starter battery. However, according to reference [31], a large amount of LA was installed in about 50,000 solar households in Morocco from 1995 to 2009 for the target of rural electrification. The number for Bangladesh is 3,500,000 solar households. Mass production of LA batteries for application in the stationary system might lead to a price reduction. Furthermore, researchers worldwide are continuously researching effective improvement for traditional LA to overcome its drawbacks. The presence of many advanced LA versions, for example, “ultrabattery” which is an enhancement of negative electrode with ultracapacitor to increase charge/discharge rates is an evidence for that effort.

b. Nickel-cadmium and nickel metal hydride battery

NiCd and NiMH batteries were commercially introduced around 1915 and 1995 respectively. In comparison with LA battery, they are more expensive. However, the significant advantage of those batteries is good performance even at the low temperature which is around the range of $-20\text{ }^{\circ}\text{C}$ to $-40\text{ }^{\circ}\text{C}$. In addition, they also perform higher power density, higher cycle life and slightly higher energy density than LA battery. Technical comparison of three types of battery can be seen in Table 3.1

Similar to LA battery, NiCd battery contains toxic material that is cadmium. Therefore, it is commonly used for stationary applications under vented NiCd battery and officially prohibited in Europe in 2006 for consumer use.

On the other hand, NiMH battery which has the same advantages of NiCd battery excluding low nominal capacity was initially created to replace NiCd battery due to the toxic issue. The nominal capacity of NiMH battery is ten times less than NiCd and LA but higher energy density. Its price is equal to the lithium-ion battery but it is preferable to apply in the hybrid vehicle because of robust and safe advantages. On the contrary, lithium-ion battery now replaces NiMH battery in the portable applications.

Table 3.1 Technical review of LA, NiCd and NiMH battery [30]

Technical parameters	Battery technologies		
	<i>Lead Acid</i>	<i>NiCd Vented Sealed</i>	<i>NiMH sealed</i>
<i>Nominal Voltage (V)</i>	2	1.2	1.2
<i>Capacity per cell (Ah)</i>	1 -4000	2 - 1300 0.05 - 25	0.05 - 110
<i>Response Time</i>	< sec	< sec	< sec
<i>Energy Density (Wh/kg)</i>	30 - 45	15 - 40 30 -45	40 -80
<i>Energy Density (Wh/l)</i>	50 -80	15 - 80 80 -110	80 - 200
<i>Power Density (W/l)</i>	90 - 700	75 - 700 (vented)	500 - 3000
<i>Typical Discharge Time</i>	hours	hours	hours
<i>Energy Efficiency Wh (%)</i>	75 - 90	60 -80 60 -70	65 - 75
<i>Typical Cycle Lifetime (cycles)</i>	250 - 1500	1500 - 3000 500 - 800	600 - 1200
<i>Typical Application</i>	Off - Grid, Emergency Supply, Time Shifting, Power Quality	Off - Grid, Emergency Supply, Time Shifting, Power Quality	Electric Vehicle

c. Lithium-ion battery

Li-ion battery which was first commercially introduced in the 1990s by Sony has become the most popular application in portable electronics such as laptops, cellphones and so forth. In comparison with other technologies, Li-on batteries have the highest nominal voltage of 3.7V. This helps Li-on batteries have characteristics of high energy density and high power density, allowing them to save significant space

while providing high energy and high power. Besides, other identified advantages of Li-ion batteries are long cycle-life, very high efficiency (typically in the range of 85% to 98%), and environmental friendliness. Those good characteristics make them become a very promising option for application in next generation of electric vehicles (EVs) and plug-in hybrid EVs (PHEVs). Currently, the price of Li-ion batteries is still high with more than \$600/kWh since it needs internal overcharge protection circuit [31]. Large cost reduction is expected due to mass production coupled with the development of EVs and PHEVs. Another obstacle accompanying with Li-ion battery is safety when overheating or fire may occur with such type of battery. Therefore, protection solution should be carefully considered with the equipment of overcharging/over-discharging protection circuits and voltage balance circuit. This should be standardized with Li-ion battery production to implement in power grid.

Table 3.2 Application of Li-ion battery in power systems [31]

Project Name	Location	Energy	Application Functionality	Year of Installation
Santa Rita Jail Smart Grid Advanced Energy Storage System	California, United States	32 MW/0.25 h	Microgrid with renewable generation and large-scale energy storage, balancing load peaks and valleys	2012
Anchorage Area Battery Energy Storage System	Alaska, United States	25 MW/0.6 h	Electric energy time shift, electric supply reserve capacity spinning, load leveling, transportable transmission/distribution, upgrade deferral	2012
National Wind and Solar Energy Storage and Transmission Demonstration Project (III)	Hebei, China	3 MW/3 h	Frequency regulation, ramping, renewables capacity firming, renewables energy time shift	2012
Orkney Storage	Scotland, United Kingdom	2 MW/0.25 h	Transmission congestion relief	2013
Tehachapi Wind Energy Storage Project–Southern California Edison	California, United States	8 MW/4 h	Electric supply capacity, renewables capacity firming, transmission congestion relief, transportable transmission/distribution upgrade deferral, voltage support	2014
Giheung Samsung SDI Project	Gyeonggi-do, South Korea	1 MW/10 h	Frequency regulation, transmission congestion relief, voltage support	2015
Feldheim Regional Regulating Power Station	Brandenburg, Germany	1 MW/1 h	Frequency regulation, renewables capacity firming, transmission upgrades due to wind	2015
Rabbit Hill Energy Storage Project	Texas, United States	1 MW/0.5 h	Electric energy time shift, frequency regulation, renewables energy time shift	2016

Nowadays, various types of Li-ion batteries are existing in the effort of researchers to seek the advanced one for safe and low in cost. They are different with chemical compositions which make up anode, cathode, or electrolyte. As a result, their

price and performance are different. In that effort, it was remarkable in 1997 with the introduction of Lithium-ion phosphate (LFP) battery that the cost was reduced significantly for the first time, making scale utility application possible. As a result, some Li-ion battery projects have been implemented in power system in practice shown in Table 3.2. In those applications, with their advantages, Li-ion batteries have undertaken various supporting roles for the power grid.

d. Sodium sulphur battery

Ford Motor Company is the pioneer in the development of NaS battery which aimed to use in early-model electric cars in the 1960s. However, until the late 1990s, NaS batteries were introduced under utility-scale and then launched to the market in 2002 [31]. Different from above batteries, NaS battery requires operation at high temperature around 300 °C to 350 °C to keep their positive and negative electrodes which are made of sulphur and sodium molten. Therefore, external heating is needed for starting the operation and usually not required during charge and discharge processes when the electrochemical reaction can create heat itself. To prevent heat leakage, NaS cell is made in blocks and covered by a vacuum-insulated box. This is the main drawback of such type battery when it needs its own stored energy, resulting in partial performance reduction. Simultaneously, this is also positive point of NaS batteries because it allows them to operate in some hot and harsh environments.

About technical characteristics, NaS battery performs high energy density (100-250Wh/kg) and long cycle-life (2500-4500 cycles) shown in Table 3.3. Compared with LA battery, its power density is higher but lower than NiMH and Li-ion batteries. Those characteristics make NaS battery economically suitable for the combination of power quality and time shift supports for the power grid. According to reference [31], the application of NaS battery has been developing in Japan with a deployment of over 190 sites (about 270MW), mainly for peak shaving support. The biggest installation is a 34MW/245MWh which was installed in Northern Japan for wind stabilization. Besides, Germany, France, and United States are also the countries those have NaS batteries in operation.

e. Sodium nickel chloride battery (NaNiCl)

NaNiCl battery is well-known as the ZEBRA (Zero Emission Battery Research) battery which has been commercially distributed since 1995 [30]. Similar to NaS battery, this type of battery operates in high-temperature at around 270 °C. Its negative electrode is made of sodium while positive electrode uses nickel chloride instead of sulphur. In comparison with NaS battery, this technology is somehow safer since it can suffer limited overcharge and discharge. In addition, the nominal voltage of 2.6 V is higher than NaS batteries with 2.1V. It is a fact that NaNiCl battery has been successfully designed in several electric vehicle versions such as Think City and Smart EV. Besides, it is also suitable for fleet applications. Presently, researchers are developing advanced versions of the ZEBRA battery which improve its power density characteristic for hybrid electric vehicle application and energy density characteristic for power and industrial applications.

Table 3.3 Technical review of Li-ion, NaS and NaNiCl battery [30]

Technical parameters	Battery technologies		
	<i>Li-ion</i>	<i>NaS</i>	<i>NaNiCl</i>
<i>Nominal Voltage (V)</i>	3.7	2.1	2.6
<i>Capacity per cell (Ah)</i>	0.05 - 100	4 - 30	38
<i>Response Time</i>	< sec	< sec	< sec
<i>Energy Density (Wh/kg)</i>	60 - 200	100 - 250	100 - 200
<i>Energy Density (Wh/l)</i>	200 - 400	150 - 300	150 - 200
<i>Power Density (W/l)</i>	1300 - 10000	120 - 160	250 - 270
<i>Typical Discharge Time</i>	hours	hours	hours
<i>Energy Efficiency Wh (%)</i>	85 - 98	70 - 85	80 - 90
<i>Typical Cycle Lifetime (cycles)</i>	500 - 10000	2500 - 4500	~ 1000

Technical parameters	Battery technologies		
	<i>Li-ion</i>	<i>NaS</i>	<i>NaNiCl</i>
<i>Typical Application</i>	Off - Grid, Network efficiency Time Shifting, Power Quality Electric Vehicle	Time Shifting, Off - Grid, Network efficiency	Time Shifting, Electric Vehicle

3.1.2.2 Considered factors for battery selection

Variety of batteries existing in the market bring to investors more opportunities to select for their BESS project. The factors for battery selection that should be taken into account are pointed out in Figure 3.3 [15].

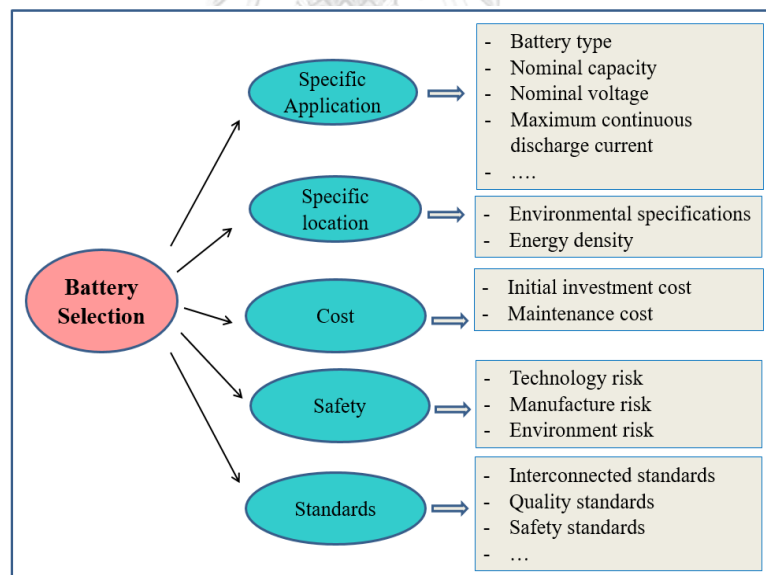


Figure 3.3 Considered aspects of battery selection

Among those factors, technical features should be considered first to meet the requirements of a particular application. If a battery is used in wrong application, it may either not satisfy operation requirement of the system or be affected dramatically its lifetime. Together with that, limitation of space and environmental operation of the battery are particular traits which must be noticed for a specific application. Besides,

different suppliers may offer different prices for their products. Investors, therefore, should analyze factors such as cost, product's performance as well as unsafe risks and prestige of supplier. Lastly, certificated standards of the battery must meet requirements of the local utility. As a result, after considering all factors, selected range is lessened quickly according to considered categories to reach the best selection for an individual project of BESS.

The battery used for voltage management application in the grid should be secondary and deep charge/discharge cycle type. In general, for each technology, corresponded standards should satisfy the requirement of local utility. Currently, various standards developed by international organizations are applicable to battery. The standards classify according to battery technologies, working environments and some other topics. Most of them are guides for traditional batteries such as lead-acid, lithium, nickel metal hydride, nickel cadmium batteries, covering technical feature, testing and system integration [30]. Noted that, battery bank with its specifications must match bidirectional converter requirement to become unified BESS.

3.1.2.3 Supporting standards for BESS integration and automation in power grid

Although many big projects of BESS have been applied in practice worldwide, they use proprietary facilities to make the work done, with integration designed on a case-by-case basis. This is because currently, no independent standard for BESS integration to utility grid now exists. It is one of the factors that contribute to high cost of battery projects due to lack of international standards applied for BESS integration. Response to this demand, IEC (International Electrotechnical Commission) has approved a new work, namely, IEC 61850-90-9 - Models for Electrical Energy Storage under a technical report. According to the reference [32], the content of this technical report in the latest draft specifies the basic functions of electrical energy storage system and describes integration model between electrical energy storage system as DER (distributed energy resource) unit and intelligent power grids. The work is progressing and expected to be published soon.

Furthermore, IEC 61850-90-9 is an extension, lying in IEC 61850 framework that standardizes communication networks and systems for power utility automation with series of standards depicted in Figure 3.4. This document with specified object

models for BESS closely associated with following standards supports for automation target of BESS in power system [33-35].

- “IEC 61850 -7-4: Basic communication structure – Compatible logical node classes and data object classes” published in 2010 with the second edition version. This standard specifies normative rules those can be applied to describe how control system and BESS generate and exchange information.
- “IEC 61850 -7-420: Basic communication structure – Distributed energy resources logical nodes” published in 2009 with the first edition version. However, BESS mentioned in this publication is an auxiliary system used in substations. Therefore, only discharge function of BESS is described.

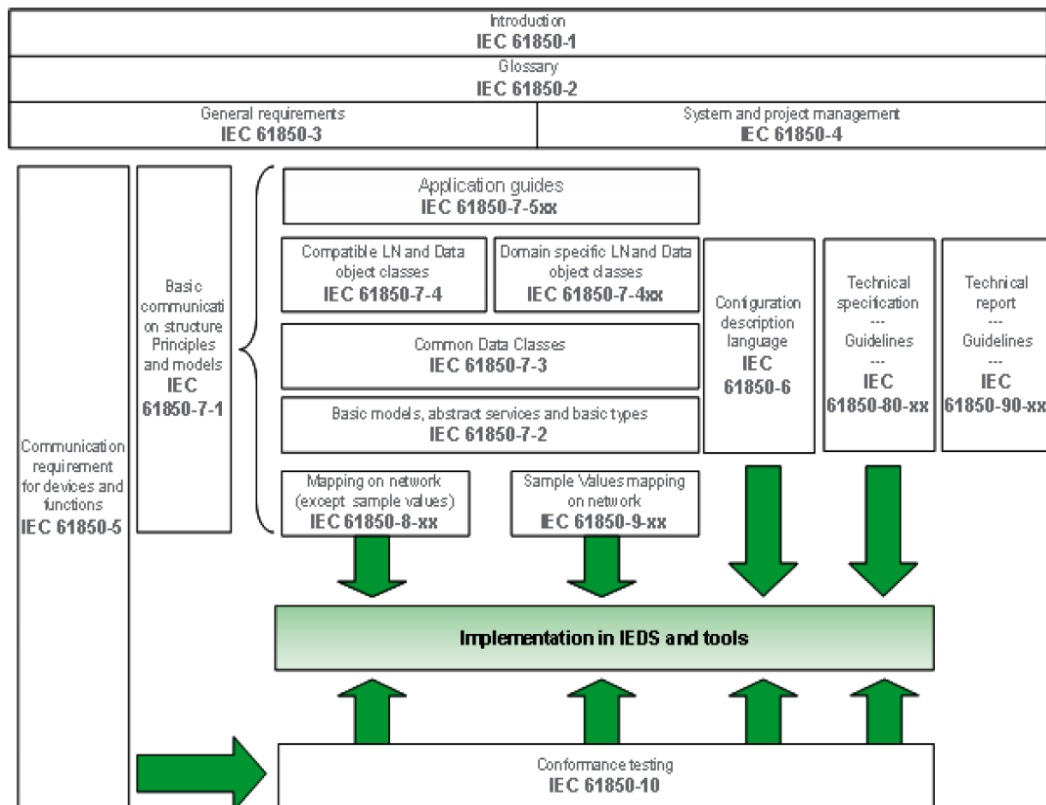


Figure 3.4 Framework of the IEC 61850 [33]

- “IEC/TR 61850 -90- 7: Object models for power converters in distributed energy resources (DER) systems” published in 2013 with the first edition version. In this part, functions of converters of DER systems including BESS are described in conjunction with the model of exchanged information between converter-based DER systems and control center or

others. The content of the voltage management through described functions, operation modes (illustrated in Figure 3.5) of the converter is also defined in this part.

Since, fully- completed standard for BESS integration to power system has not been published yet, BESS should comply grid interconnection code, testing and general standards specified by local utilities. Besides, it must be capable of smart control to adapt designed application (such as charge/discharge scheduling) as well as the safe and effective operation itself.

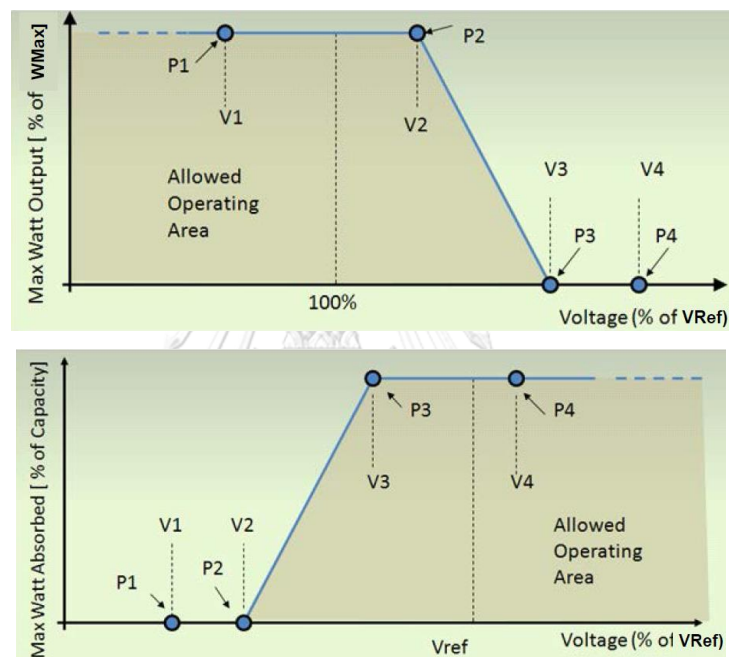


Figure 3.5 Examples of setting modes of converters for voltage support [33]

3.2 Battery modeling for economic assessment of BESS project

Battery is still a challenge for modeling due to its complexities in state description contributed by various influential factors. Thus, each model has its own scope of application with some simplified assumptions. This section aims to give the overview of battery characteristics and complex relationships among operation parameters and their influential factors. It is noted that those descriptions do not focus on any type of battery and the characteristic curves in the figures are used only for illustration purpose. Then different battery models are described to understand how precise of each model and its scope of application. Lastly, some simple methods of

battery lifetime estimation commonly used for economic assessment in the literature are reviewed.

3.2.1 Basic battery concepts

Before going further to understand about battery modeling, the understanding of battery terminologies are provided in subsection 3.2.1.1 [36]. Conditioned characteristics of battery parameters are described in subsection 3.2.1.2.

3.2.1.1 Battery terminology

Battery parameters depend on operation conditions. As a result, specifications of a battery provided by the manufacturer are basically based on specific condition (standard condition). Battery terminologies include the terminologies describing the technical specification of a battery which usually provided by the battery manufacturer and the terminologies describing operating state of a battery.

❖ Terminologies describing battery technical specifications

✚ Nominal Voltage (V)

“Nominal” voltage is known as designed voltage or reference of the battery that is defined by cell-voltage and number of cell in series.

✚ Cut-off Voltage

Cut-off voltage is the lowest voltage at which battery must be cut out in discharging process for purpose of damage prevention. It contains the meaning of the empty state of the battery.

✚ Capacity or Nominal Capacity (C)

Battery capacity, a measure in Ah, Wh or kWh is the total amount of stored energy that can be drawn from full state to the empty state at a certain condition (temperature, discharge current).

Nominal capacity is a reference reported by the manufacturer.

Actual capacity is calculated by multiplying the discharge current (in Amps) by the discharge time (in hours) and decreases with increasing C-rate.

✚ Cycle-Life

Cycle-life is measured by the number of operating cycles of a battery before it meets specific performance criteria supposed the end of life. Degradation of 20%

original capacity is an example of applied criteria. Cycle-life is reported for a specific charge and discharge condition and influenced by the rate and depth of discharge (DOD) and by environmental conditions such as temperature and humidity.

✚ *Specific Energy (Wh/kg)*

Specific energy is also known as gravimetric energy density which measures the nominal battery energy per unit mass. Specific energy is particular for each type of battery technology through the characteristic of the battery chemistry and packaging. With this information, the weight of the battery is estimated for the desired energy for supplying.

✚ *Specific Power (W/kg)*

Similar to specific energy, specific power is particular for each battery technology through the characteristic of the battery chemistry and packaging but measured by the maximum available power per unit mass. With this information, the weight of the battery is estimated for the desired power for supplying.

✚ *Energy Density (Wh/L)*

Energy density is also known as the volumetric energy density which is measured by the nominal battery energy per unit volume. Energy density is particular for each type of battery technology through the characteristic of the battery chemistry and packaging. With this information, the size of the battery is estimated for the desired energy for supplying.

✚ *Power Density (W/L)*

Similar to energy density, power density is particular for each battery technology through the characteristic of the battery chemistry and packaging but measured by the maximum available power per unit volume. With this information, the size of the battery is estimated for the desired power for supplying.

✚ *Maximum Continuous Discharge Current*

Maximum continuous discharge current is the maximum current which is allowable to be discharged continuously. Battery should not be discharged above this rate because this may damage or reduce battery capacity.

✚ *Maximum 30-sec Discharge Pulse Current*

Beside maximum continuous discharge current, maximum 30-sec discharge pulse current defines the maximum current which is allowable to be discharged for pulses of up to 30 seconds.

✚ Charge Voltage

The voltage that the battery is charged to when it is full. Charging schemes generally consist of a constant current charging until the battery voltage reaching the charge voltage, then a constant voltage charging, allowing the charge current to taper until it is very small. The concepts related to charging process of a battery are depicted in Figure 3.6

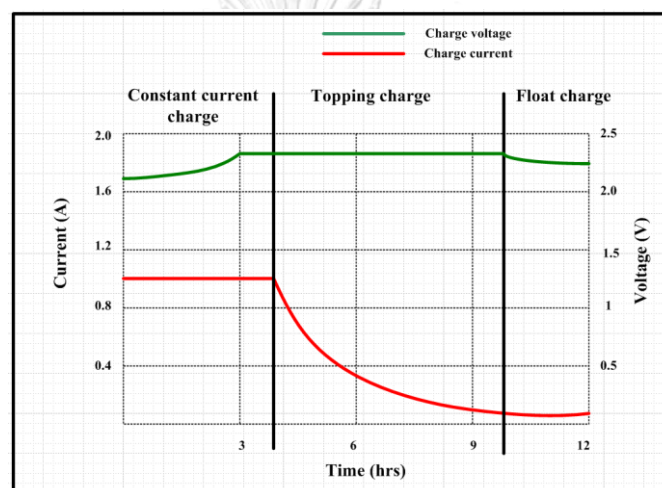


Figure 3.6 Charging process of typical lead acid battery

✚ Float Voltage จุฬาลงกรณ์มหาวิทยาลัย

Float voltage is the voltage to keep battery full capacity after it is charged to 100% state of charge by compensating for self-discharge of the battery.

✚ Recommended Charge Current

Recommended charge current is the constant current that the battery should be charged before changing to constant voltage charging at around 70% state of charge.

✚ Internal Resistance

Internal resistance represents for energy loss during charging and discharging processes. Internal resistance changes according to state of charge and differently for two processes [36].

❖ Battery operating terminologies

✚ State of Charge

State of charge (SOC) represents available energy level in battery in percentage expressed in the equation (3.1). It plays a role as an indicator to let users know how much energy left they have or how long they can use, in turn preventing battery damage caused by overcharge or over-discharge.

$$\text{SOC} = \frac{E}{C} * 100\% \quad (3.1)$$

Where

- E is available energy in the battery (Wh)
- C is reference capacity of the battery (Wh)

Depth of discharge

Depth of discharge (DOD) of a battery is represented in percentage of the ratio between the discharged energy and the maximum capacity of the battery. It is usually considered for an operating cycle of battery and expressed in formula (3.2). Operating DOD should not exceed maximum DOD specified by battery manufacturer.

$$\text{DOD} = \frac{E_d}{C} * 100\% \quad (3.2)$$

Where

- E_d is discharged energy of the battery (Wh)
- C is reference capacity of the battery (Wh)

Charge and discharge rate

Charge and discharge rates refer to the speed of charge or discharge. They can be measured in quantity of current, power or C-rate.

C-rate is a measure of charge and discharge rate of a battery which is relative to its maximum capacity [36]. A C-rate means that entire capacity is charged or discharged in 1 hour. For example, if 50 Ah battery discharges at 1C, 2C or C/2, the discharge current will be 50A, 100A or 25A, respectively, and corresponding discharge times will be 1h, 0.5h or 2h. By this way, from C-rate, the time for charging or discharging entire capacity of a battery is deduced.

State of Health and End of Life

In general, there is no universal definition of battery state of health (SOH), and its meaning is largely application-dependence. However, in all cases, battery SOH quantifies the extent a battery's performance that has been reduced, and it is usually

expressed in terms of a percentage. A new battery would, therefore, have a SOH of 100%, and a battery that has reached its minimum level of acceptable performance, or end-of-life (EOL), could be said to have a SOH of 0%. In stationary and hybrid-vehicle applications, capacity is often the primary metric of interest, and so SOH will refer to the amount of capacity loss that a battery has experienced. EOL, in turn, will identify the minimum allowable capacity before the battery is said to have failed. For starter batteries where peak power output is the most important battery characteristic, SOH could be defined in terms of increases in internal resistance.

3.2.1.2 Conditioned characteristics of battery parameters

The section states the key parameters used to characterize batteries and shows how these parameters may vary with the operating conditions. Conditioned characteristics of the battery parameters are described in various specific conditions.

❖ Conditioned characteristics of battery capacity

Sustained capacity of a battery decreases along the operation life due to aging degradation (illustrated in Figure 3.7). This occurs with all battery chemistries. Speed of aging or capacity reduction is influenced by multiple factors which will be discussed later.

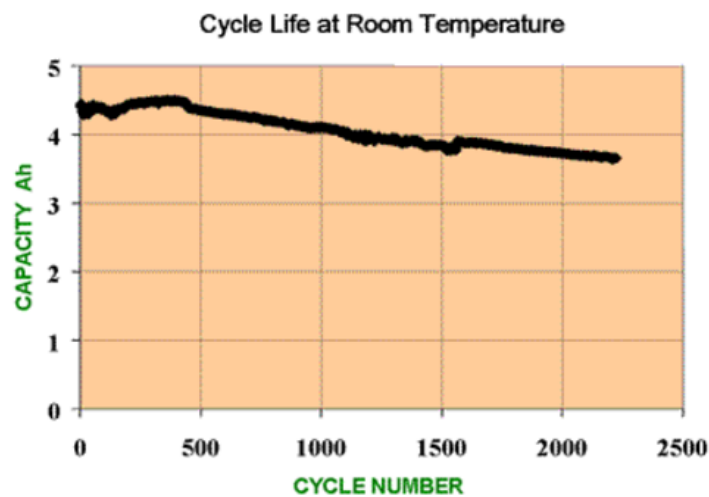


Figure 3.7 Degradation of battery capacity [37]

However, for a certain time of the life, delivered capacity varies depending on charge/discharge current and ambient temperature. The higher temperature is the higher capacity is extracted while reversed correlation is observed with charge/discharge rate.

This can be explained for the fact that temperature helps chemical reaction more quickly, resulting in higher available energy while higher charge/discharge rates would not provide enough time for completing the reaction and moving of components to necessary positions, in turn, low energy is available. The curves in Figure 3.8 are taken from the tests of a Lithium-ion battery [38] to see the effects of ambient temperature and discharge rate on its capacity. It can be seen that, for the lithium-ion battery, the influence of the discharge rate is relatively smaller in comparison with the temperature.

Besides, the nonlinear relationship between discharge current and delivered capacity has been investigated by a German scientist with proposed Peukert's law which is represented in equation (3.3) for the lead-acid battery.

$$C = I^p \cdot t \quad (3.3)$$

where:

- C is capacity of battery at 1A discharge rate (Ah)
- I is actual discharge current (A)
- t is duration of discharge (h)
- p is the Peukert coefficient

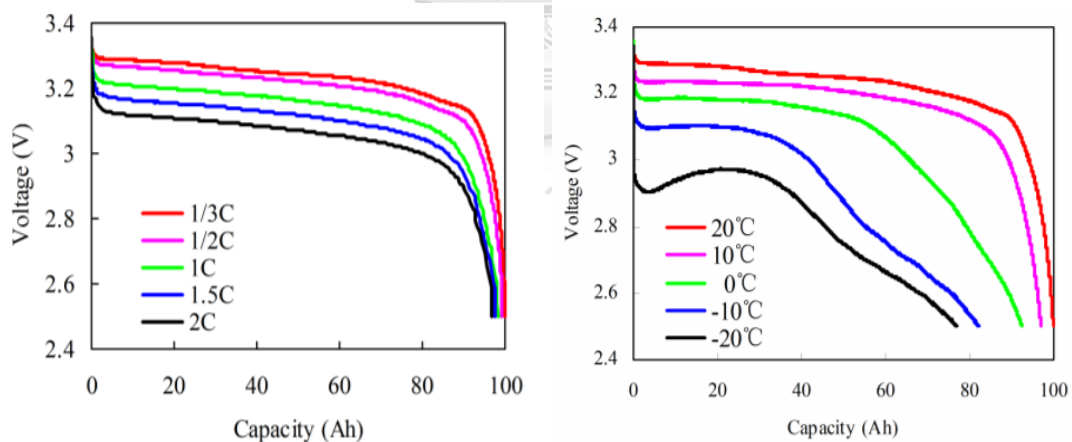


Figure 3.8 Effects of discharge rates and ambient temperatures on discharged capacity [38]

From the presented characteristic curves, they indicate that battery capacity is not a fixed number. It is influenced by many factors including aging status, operating conditions. Different battery technologies with their particular characteristics exhibit different influential curves.

❖ Conditioned characteristics of battery voltage

There are multiple parameters which influence voltage of a battery. Among these parameters, SOC of the battery is most important for voltage determination and vice versa. Relationships between voltage and SOC are different for charge and discharge processes represented in Figure 3.9.

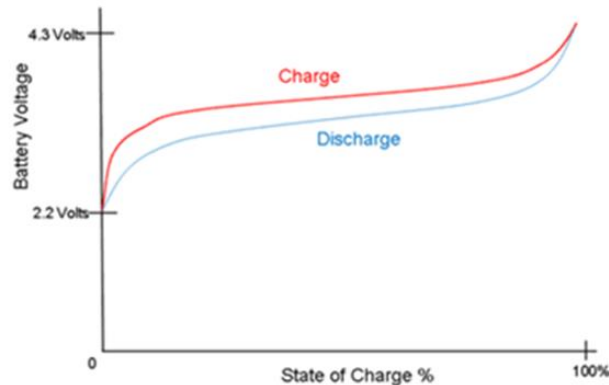


Figure 3.9 Charge/discharge profiles [37]

In addition, temperature also considerably affects the voltage of battery due to its effects on chemical reactions and internal resistance of the battery. In general, the battery voltage will be higher in cold weather and lower in hot weather. As a result, SOC estimation can be based on battery voltage with temperature correction.

❖ Conditioned characteristics of battery lifetime

Battery lifetime reflects the aging speed of battery which is affected by environmental conditions and how it is used. There are many factors that influence battery lifetime, even kill battery immediately such as operating in undersigned conditions. In this consideration, only general operating factors in operating condition are discussed for purpose of understanding aging models. For normal operation, battery goes to the end of life when performance criterion reaches a specified value. Aging degradation can be observed through the reduction in battery capacity or increase in internal resistance of the battery in which 80% initial capacity and 1.3 times or double initial internal resistance are criteria usually applied.

Among environmental factors, the temperature is the most influential factor because it plays an important role for chemical reactions inside the battery. Figure 3.10 gives an example illustrating the effect of temperature on the lifetime of a battery [39].

In this example, temperature increase causes a reduction in lifetime of the battery which is represented by cycle-life. The different temperature ranges are recommended by the manufacturer for different types of battery and it is certain that the effects are different.

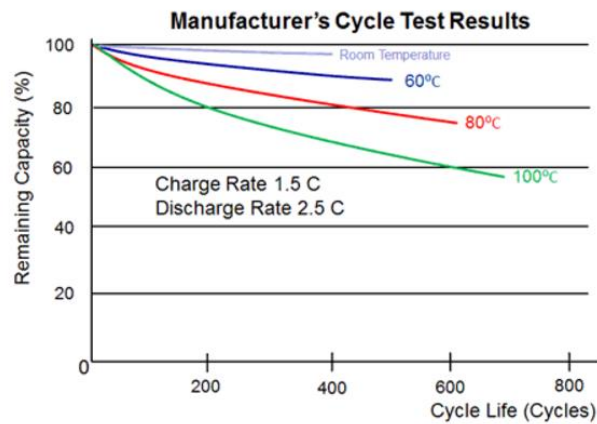


Figure 3.10 Effect of the temperature on battery lifetime [39]

Besides, without environmental consideration, how a battery is operated also affects its lifetime. Regarding operation factors, cycle-life is usually used. It measures how many cycles that battery can serve until the end of life. However, number of cycles varies according to how deep of discharge which is commonly provided in data sheet by battery manufacturer (illustrated in Figure 3.11). This is because battery life depends on the total energy throughput that the active chemicals can tolerate.

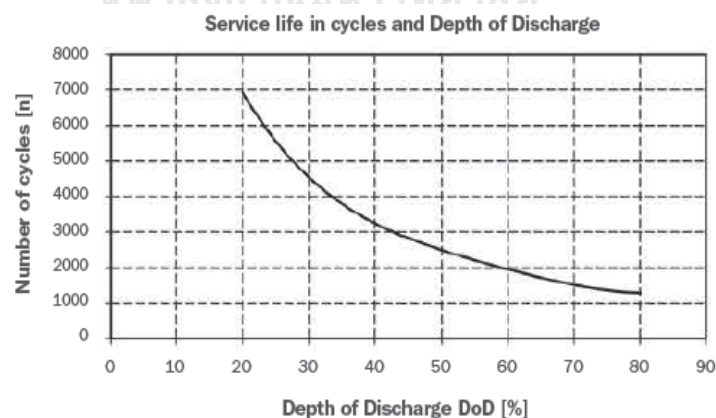


Figure 3.11 Relationship between number of cycles and DOD [15]

Similarly, charge and discharge rates are also factors affecting the effectiveness as well as the lifetime of a battery. From Figure 3.12, it can be seen that higher

charge/discharge rates cause quicker capacity losses. Consequently, battery reaches the end of life faster.

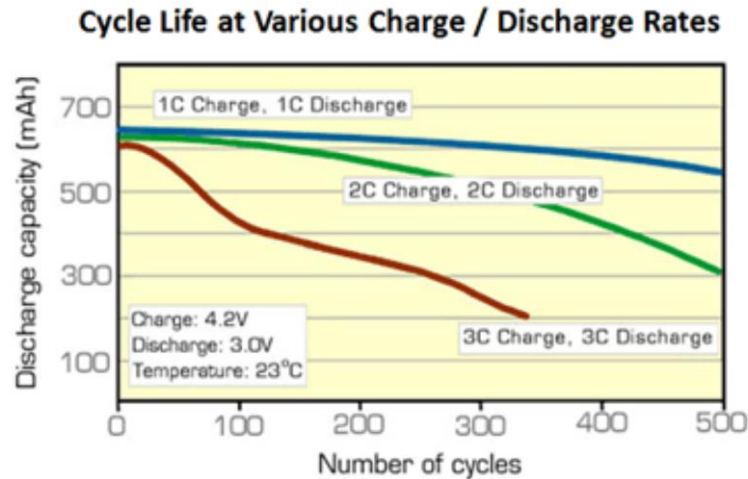


Figure 3.12 Effect of charge/discharge rates on the lifetime of a battery [39]

3.2.2 Battery modeling and lifetime estimation methods

This subsection gives an overview of battery modeling and reviews some lifetime estimation methods for economic assessment application.

3.2.2.1 Overview of battery modeling

Interaction of battery parameters makes it complex to model precisely operation parameters those are used for different applications. Hence, battery models are distinguished, basing on which characteristic they describe and the methods of modeling. Main classifications of battery modeling are summarized and demonstrated in Figure 3.13.

Basing on modeling methods, various specified methods for modeling battery can also be seen in the Figure 3.13. They comprise the methods, from very complex in spectroscopy and electrochemical technique model to very simple in statistical models. Each type of model requires a particular inputs and exhibits complexity its self. However, how precise of the model does not determine the range of application. For instance, electrochemical models perform very well characteristic of the battery but cannot be applied directly to other batteries. Whereas, statistical models are quite flexible and easy to modify for other batteries [40]. As a result, each application requires a rate of accuracy and flexibility of the model.

Three battery characteristics are mostly modeled for different modeling purposes. Performance models which include voltage and charge modeling focus on modeling operating parameters of the battery and usually are implemented in battery management system. Depending on how detailed of the outputs, performance models are different. While charge models focus on estimating SOC of the battery which is the most important parameter considered by general users such as laptops, electric vehicle and so forth, more detailed modeling can be seen in voltage models, in turn, more outputs can be released. On the other hand, lifetime models describe the aging process of the battery with consideration of influential factors on expected lifetime during operation to utilize for various application purposes. Lifetime estimation of a battery which is necessary for economic assessment of battery project is one of the important applications. It should be noted that lifetime model can be independent of performance models or integrated with them to make effort in modeling completely a battery system [41].

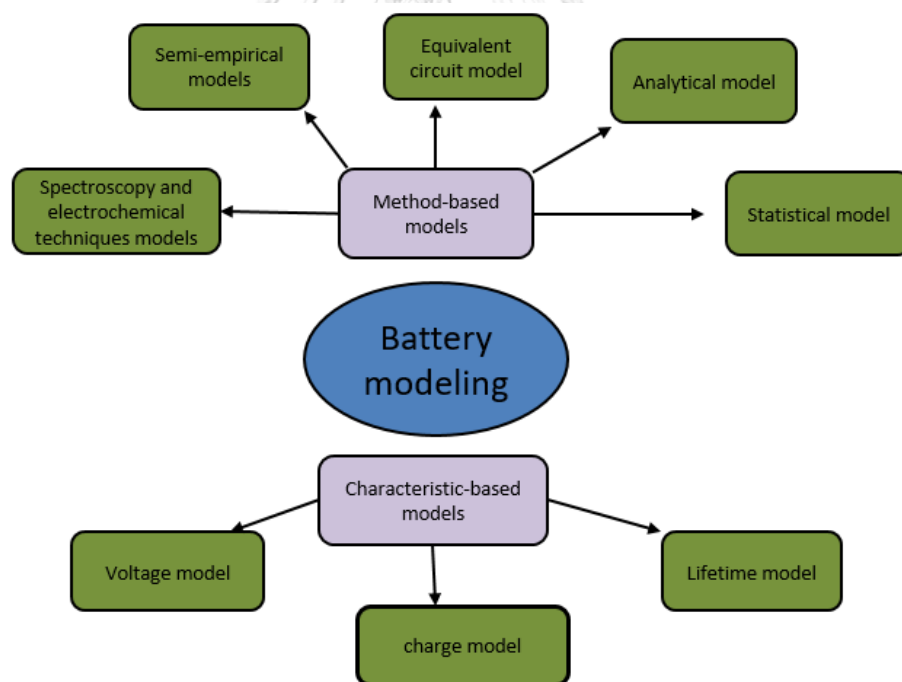


Figure 3.13 Battery modeling classification

3.2.2.2 Review of battery lifetime estimation methods

Accurate estimation of battery lifetime still is a challenge due to the complexity of the aging mechanism. With economic assessment of battery projects where any type

of batteries are taken into account as well as various operating strategies are considered. They make a challenge in lifetime estimation. Hence, in the literature, there are not few studies which use lifetime data provided by battery manufacturers with regardless of operating conditions. This makes the cost of battery very uncertain. Fully aware of flexibilities of the application, this section reviews some simple models those were applied to estimate the lifetime of the battery for economic assessment [19, 41, 42]. The approaches were based on the analysis of measured data provided in datasheet by the manufacturers or from experimental results. They include Ah-throughput counting, cycle counting, and linear aging degradation model.

❖ Ah-throughput counting based model

Ah-throughput is a major parameter reflecting the aging process of the battery. According to this model, it is assumed that each battery can tolerate a fixed amount of energy going through it before it dies. As a result, aging status and lifetime of the battery can be estimated based on measured energy going through battery during the operation cycle. This comes from the observed data of different operating conditions such as different depth of discharge. It indicates that Ah-throughputs calculated from the number of cycles multiplied by the discharged energy per cycle change not much. The Ah-throughputs calculated for different operating conditions are illustrated in Figure 3.14. For this model, Ah-throughput is assumed flat.

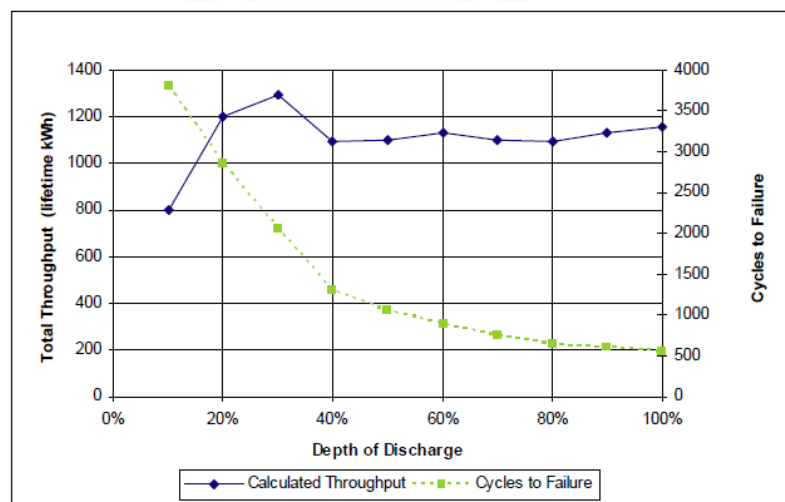


Figure 3.14 Ah curve calculated from data sheet [41]

With that assumption, Ah-throughput can be estimated by formula (3.4)

$$\text{Ah-throughput} = \frac{\sum_{i=1}^N \text{DOD}_i * \text{NC}_i * \text{C}_{\text{nom}}}{N} \quad (3.4)$$

Where

C_{nom} is the nominal capacity of battery

DOD_i is the depth of discharge corresponding operating condition i

NC_i is the number of cycles to failure corresponding operation condition i

N is the number of considered operation conditions

Throughput calculation can be represented either in Amp-hours or Watt-hours for more flexible use. It exhibits simplicity in modeling. Therefore, the extended Ah-throughput attempts to consider more effects of some other factors on aging process by introducing weighting factors in their calculation. The disadvantage of this model is that end of life criterion is predefined by manufacturer and datasheets are provided for specific conditions.

❖ Cycle counting based method

Similar to Ah-throughput counting, cycle counting based method also utilizes datasheet provided in Figure 3.14. However, spending lifetime in this model is calculated for each operation cycle with the consideration of the depth of discharge. Thus, the lifetime of the battery is calculated based on counting number of operation cycle or spending lifetime for each operation cycle which is popularly known as rain-flow counting algorithm.

For convenience, the number of cycles is represented as a function of DOD by a fitting function. The fitting function is an exponential function according to Levenberg–Marquardt method [42] represented in (3.5)

$$\text{NC} = a_1 + a_2 * e^{\alpha * \text{DOD}} + a_3 * e^{\beta * \text{DOD}} \quad (3.5)$$

Where

$a_1, a_2, a_3, \alpha, \beta$ are fitting constants

NC is number of cycles corresponding to given DOD

Spending lifetime for individual operation cycle can be represented as a fraction of its lifetime. Battery lifetime in a year is estimated as follows [42]

$$T = \frac{1}{\sum \text{NC}_i^{-1}} * \frac{T_s}{T_{\text{yr}}} \quad (3.6)$$

Where

T is estimated lifetime of the battery

NC_i is number of cycles for a given DOD i

T_s is simulation time

T_{yr} represents 1 year

This model overcomes the flattening of Ah-throughput model across depths of discharge. However, the users can not define the end of life criterion for their model. For instant, the users may expect a longer life based on reducing EOL criterion, for example, from 80% to 60% of nominal capacity but no data is provided for that assumption.

❖ Linear aging degradation model

Aging process of battery reflects the degradation of battery capacity during its operation. Depending on operation conditions, observed capacities lie in the capacity space with a downward trend over operating cycles which is illustrated in Figure 3.15. To seek a simplicity, the capacity loss is assumed linear according to state of charge represented by linear aging coefficient [16, 19, 20]. This model was primarily proposed in [19] based on the experimental results conducted by INES institute which were carried out for different battery technologies [43].

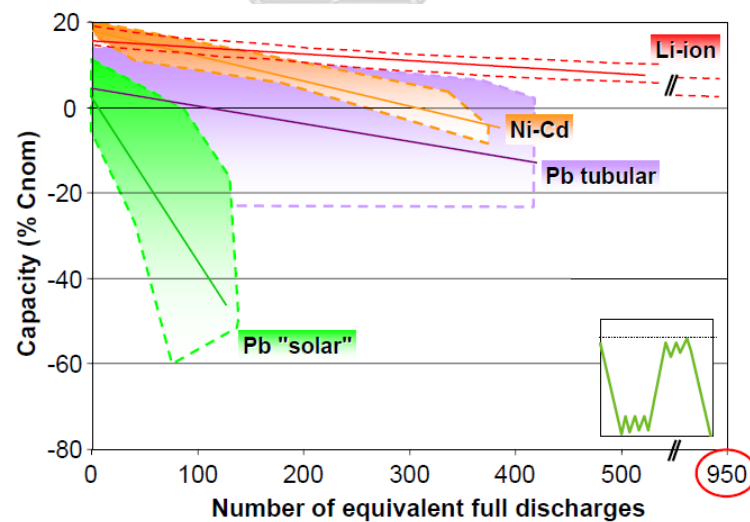


Figure 3.15 Capacity loss due to aging degradation [43]

According to this model, if aging process is represented only through discharge process. The capacity loss is calculated for that period presented in the formula (3.7).

$$\Delta C = Z \cdot C_{B,nom} \cdot (SOC_{bf} - SOC_{af}) \quad (3.7)$$

Where

Z is the linear aging coefficient

SOC_{bf}	is state of charge of the BESS before discharge
SOC_{af}	is state of charge of the BESS after discharge
ΔC	is capacity loss during the discharge process (kWh)
$C_{B,nom}$	is the nominal capacity of battery (kWh)

Capacity-loss can be measured either in Ah or Wh. The advantage of this model is modeling dynamic conversion of battery capacity along the life. Lifetime can be estimated until EOL criterion is met. Normally, 80% of nominal capacity is used as the EOL criterion. However, in practice battery might still continue working. This model allows the user to be more flexible in EOL definition.



CHAPTER 4

COST MINIMIZATION METHODS OF BESS FOR VOLTAGE MANAGEMENT IN LV NETWORK

As previously specified, BESS is investigated in this dissertation in order to manage network voltages within acceptable limits. For that purpose, utilities may expect to know optimum resolutions as well as the minimum expense they need to pay for their resolutions. Therefore, wholly optimum strategies which are applied for long-term planning and operation planning are presented in this chapter. First, a formulation for the minimum cost of BESS is formulated in conjunction with the operation constraints of BESS and network voltages through an optimization problem. Then, the optimization problem is developed for two optimum strategies of BESS. Consequently, siting and sizing of BESSs are formulated in Section 4.2 while optimum scheduling is considered in Section 4.3. Main ideas of the proposed methods are demonstrated in Figure 4.1 with convention of power flows in the network is specified in Figure 4.2

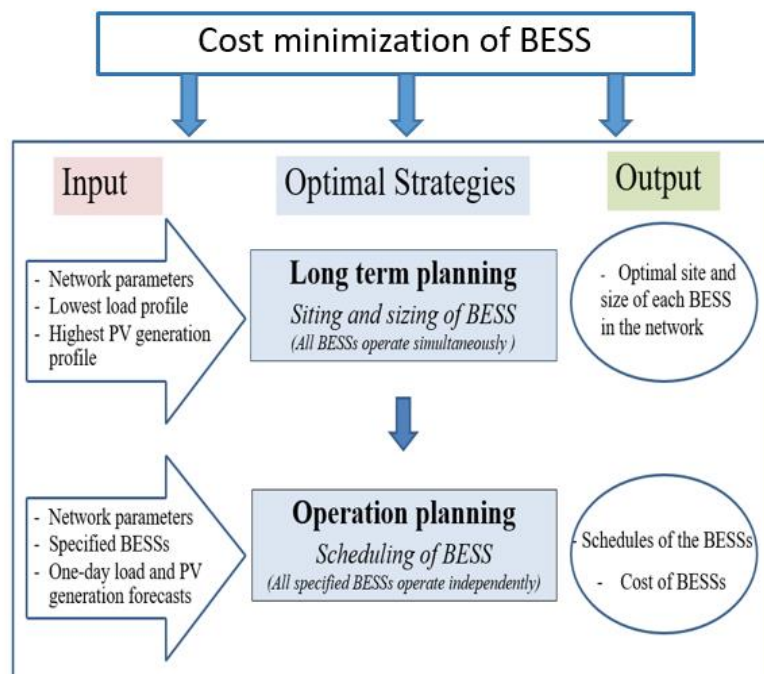


Figure 4.1 Contents of the proposed methods

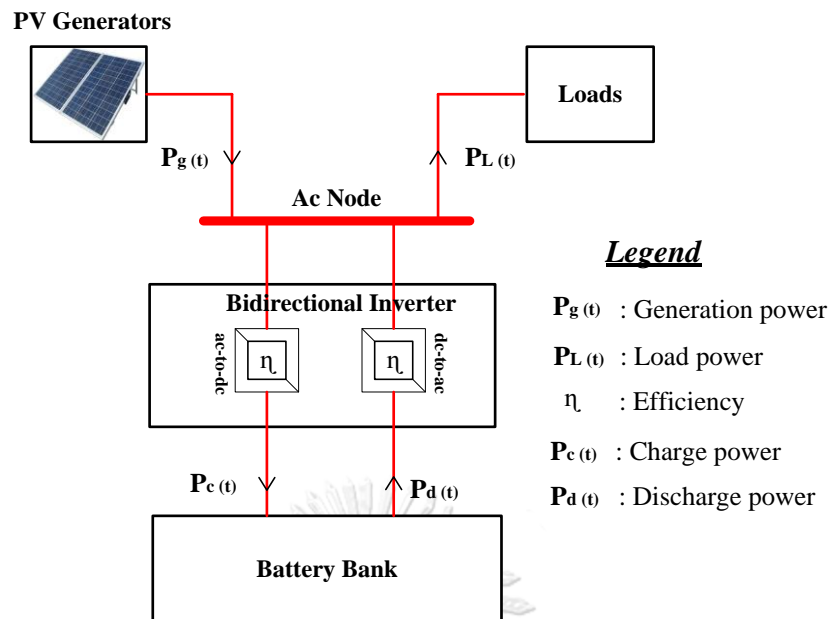


Figure 4.2 Convention of power flows in the network

4.1 Cost minimization of BESS

This section presents the main idea for cost minimization of a BESS with consideration of the aging degradation. The aging model is inherited from the reference [19] which is formulated in this chapter together with other specified expenses and operation requirements for purpose of economic evaluation of the BESS. In addition, in order to manage voltage of the network within acceptable range, the minimum cost of the BESS is obtained based on an optimal schedule of the BESS as well as its size, simultaneously satisfying both voltage requirement and operating conditions of the BESS.

4.1.1 Objective function

Cost of the BESS for duration D represented by objective function F can be separated into 2 categories as shown in (4.1). The first element is the cost for capacity losses by aging process during operation of the BESS while the second element is the additional cost that is proportional to the installed capacity of the BESS in the considered duration D . In this dissertation, the cost for accessing bank loan through interest rate and the cost for operation and maintenance (O&M) of the BESS are taken

into account as the additional cost. As a result, the additional cost per unit investment capacity for a day can be calculated in (4.2).

$$\underbrace{\text{Minimize } F}_{P_d(t), P_c(t), C(t), E(t), C_{B,nom}} = \lambda \cdot (\sum_{t=1}^T \Delta C_{(t)}) + \beta \cdot D \cdot C_{B,nom} \quad (4.1)$$

Where

λ is cost per unit capacity loss of the BESS (\$/kWh)

$\Delta C_{(t)}$ is capacity loss in t^{th} time interval (kWh)

(t) is time index indicating t^{th} time interval

β is additional cost per unit investment capacity of the BESS and duration (\$/kWh.day)

$C_{B,nom}$ is the nominal capacity of the BESS (kWh)

T is number of time intervals in considered duration D

D is operation duration (day)

Capacity of a battery reduces during its operating time. Life-span of the BESS is determined as the time period from the first use until the usable capacity of the battery reaches a specific level defined as the end of life, normally 80% of the nominal capacity for lead acid [42, 44]. As a result, cost of BESS per capacity-loss can be determined in (4.3) while aging phenomenon is based on the model in references [16, 19, 20] with the assumption that it only occurs during discharge processes. Therefore, capacity losses are given in (4.4) and in simplified formulas (4.5) and (4.6) with capacity loss neglected between two consecutive intervals.

$$\beta = \frac{(r + OM) \cdot C_0}{365} \quad (4.2)$$

$$\lambda = \frac{\text{Investment cost}}{\text{Capacity losses}} = \frac{C_0 \cdot C_{B,nom}}{20\% \cdot C_{B,nom}} \quad (4.3)$$

$$\Delta C_{(t)} = Z \cdot C_{B,nom} \cdot (\text{SOC}_{(t-1)} - \text{SOC}_{(t)}) \quad (4.4)$$

$$\approx Z \cdot C_{B,nom} \cdot \frac{E_{(t-1)} - E_{(t)}}{C_{(t-1)}} \quad (4.5)$$

$$\approx Z \cdot C_{B,nom} \cdot \frac{P_{d(t)} \cdot \Delta t}{C_{(t-1)}} \quad (4.6)$$

Where

C_0 is cost per unit investment capacity of the BESS (\$/kWh)

r is annual interest rate

OM is annual O&M rate of the BESS

- Z is linear aging coefficient
 $SOC_{(t)}$ is state of charge of the BESS in t^{th} time interval
 $E_{(t)}$ is available energy in the BESS in t^{th} time interval (kWh)
 $C_{(t)}$ represents capacity of BESS in t^{th} time interval (kWh)
 $P_{d(t)}$ is discharge power of the BESS in t^{th} time interval (kW)
 $P_{c(t)}$ is charge power of the BESS in t^{th} time interval (kW)
 Δt is time interval (h)

4.1.2 Constraints

The following constraints are taken into account to obtain the optimum values of the optimization problem. Those constraints need to be satisfied simultaneously the operating conditions of the BESS and voltage requirement of the grid.

4.1.2.1 Operating conditions of the BESS

❖ Dynamics of BESS

Cumulative energy in BESS is defined as a sum of energy of the previous time and added energy in the current interval.

$$E_{(t)} = E_{(t-1)} + P_{c(t)} \cdot \Delta t - P_{d(t)} \cdot \Delta t \quad (4.7)$$

❖ Charge and discharge status

Charge and discharge processes are not operated simultaneously.

$$P_{c(t)} \cdot P_{d(t)} = 0 \quad (4.8)$$

❖ Rates of charge and discharge

Maximum charge and discharge rates are provided by manufactures or can be calculated based on the minimum charge and discharge times. Since the capacity of battery degrades along the battery operation time, charge and discharge rates reduce correspondingly. Therefore, the selected battery must guarantee the requirement of charge and discharge powers until the end of life (80% of the nominal capacity).

$$P_{c(t)} \leq \frac{80\% \cdot C_{B,nom}}{T_c} \quad (4.9)$$

$$P_{d(t)} \leq \frac{80\% \cdot C_{B,nom}}{T_d} \quad (4.10)$$

Where

- T_c is minimum charge time

T_d is minimum discharge time

❖ State of charge (SOC)

Cycle-Life of a BESS is considerably influenced by how deep of discharge. In addition, a battery may be damaged by over-charge or over-discharge. Thus, SOC of the BESS should be operated within a designed range.

$$SOC_{\min} \leq SOC_{(t)} \leq SOC_{\max} \quad (4.11)$$

Where

SOC_{\min} is minimum state of charge that the BESS is allowed to operate

SOC_{\max} is maximum state of charge that the BESS is allowed to operate

SOC of the BESS at time interval t is given in the formula (4.12)

$$SOC_{(t)} = \frac{E_{(t)}}{C_{(t)}} \cdot 100\% \quad (4.12)$$

❖ Capacity loss of the BESS due to the aging process

According to the aging model in references [16, 19, 20], capacity losses in t^{th} time interval is formulated in (4.13)

$$\Delta C_{(t)} = Z \cdot C_{B,\text{nom}} \cdot \frac{P_{d(t)} \cdot \Delta t}{C_{(t-1)}} \quad (4.13)$$

Hence, usable capacity in t^{th} time interval can be determined by usable capacity at the previous time interval and the capacity loss in the current time interval.

$$C_{(t)} = C_{(t-1)} - \Delta C_{(t)} \quad (4.14)$$

And, nominal capacity of the BESS is obtained in (4.15).

$$C_{B,\text{nom}} = C_{(0)} = C_{(1)} + \Delta C_{(1)} \quad (4.15)$$

4.1.2.2 Voltage requirement

Voltages of electrical network must be maintained within acceptable limits.

$$V_{\min} \leq V_{(t)}^k \leq V_{\max} \quad (4.16)$$

Where

k is index indicates k node

$V_{(t)}^k$ is voltage at node k and in t^{th} time interval (pu)

V_{\min} and V_{\max} are the minimum and maximum acceptable voltages (pu)

It is assumed that load and generation profiles are known. Voltages of the network are state variables which can be represented as a function of charge and

discharge powers as shown in (4.17). It is noted that efficiencies of BESS for charge and discharge processes are assumed equal and also considered in the function through a unique parameter (η). Furthermore, in this dissertation, Newton-Raphson method is used to check voltage condition in each iteration of the optimization problem. Load flow calculation based on Newton-Raphson method is presented in Appendix A.

$$V_{(t)}^k = f(P_{c(t)}, P_{d(t)}) \quad (4.17)$$

4.2 Siting and sizing strategy of BESSs

There is a fact that voltage varies across locations. Consequently, effectiveness of a BESS is different depending on its location. Therefore, siting and sizing of BESSs, the work in long-term planning also play an important role to minimize BESSs cost. As a result, cost minimization of BESSs is formulated in this section to find the optimal locations and sizes of the BESSs, simultaneously satisfying operating conditions of the BESSs and voltage requirement of the network. To determine the optimal locations and sizes of BESS within the network, all considered locations for battery installation are treated fairly with the same conditions, i.e.:

- Specifications of batteries are identical.
- BESSs operate simultaneously and keep the same contribution percentage during charge/discharge processes.

Variable a^k is introduced to represent optimal contribution-percentage of BESS at node k in comparison with the total BESSs through charge/discharge processes. It reflects voltage regulation effectiveness of the BESS at node k . Since those contribution percentages keep unchanged over time intervals, charge/discharge powers are, therefore, proportional to their size. Consequently, a^k is also the optimal size-percentage of the BESS at node k defined in (4.18) and relevant constraints are in (4.19) and (4.20).

$$a^k = \frac{P_{d(t)}^k}{P_{d(t)}^{\Sigma}} \cdot 100\% = \frac{P_{c(t)}^k}{P_{c(t)}^{\Sigma}} \cdot 100\% = \frac{C_{B,nom}^k}{C_{B,nom}^{\Sigma}} \cdot 100\% \quad (4.18)$$

$$C_{B,nom}^{\Sigma} = \sum_{k=1}^n C_{B,nom}^k \quad (4.19)$$

$$\sum_{k=1}^n a^k = 100\% \quad (4.20)$$

Where

$P_{c(t)}^k, P_{d(t)}^k$ are charge power, discharge power of the BESS at node k in t^{th} time interval (kW)

$P_{c(t)}^\Sigma, P_{d(t)}^\Sigma$ are total charge power, total discharge power of the BESSs in t^{th} time interval (kW)

$C_{B,nom}^k, C_{B,nom}^\Sigma$ are nominal capacity of the BESS at node k and total nominal capacity of the BESSs (kWh).

N is number of considered locations for BESS installation in the network

Furthermore, to solve the problem easier, the number of variables should be lessened. Therefore, the optimization problem is formulated with variables representing the operation parameters of total BESSs and variables representing their contributions (a^k). The main content of cost minimization of BESSs is based on the formulation in Section 4.1. The optimization problem becomes as follows.

4.2.1 Objective function

Similarly, cost of total BESSs are taken into account, including the aging cost and the additional cost of the BESSs formulated in (4.21)

$$\underbrace{\text{Minimize } F1}_{P_{d(t)}^\Sigma, P_{c(t)}^\Sigma, C_{(t)}^\Sigma, E_{(t)}^\Sigma, C_{B,nom}^\Sigma, a^k} = \sum_{t=1}^T \lambda \cdot \Delta C_{(t)}^\Sigma + \beta \cdot D \cdot C_{B,nom}^\Sigma \quad (4.21)$$

Where

$\Delta C_{(t)}^\Sigma$ is capacity loss of total BESSs in t^{th} time interval (kWh)

4.2.2 Constraints

The main constraints comprise the operating conditions of the BESSs, voltage requirement of the network and constraint regarding the new variables which have introduced and defined in (4.18) for sitting and sizing strategy.

4.2.2.1 Operating conditions of the BESSs

Operating conditions of the BESSs are summarized in Table 4.1 with variables representing operation parameters of total BESSs denoted by the Σ symbol.

With

$E_{(t)}^\Sigma$ is available energy of total BESSs in t^{th} time interval (kWh)

$C_{(t)}^\Sigma$ is capacity of total BESSs in t^{th} time interval (kWh)

$SOC_{(t)}^{\Sigma}$ is state of charge of total BESSs in t^{th} time interval

Table 4.1 Operating conditions of BESSs

Meaning	Operating Conditions
Dynamics of BESSs	$E_{(t)}^{\Sigma} = E_{(t-1)}^{\Sigma} + P_{c(t)}^{\Sigma} \cdot \Delta t - P_{d(t)}^{\Sigma} \cdot \Delta t$ (4.22)
Charge and discharge status	$P_{c(t)}^{\Sigma} \cdot P_{d(t)}^{\Sigma} = 0$ (4.23)
Rates of charge and discharge	$P_{c(t)}^{\Sigma} \leq \frac{80\% \cdot C_{B,nom}^{\Sigma}}{T_c}$ (4.24)
	$P_{d(t)}^{\Sigma} \leq \frac{80\% \cdot C_{B,nom}^{\Sigma}}{T_d}$ (4.25)
State of charge (SOC)	$SOC_{min} \leq SOC_{(t)}^{\Sigma} \leq SOC_{max}$ (4.26)
	$SOC_{(t)}^{\Sigma} = \frac{E_{(t)}^{\Sigma}}{C_{(t)}^{\Sigma}} \cdot 100\%$ (4.27)
Capacity loss of BESSs due to the aging process	$\Delta C_{(t)}^{\Sigma} = Z \cdot C_{B,nom}^{\Sigma} \cdot \frac{P_{d(t)}^{\Sigma} \cdot \Delta t}{C_{(t-1)}^{\Sigma}}$ (4.28)
	$C_{(t)}^{\Sigma} = C_{(t-1)}^{\Sigma} - \Delta C_{(t)}^{\Sigma}$ (4.29)
	$C_{B,nom}^{\Sigma} = C_{(0)}^{\Sigma} = C_{(1)}^{\Sigma} + \Delta C_{(1)}^{\Sigma}$ (4.30)

4.2.2.2 Voltage requirement

Voltages of the network must be maintained within acceptable range.

$$V_{min} \leq V_{(t)}^k \leq V_{max} \quad (4.31)$$

Charge and discharge powers of each BESS are directly proportional to total charge and discharge powers. Therefore, voltages, in this case, are represented as a function of total charge and discharge powers and the contribution percentages with consideration of the efficiency of BESSs.

$$V_{(t)}^k = f(\vec{a}^k, P_{c(t)}^{\Sigma}, P_{d(t)}^{\Sigma}) \quad (4.32)$$

Where

N^k is set of considered locations for BESS installation

4.2.2.3 Assumption constraint

Constraint (4.33) is deduced from the definitions of the variables.

$$\sum_{k=1}^n a^k = 100\% \quad (4.33)$$

4.3 Scheduling of the installed BESSs

After locations and sizes of BESSs are specified with the proposed method in Section 4.2. Now, they are known parameters. Optimum strategy of operation planning is developed in this section, based on one-day load and PV generation forecast. Schedules of the BESSs are derived independently for each BESS to obtain their minimum total cost with the assumption that locations, sizes as well as the aging status of the installed BESSs are given parameters.

The main content of cost minimization of total BESSs is similar to previous formulations. Accordingly, cost minimization of total BESSs is formulated in this section to find the optimal schedules of the installed BESSs, simultaneously satisfying operating conditions of the BESSs and voltage requirement of the network. The difference is that the installed BESSs can operate independently to obtain the minimum total cost. Therefore, operation condition constraints are applied for each BESS but the objective function is the sum of their cost. Simultaneously, number of variables increases significantly according to number of installed BESSs. The optimization problem becomes as follows.

4.3.1 Objective function

The objective function is the total cost of the installed BESSs

$$\underbrace{\text{Minimize } F2}_{P_{d(t)}^k, P_{c(t)}^k, C_{(t)}^k, E_{(t)}^k, C_{B,nom}^k} = \sum_k^{\Omega^k} (\sum_{t=1}^T \lambda \cdot \Delta C_{(t)}^k + \beta \cdot D \cdot C_{B,nom}^k) \quad (4.34)$$

Where

$\Delta C_{(t)}^k$ is capacity loss of the BESS at node k in t^{th} time interval (kWh)

$C_{B,nom}^k$ is the nominal capacity of the BESS at node k (kWh)

Ω^k is set of the installed BESSs

Although the second term in the objective function is predetermined and does not play a role in the cost minimization, it is still taken into account to represent a part of total cost of BESSs in duration D .

4.3.2 Constraints

Similarly, the constraints that are taken into account are operating conditions of the installed BESSs and voltage requirement of the network.

4.3.2.1 Operating conditions of the installed BESSs

Operating conditions must be satisfied independently for all installed BESSs. Those constraints are summarized in Table 4.2 and represented for BESS installed at node k .

Table 4.2 Operating conditions of the installed BESSs represented for BESS at node k .

Meaning	Operating Conditions of BESS installed at node k
<i>Dynamics of BESS</i>	$E_{(t)}^k = E_{(t-1)}^k + P_{c(t)}^k \cdot \Delta t - P_{d(t)}^k \cdot \Delta t \quad (4.35)$
<i>Charge and discharge status</i>	$P_{c(t)}^k \cdot P_{d(t)}^k = 0 \quad (4.36)$
<i>Rates of charge and discharge</i>	$P_{(c)}^k \leq \frac{80\% \cdot C_{B,nom}^k}{T_c} \quad (4.37)$
	$P_{d(t)}^k \leq \frac{80\% \cdot C_{B,nom}^k}{T_d} \quad (4.38)$
<i>State of charge (SOC)</i>	$SOC_{min} \leq SOC_{(t)}^k \leq SOC_{max} \quad (4.39)$
	$SOC_{(t)}^k = \frac{E_{(t)}^k}{C_{(t)}^k} \cdot 100\% \quad (4.40)$
<i>Capacity loss of BESS due to the aging process</i>	$\Delta C_{(t)}^k = Z \cdot C_{B,nom}^k \cdot \frac{P_{d(t)}^k \cdot \Delta t}{C_{(t-1)}^k} \quad (4.41)$
	$C_{(t)}^k = C_{(t-1)}^k - \Delta C_{(t)}^k \quad (4.42)$
	$C_{int}^k = C_{(1)}^k + \Delta C_{(1)}^k \quad (4.43)$

Where

$E_{(t)}^k$ is available energy of the BESS at node k in t^{th} time interval (kWh)

$\text{SOC}_{(t)}^k$ is state of charge of the BESS at node k in t^{th} time interval

$C_{(t)}^k$ is capacity of the BESS at node k in t^{th} time interval (kWh)

C_{int}^k is initial capacity of the BESS at node k (kWh)

4.3.2.2 Voltage requirement

Voltages of the electrical network must be maintained within acceptable limits.

$$V_{\min} \leq V_{(t)}^k \leq V_{\max} \quad (4.44)$$

With forecasted load and PV generation, voltages of the network can be represented as a function of charge and discharge powers of the installed BESSs

$$V_{(t)}^k = f(\overbrace{P_{c(t)}^k, P_{d(t)}^k}^{\Omega^k}) \quad (4.45)$$

CHAPTER 5

SIMULATION NETWORK

This chapter gives the detailed descriptions about the network for simulation. Some notices about the scenarios selected for simulation are also specified.

5.1 Network configuration

The simplified networks for simulation are derived from the typical characteristics of low-voltage networks in the jurisdiction of MEA (Metropolitan Electricity Authority), Thailand [45]. Most of LV networks are still overhead lines while some of them are underground cables which concentrate in the center of Bangkok. Typical conductors of main feeders and laterals are 400AW70OH3 and MLINK3, respectively. Network for simulation is depicted in Figure 5.1. Length of the main feeder is 3 kilometers. Nine laterals come from the main feeder supplying electricity to groups of households. The details of the electrical network can be found in Table 5.1.

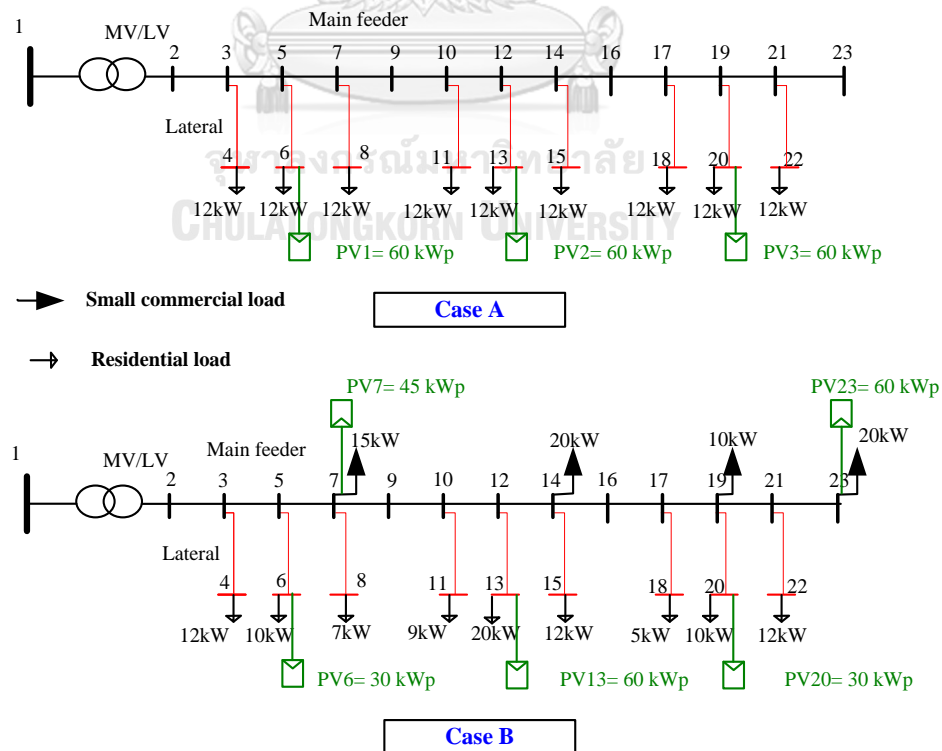


Figure 5.1 Configurations of the simulated network

Table 5.1 Network parameters in per unit with $S_{base} = 100\text{MVA}$, $U_b = 380\text{V}$.

Branch	From node	To node	R (pu)	X (pu)	B (pu)
1	1	2	0.47778	16.65982	0
2	2	3	10.45833	12.59375	0
3	3	4	27.07406	3.59031	0
4	3	5	20.91667	25.18750	0
5	5	6	27.07406	3.59031	0
6	5	7	20.91667	25.18750	0
7	7	8	27.07406	3.59031	0
8	7	9	10.45833	12.59375	0
9	9	10	10.45833	12.59375	0
10	10	11	27.07406	3.59031	0
11	10	12	20.91667	25.18750	0
12	12	13	27.07406	3.59031	0
13	12	14	20.91667	25.18750	0
14	14	15	27.07406	3.59031	0
15	14	16	10.45833	12.59375	0
16	16	17	10.45833	12.59375	0
17	17	18	27.07406	3.59031	0
18	17	19	20.91667	25.18750	0
19	19	20	27.07406	3.59031	0
20	19	21	20.91667	25.18750	0
21	21	22	27.07406	3.59031	0
22	21	23	10.45833	12.59375	0

In order to demonstrate fully usefulness of the proposed methods, the configurations of the network are investigated with two cases as seen in Figure 5.1. The two cases, i.e. Case A and Case B, share the same network parameters but different distributions of load and PV generation. While loads and PV rooftops in Case A distribute evenly along the feeder, the ones in Case B are random, additionally containing small commercial loads. For the sake of simplicity, load types and PV generation at household are assumed to share the same power factor and line losses are

neglected between households and connected nodes. Loads and PV generations for Case A and Case B are respectively summarized in Tables 5.2 and 5.3.

Table 5.2 Loads and PV generations of Case A

Node	Load		PV generation	
	Size (kW)	Power factor	Size (kWp)	Power factor
Node 4	12	0.98		
Node 6	12	0.98	60	1
Node 8	12	0.98		
Node 11	12	0.98		
Node 13	12	0.98	60	1
Node 15	12	0.98		
Node 18	12	0.98		
Node 20	12	0.98	60	1
Node 22	12	0.98		

Table 5.3 Loads and PV generations of Case B

Node	Load		PV generation	
	Size (kW)	Power factor	Size (kWp)	Power factor
Node 4	12	0.98		
Node 6	10	0.98	30	1
Node 7	15	0.9	45	1
Node 8	7	0.98		
Node 11	9	0.98		
Node 13	20	0.98	60	1
Node 14	20	0.9		
Node 15	12	0.98		
Node 18	5	0.98		
Node 19	10	0.9		
Node 20	10	0.98	30	1
Node 22	12	0.98		
Node 23	20	0.9	60	1

5.2 Load and PV generation profiles

Voltage problem regarding PV generation occurs with the daily cycle. Therefore, one-day length with a time interval of one hour is selected for the simulations to demonstrate the effectiveness of the proposed methods. Furthermore, simulation also intends to find the size of the BESSs, therefore the worst day is selected for simulation. The worst day is considered for whole year data with the maximum mismatch between load and PV generation profiles. In this dissertation, load profiles in 2015 database of MEA [46] and PV generation profiles recorded in the year 2013 of the 1.2 kWp PV rooftop installed at Engineering building 4, Chulalongkorn University, Thailand [47] are selected and analyzed for simulation. Based on the recorded database of MEA, although Bangkok has three main seasons, namely summer season, rainy season and winter season, the load profiles are nearly similar along the year due to narrow temperature range. The lowest load profile coupled with the highest PV generation profile is selected as the worst case for siting and sizing of BESS. On the other hand, to demonstrate the effectiveness of the proposed method in operation planning of BESS, certain load and PV generation profiles can be used for simulation as the forecasted data. However, the worst case is selected again for the simulation to make a comparison with the results obtained from the siting and sizing strategy. Load and PV generation profiles of the households are shown in Fig. 5.2 with the size of 1 kWp. With this profiles, they are scaled up to designed sizes as shown in Figure 5.1.

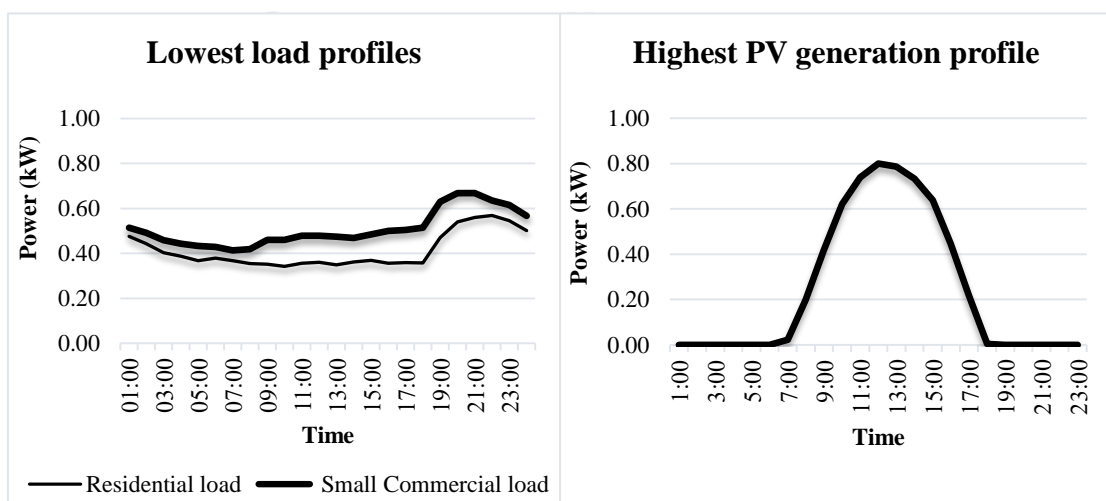


Figure 5.2 Load and PV generation profiles of the worst case.

Table 5.4 Typical load profiles for one-month cost evaluation application of BESS

Typical loads						
	Commercial load_1kW			Residential load_1kW		
Time	Workingday	Saturday	Sunday	Workingday	Saturday	Sunday
01:00	0.590722	0.583354	0.578821	0.567400	0.575058	0.577552
02:00	0.550757	0.544458	0.543302	0.517683	0.520510	0.530838
03:00	0.518581	0.512348	0.511606	0.485602	0.483172	0.489029
04:00	0.494254	0.488828	0.486392	0.449757	0.453363	0.457660
05:00	0.482911	0.473878	0.468378	0.451246	0.448523	0.434238
06:00	0.483393	0.465605	0.452904	0.429308	0.433750	0.414370
07:00	0.491673	0.452500	0.429177	0.405413	0.400636	0.385259
08:00	0.592250	0.498117	0.450748	0.371429	0.399516	0.378255
09:00	0.708608	0.594826	0.489358	0.402140	0.414121	0.388370
10:00	0.747984	0.638407	0.499670	0.390086	0.407371	0.381226
11:00	0.771828	0.665121	0.508346	0.393783	0.414412	0.394834
12:00	0.763450	0.661744	0.506284	0.405013	0.426910	0.412282
13:00	0.701955	0.599406	0.505070	0.384803	0.420867	0.419630
14:00	0.791714	0.659413	0.515298	0.419710	0.432549	0.429265
15:00	0.800542	0.668845	0.522657	0.422936	0.437503	0.434742
16:00	0.790592	0.662402	0.529494	0.416200	0.427534	0.432611
17:00	0.762527	0.627037	0.530584	0.422285	0.410266	0.420578
18:00	0.663190	0.571438	0.539873	0.395652	0.391204	0.418399
19:00	0.705288	0.633594	0.640463	0.487830	0.472527	0.513044
20:00	0.729928	0.672302	0.681602	0.586741	0.558145	0.592708
21:00	0.739441	0.681468	0.705019	0.678524	0.616596	0.674307
22:00	0.717860	0.674171	0.690433	0.686884	0.674829	0.703273
23:00	0.689571	0.659156	0.675129	0.671775	0.671063	0.682213
24:00	0.642226	0.624843	0.635467	0.624965	0.634369	0.633943

For purpose of one-month cost evaluation application of the BESSs, typical load and generation profiles are selected for simulation. While typical load profiles are

derived by averaging data in one year categorized into working-day, Saturday and Sunday for each load type, namely, Com-WorkingDay, Com-Saturday, Com-Sunday, Res-WorkingDay, Res-Saturday and Res-Sunday, summarized in Table 5.4, typical generation profile is averaged for the whole year, namely, Typ-Generation which is represented in Figure 5.3 in conjunction with typical load profiles.

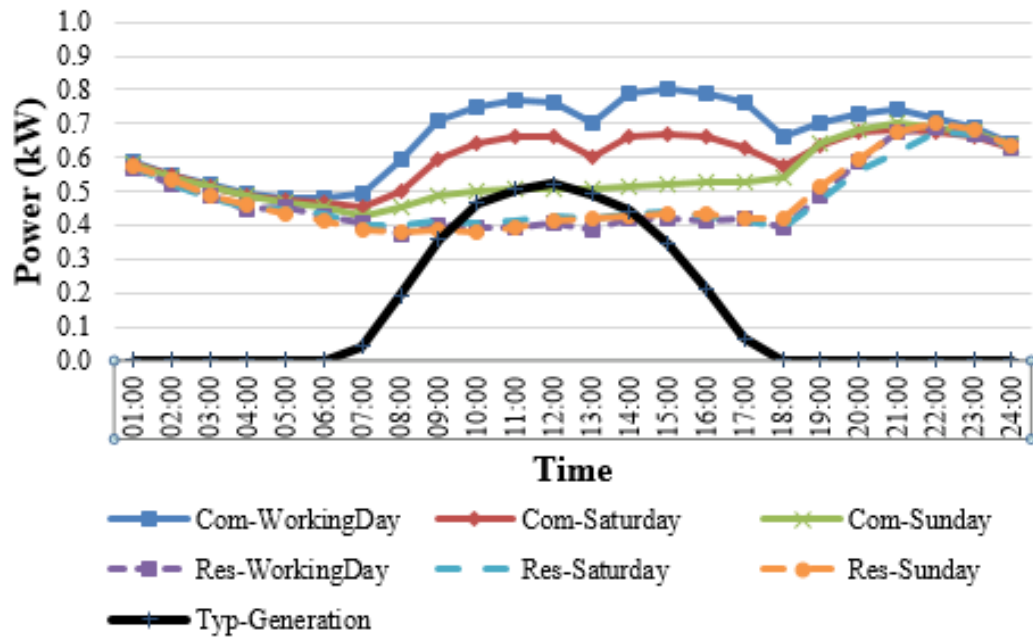


Figure 5.3 Load and PV generation profiles for one-month cost evaluation of BESS.

5.3 Technical and economic parameters for BESS simulation

Lead acid battery with the linear aging coefficient (Z) of $3.10 \cdot 10^{-4}$ [16, 19, 20] is selected for most simulations since it is cheapest and mature technologies in comparison with others for stationary storage application. Basing on technical characteristics of LA which were described in Chapter 3 and looking on LA market [48-50], initial assumptions for simulation with technical and economic parameters of BESSs and electric grid are provided in Table 5.5. It should be noted that price of BESS (600\$/kWh) includes the price of LA battery (200\$/kWh) and 400\$/kWh for the converter and other components.

In addition, lithium-ion battery is assessed as a very promising option for utility application due to high charge/discharge rate and long cycle-life although its price is still much higher than LA battery. This dissertation also makes a comparison between two options for the simulation cases. Their technical and economic parameters are

presented in Table 5.6 [16, 19, 20, 48-50]. Those are only typical values since prices of battery, as well as their technical characteristics, vary quite largely across different battery options and suppliers. For more exactly, consultancy should be made for a specific battery project as well as provided by a specific supplier. It is also noted that linear aging coefficient of the lithium-ion battery was not directly provided by the authors in reference [19] who proposed linear aging degradation model based on the experimental results conducted by INES institute [43]. However, in this research, experiments were also carried out for other battery technologies including lithium-ion. Therefore, by the same way, a linear aging coefficient is deduced for lithium-ion battery and provided in Table 5.6.

Table 5.5 Initial assumptions for simulations of BESSs using LA technology

Residential load	Power factor	0.98
Small commercial load		0.90
PV generation		1.00
BESS	η	0.90
	SOC_{min}	0.20
	SOC_{max}	0.90
	$T_c = T_d$	3 h
	$SOC_{(0)} = SOC_{(T)}$	0.20
	Power factor	1.00
Grid	V_{min}	0.9 pu
	V_{max}	1.1 pu
Financial parameters	r	0.06
	OM	0.02
	C_0	600 \$/kWh

Table 5.6 Technical and economic characteristics of battery technologies

Parameters	Battery Technologies	
	Lead-acid	Li-ion
Z	3.10^{-4} [16, 19, 20]	$1.7.10^{-5}$ [19, 43]
η	0.9	0.98
SOC_{min}	0.2	0.15
SOC_{max}	0.9	0.95
$T_c = T_d$	3	1
C_0 (\$/kWh)	600	1400



CHAPTER 6

APPLICATION OF THE PROPOSED METHODS

One by one, effectiveness and applications of the proposed methods are demonstrated in this chapter. Firstly, the basic cost minimization of BESS is illustrated for a specific case which BESS is used for voltage management purpose and applicable as an analytic tool to assess the influential factors to BESS cost. Secondly, the method of BESS siting and sizing is exhibited for two cases of the network to emphasize the effectiveness of the method and at the same time observe the effect of load and PV generation dispersion on the determination of BESS site and size. Lastly, optimal schedules and cost evaluation of BESSs are results derived from simulating the third method for different battery technologies which are also demonstrated in this chapter.

6.1 Cost minimization of BESS – An economically analytic tool of BESS

Simulations are illustrated for a duration of one-day length which the worst day with 24 time-intervals is selected. In addition, lead-acid battery with the linear aging coefficient (Z) of $3.10 \cdot 10^{-4}$ [16, 19, 20] and other initial assumptions are given in Table 5.5 those are input parameters for Case B simulation. Because Case B is more common in practice.

6.1.1 Case study for basic cost minimization of BESS

Simulation network is depicted in Figure 6.1. It is assumed that node 23 is considered for BESS installation since this node is far away from the substation and connected with large amount of PV generation.

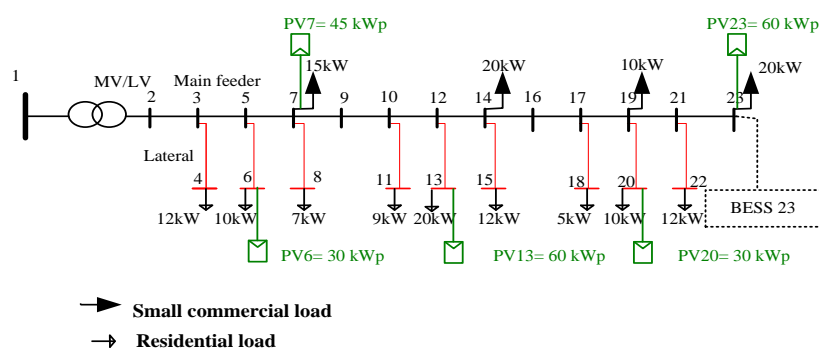


Figure 6.1 Case B with BESS installed at node 23

The optimization problem is solved on Matlab 2015b using `fmincon` function with code supported in Matpower 6.0 for power flow calculation. As a result, the minimum size which is required for the BESS is approximately 123 kWh and the minimum cost of the BESS for the simulated day is \$93.80. The effectiveness of voltage management by the BESS is demonstrated in Figure 6.2. This figure compares the voltage profiles before and after applying the BESS. From the figure, it can be seen that the overvoltages occurring from node 12 to the end of the main feeder during peak power generation and the under-voltages occurring at nodes 20, 21, 22, 23 in night time at peak demand are overcome with the support of the BESS. All node voltages of the network, therefore, are maintained within the acceptable range during the considered time.

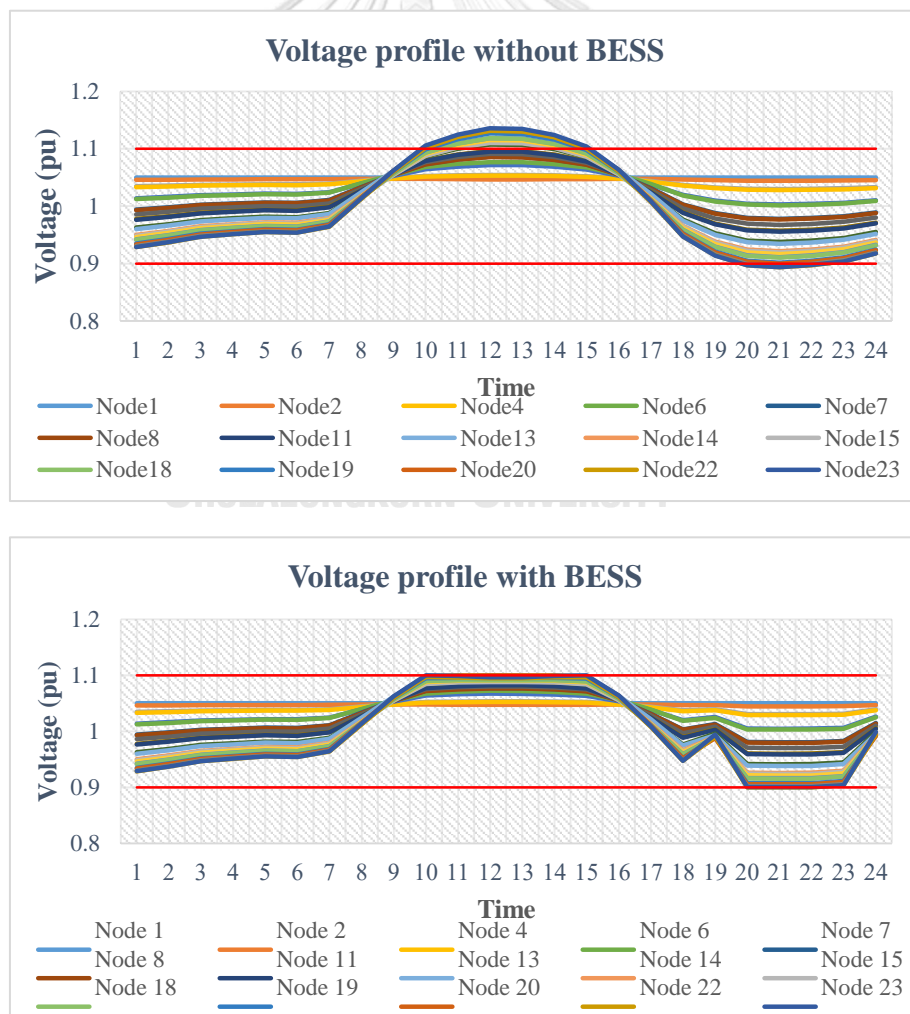


Figure 6.2 Voltages of the network with and without BESS support

Table 6.1 Simulation result for Case B with BESS installed at node 23

BESS size = 123.16 kWh, Minimum cost for simulated day = 93.80\$				
Time interval	Discharge power (kW)	Charge power (kW)	State of charge	Available energy (kWh)
1	0.0000	0.0000	0.2000	24.6320
2	0.0000	0.0000	0.2000	24.6320
3	0.0000	0.0000	0.2000	24.6320
4	0.0000	0.0000	0.2000	24.6320
5	0.0000	0.0000	0.2000	24.6320
6	0.0000	0.0000	0.2000	24.6320
7	0.0000	0.0000	0.2000	24.6320
8	0.0000	0.0000	0.2000	24.6320
9	0.0000	0.0000	0.2000	24.6320
10	0.0000	3.3102	0.2269	27.9422
11	0.0000	16.3116	0.3593	44.2538
12	0.0000	24.5701	0.5588	68.8238
13	0.0000	23.7804	0.7519	92.6042
14	0.0000	15.7896	0.8801	108.3938
15	0.0000	2.4500	0.9000	110.8438
16	0.0000	0.0000	0.9000	110.8438
17	0.0000	0.0000	0.9000	110.8438
18	0.0000	0.0000	0.9000	110.8438
19	1.0656	0.0000	0.8914	109.7783
20	1.2244	0.0000	0.8814	108.5538
21	2.6893	0.0000	0.8596	105.8645
22	15.5525	0.0000	0.7333	90.3120
23	32.8426	0.0000	0.4667	57.4694
24	32.8426	0.0000	0.2000	24.6268

The operating parameters of the BESS are provided in Table 6.1 while aging degradation of the BESS during simulated day represented by the reduction of its

capacity is drawn in Figure 6.3. It is noted that peak shaving is not considered in the scope of this dissertation.

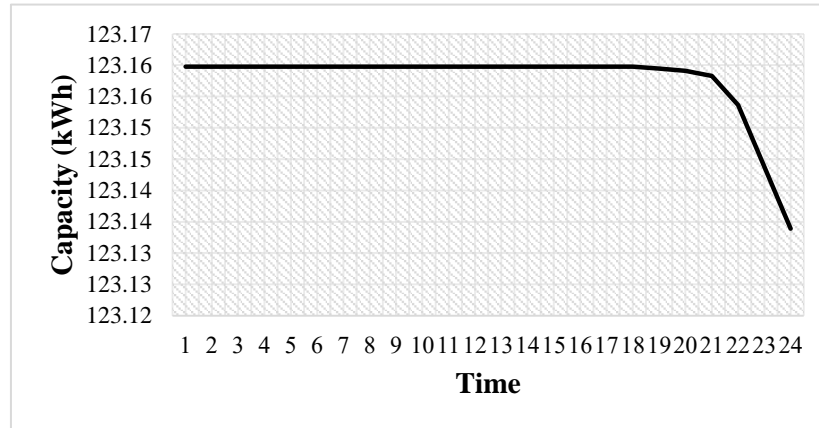


Figure 6.3 Capacity degradation of the BESS

Obviously, in this simulation, to satisfy both network voltage requirement and minimum BESS cost, the BESS only charges during peak PV generation when overvoltage occurs and discharges in the night time for peak demand support and under-voltage prevention. Discharge powers have not been involved in electricity price with time slots but limited by allowed maximum discharge power with the minimum size of BESS.

If the simulation duration is extended, the average daily cost of the BESS is expected lower due to the smaller mismatch of load and PV generation profiles and refreshed condition for a new cycle of the BESS.

Moreover, the lifespan and cost of the BESS for whole operation life can also be obtained by the recursive method proposed in the research [16] until the capacity of BESS reaches the end of life (80% of nominal capacity).

6.1.2 Effect of the installation sites on the cost and size of the BESS

In this subsection, the proposed method is used as a tool to investigate influential factors to the cost and size of the BESS. Installation site is one of the most important factors that greatly affect the effectiveness of voltage regulation reflected through the required size and cost of BESS which is evaluated by the simulations. The simulations are carried out for different sites of Case B and the results are demonstrated in Figure 6.4.

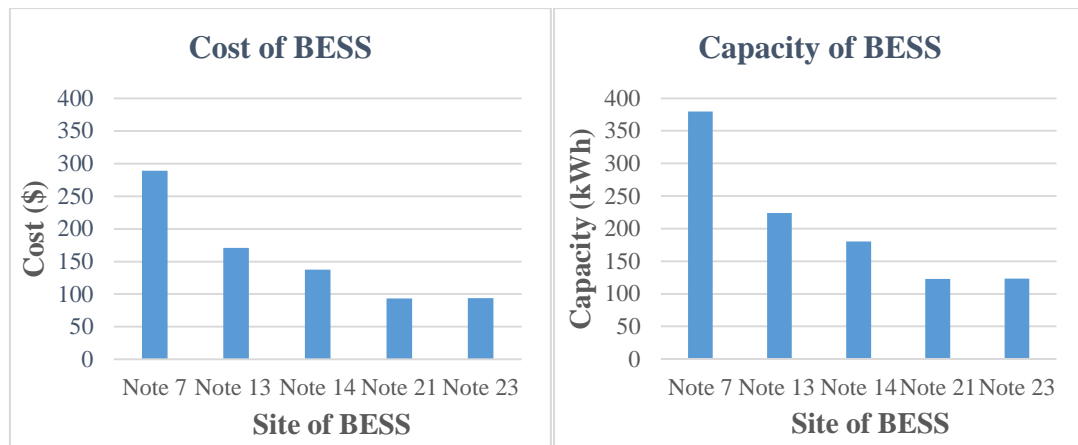


Figure 6.4 Required cost and size of BESS depending on installation sites

For voltage management target, the cost and size of the BESS installed at node 7 are required nearly three times as large as the one installed at node 21. For this specific network, BESS should be installed at nodes near the end of the main feeder. This is because PV penetration is high at those nodes and far from the source. Consequently, the surplus power causes overvoltage more seriously and BESS located at those nodes are more effective. Therefore, installation site should be specially considered in order to reduce BESS cost

In order to find the optimum installation site in the network, the simulation could run many times to examine all nodes. This may take a long time in case of a large network. In addition, this simulation only measures individual site. A certain combination that returns a better result might exist. For that wonder, the second method is developed for that purpose.

6.2 Strategy of siting and sizing of BESSs

Both Case A and Case B are used for simulation to demonstrate the effectiveness of the proposed method. Because Case A is simple and easy to achieve a good result from theoretical analysis and the proposed method is utilized to verify that theory. On the other hand, Case B is more common in practice due to random load sizes and various load types. Again, the lead-acid battery is illustrated for those simulations.

6.2.1 Case-study for siting and sizing strategies of BESS

It is assumed that, for Case A, the utility takes into account only 3 locations, for example, nodes 6, node 13 and node 20 for BESS installation. Because, only three

locations in the network are implemented large amounts of PV generation or convenient for BESS installation. On the other hand, Case B does not have any boundary of the locations for BESS installation. Therefore, all nodes are taken into account. Figure 6.5 depicts case-studies with those considerations.

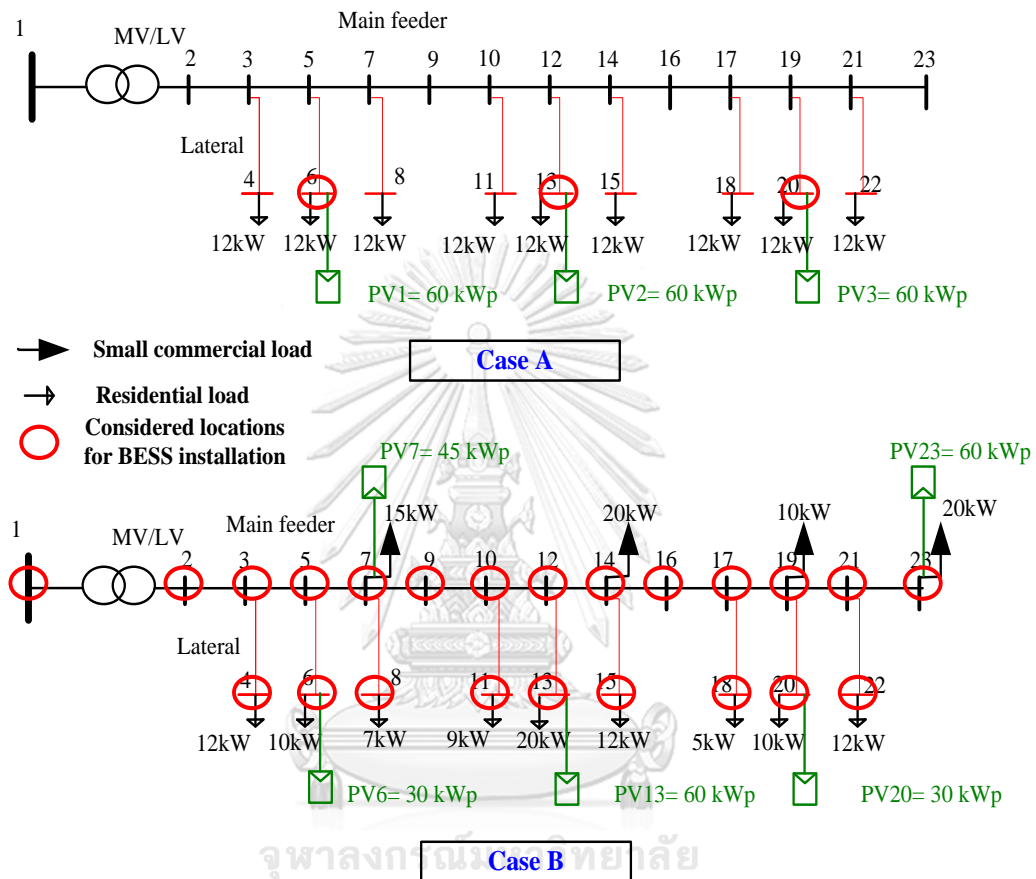


Figure 6.5 Case A and Case B with considered locations for BESSs installation

Different from previous simulations, the load and generation profiles selected for simulation only play the role of illustration. In this simulation, they should be carefully considered. First, they should represent the real load and PV generation profiles of the network. Second, they should create enough reserves in term of BESS size that can solve the biggest voltage problem for the whole year consideration. Therefore, the worst case of load and PV generation profiles are selected for the simulation. In contrast, the objective function which returns the cost of BESS only play a role in measuring the candidates to achieve the optimum result.

The optimization problem is solved on Matlab 2015b using `fmincon` function with code supported in Matpower 6.0 for power flow calculation. The optimum results of two cases are summarized in Table 6.2.

Table 6.2 Simulation results for Case A and Case B

Optimum parameters	Case A		Case B	
F1	97.723 \$		91.79 \$	
$C_{B,norm}^{\Sigma}$	128.32 kWh		120.53 kWh	
Dispatched capacity percentage	a^{20}	100%	a^{23}	85%
	a^{13}	0%	a^{20}	15%
	a^6	0%	a^k ($k \neq 20, 23$)	0%

For Case A, the results suggest that batteries should be clustered at node 20. This is the unique optimum location to install BESS and voltage regulation at this node is the most effective. Differently, for Case B, batteries should be distributed 85% capacity at node 23 and 15% capacity at node 20 to obtain the minimum cost of BESSs for the regulated duration. Influential factors which govern the obtained results are load and PV generation profiles, dispersion of load and PV rooftops as well as network parameters. Therefore, for Case A, which the network is simple, the optimum site for BESS installation can be obtained easily from the qualitative analysis and conform to the simulation result. However, Case B is more complex and the optimum site for BESS installation is not easy to be obtained from qualitative analysis. Only quantitative analysis from the simulation can be achieved. The obtained results are also reasonable when two suggested sites are node 23 and node 20. They are all near the end of the feeder, close each other with a large amount of PV generation. At peak power generation, overvoltage is most serious at node 23, with the support of PV generation of node 20 (very close to node 23), overvoltage level increases. Whereas, other nodes with high PV generation are quite far from node 23 and surrounded by many other loads, so reducing their effect on node 23.

It is obvious that the suggestion from the obtained results has much meaning in planning battery projects in term of siting and sizing BESSs. Moreover, to coordinate BESSs for overvoltage prevention, the simulation in the reference [14] used voltage sensitivity to decide which and how much each BESS should operate. Accordingly, some BESSs operate very frequently in the meanwhile some others are rarely used. Consequently, the rarely used ones met calendar life before cycle life. This leads to battery waste. The cost of BESSs was higher than they should be. With the proposed method, the site and size of BESSs are determined with the consideration of how frequent of their operation. Therefore, this method is better in term of avoiding battery waste due to infrequent operation.

6.2.2 Effect of PV rooftop dispersion on siting and sizing of BESSs

As above discussion, the factors governing optimal strategy of BESS are characteristic of load and PV generation profiles, dispersion of loads and PV rooftops as well as network parameters.

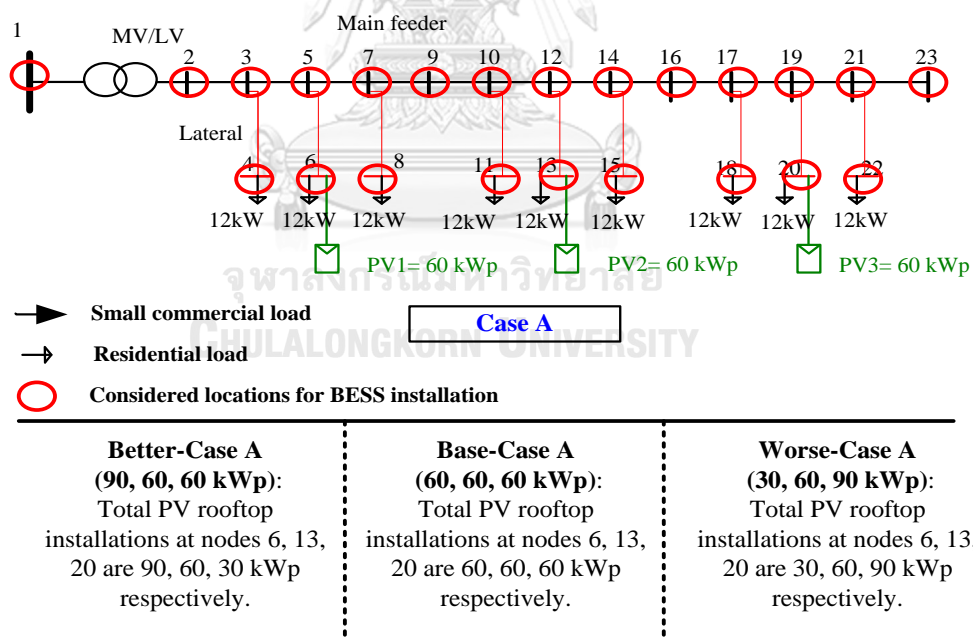


Figure 6.6 Scenarios of PV rooftop dispersions of Case A

Based on modified Case A, three scenarios of PV rooftop dispersion are examined to understand the effect of PV rooftop dispersion on siting and sizing of BESSs. In addition, different from the previous simulation which only 3 locations are considered for BESS installation, in this simulation, all locations are evaluated depicted

in Figure 6.6 to find the optimal result. Consequently, optimal strategies of BESSs for 3 scenarios are summarized in Table 6.3.

Table 6.3 Optimal strategies of BESSs

Optimum parameters	Better Case A (90, 60, 30 kWp)	Base case A (60, 60, 60 kWp)	Worse Case A (30, 60, 90 kWp)
F1	15.706 \$	97.723 \$	198.98 \$
$C_{B,norm}^{\Sigma}$	20.623 kWh	128.32 kWh	261.277 kWh
$a^k (k \neq 13, 20)$	0%	0%	0%
a^{13}	95.09%	0%	0%
a^{20}	4.91%	100%	100%

Obviously, three scenarios share the same level of solar power penetration. However, the total capacity requirement of BESSs, as well as the operation cost, are smallest for Better case A and largest for Worse Case A. This is because when PV generation is gathered more at the end of the feeder, voltage violation is more serious. As a result, the higher cost and larger size of BESSs are required. Especially, having a look on Better Case A where PV rooftops have a very high density near the source and low density near the end of the feeder, node 20 is no longer the best site for battery installation because only some surplus power is required to be compensated there. This is why the result suggests 95.09% of battery capacity should be installed at node 13 and 4.91% at node 20.

6.3 Operation planning and cost evaluation of BESSs

The main contribution of the proposed method is used for operation planning of the installed BESSs in the network to obtain their minimum total cost. Therefore, in this section, simulation is run to illustrate the application based on one-day ahead load and PV generation forecast. Besides, cost evaluation is also derived from the simulation. Hence, cost evaluation for one month is also carried out based on one-month typical load and PV generation profiles.

6.3.1 Operation planning of the BESSs

Simulation continues running for Case B after sites and sizes of the two BESSs are specified in Table 6.2 by the proposed method. The worst day is also assumed being the forecasted data for this simulation. Additionally, the simulation run for the first day that the BESSs are on duty. Therefore initial capacities of the BESSs are also their nominal capacities which are summarized and noticed in Table 6.4. The initial capacities will change during operation life. Other initial assumptions are shown in Table 5.5 with the lead-acid battery is the selection.

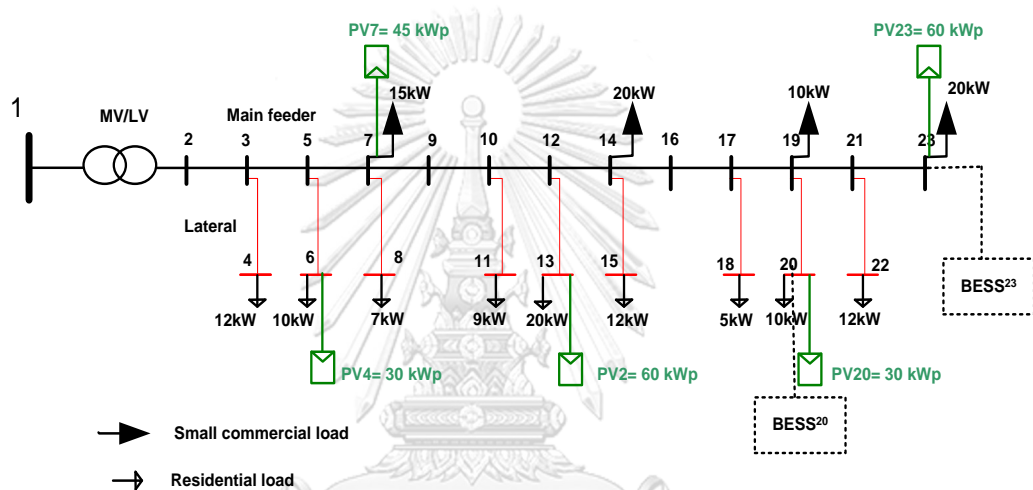


Figure 6.7 Network for operation planning simulation of the BESSs

Table 6.4 Parameters of the BESSs installed in Case B.

	Size-percentage	Size of BESS (kWh)	Initial capacity (kWh)
<i>BESS at node 20</i> (<i>BESS²⁰</i>)	15%	18.08	18.08
<i>BESS at node 23</i> (<i>BESS²³</i>)	85%	102.45	102.45
<i>Total</i>	100%	120.53	

Similarly, the optimization problem is solved on Matlab 2015b using fmincon function with code supported in Matpower 6.0 for power flow calculation. As a result, the minimum cost of the BESSs on the duty of managing node voltages of the network

within the acceptable range is \$91.74 for the forecasted day. The forecasted voltages of the network are described by the voltage curves in Figure 6.8.

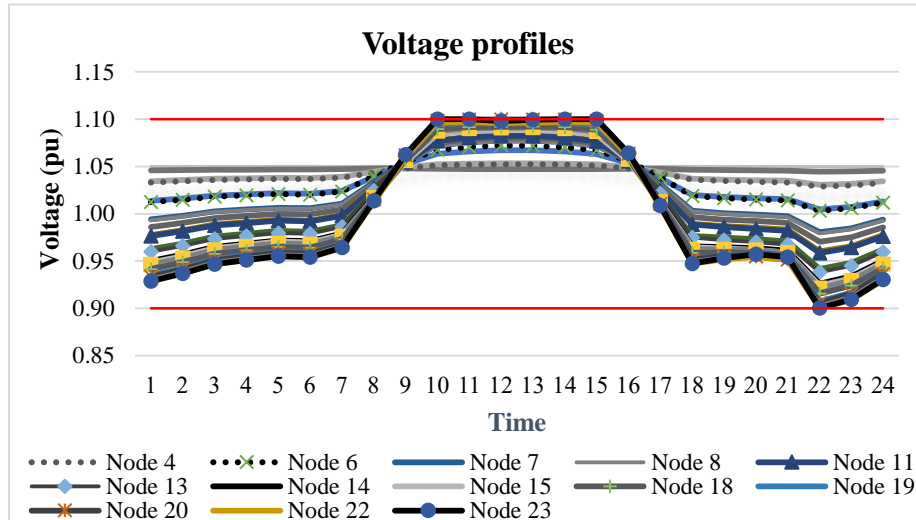


Figure 6.8 Voltage profiles of the network for the forecasted day

In order to obtain minimum cost, the BESSs should operate following the schedules shown in Figure 6.9.

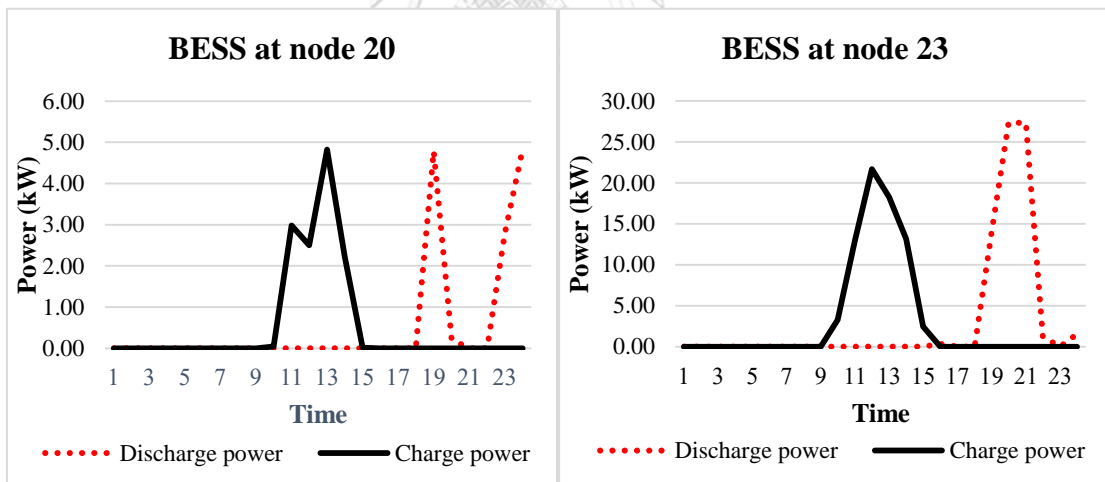


Figure 6.9 Charge/discharge schedules of the BESSs for the forecasted day

Figure 6.10 represents the state of charge of the BESSs during the simulated day while Figure 6.11 draws the curves of capacity loss caused by aging degradation during their operation.

The worst case rarely occurs in practice. Therefore, the cost of the BESSs for voltage management of one day is much lower than this number or even near to zero if voltage problems (overvoltage and under-voltage) do not occur. However, this

simulation gives an example of a forecasted data in order to compare with the previous result. It is clear that each formulation has its own goals, in turn different assumptions. While load and PV generation profiles used for siting and sizing of BESS should make a reservation for the worst case in long-term planning, the ones used for scheduling vary day by day for operation planning. BESSs for siting and sizing strategy operate simultaneously to find the best locations and sizes while for operation planning, they can operate independently to obtain minimum total cost. It can be seen that although same load and PV generation profiles are used, the cost of BESS in the simulation for scheduling is \$91.74, a little bit lower in comparison with the simulation for siting and sizing BESS of \$91.79. This is because, in the second formulation, two BESSs are pre-specified and they can operate independently to obtain the best result with independent schedules. The schedules obtained by the first formulation is only one of the good candidates for operation planning but not the best one.

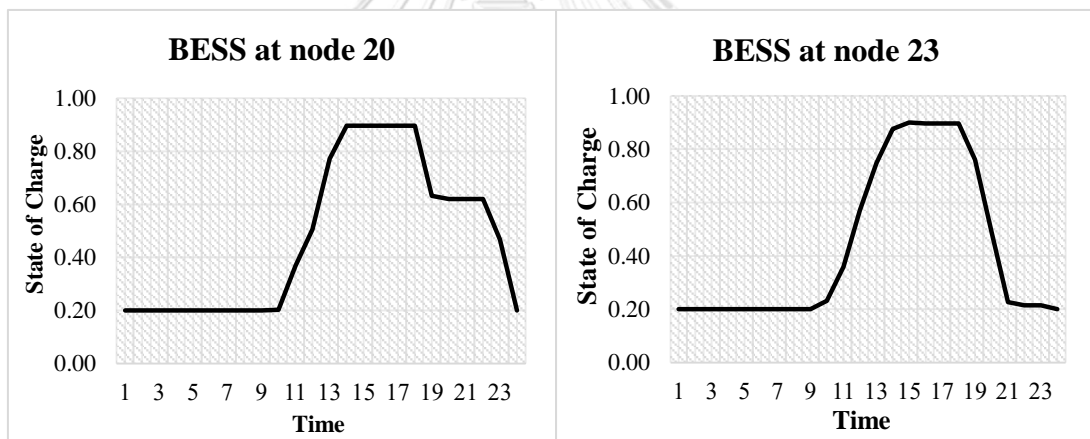


Figure 6.10 State of charge of the BESSs for the forecasted day

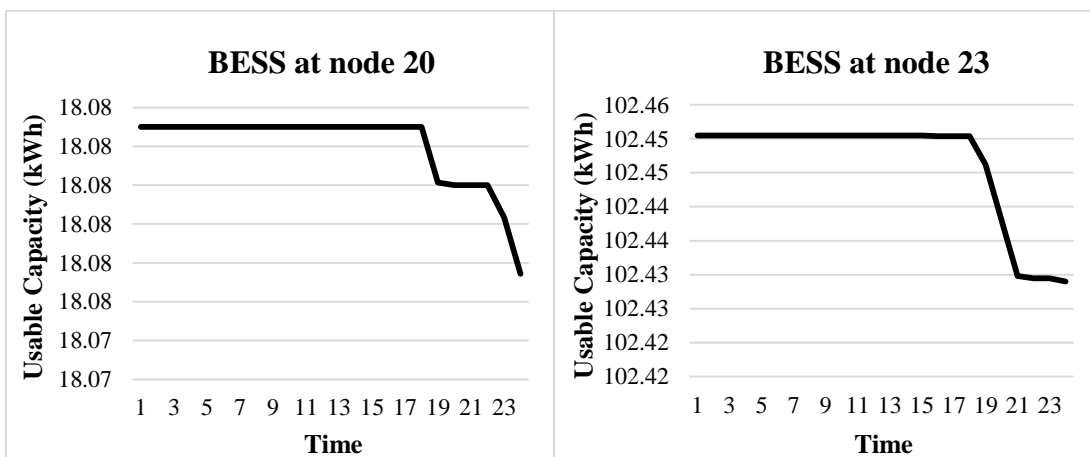


Figure 6.11 Capacity degradation of the BESSs for the forecasted day

6.3.2 Cost evaluation of the BESSs

From operation planning simulation, cost evaluation of the BESSs for the simulated day is also derived. Therefore, in this subsection, cost evaluations of the BESSs which simulations are run for Case B are carried out for one month with typical load and generation profiles given in Table 5.4 and Figure 5.2. Moreover, the simulations make comparison between two technology options of battery with same sizes for BESS installation. They are all potential technologies and very different in price as well as performance characteristics. Case study and technical and economic characteristics of the battery technologies for simulation are provided in Figure 6.12.

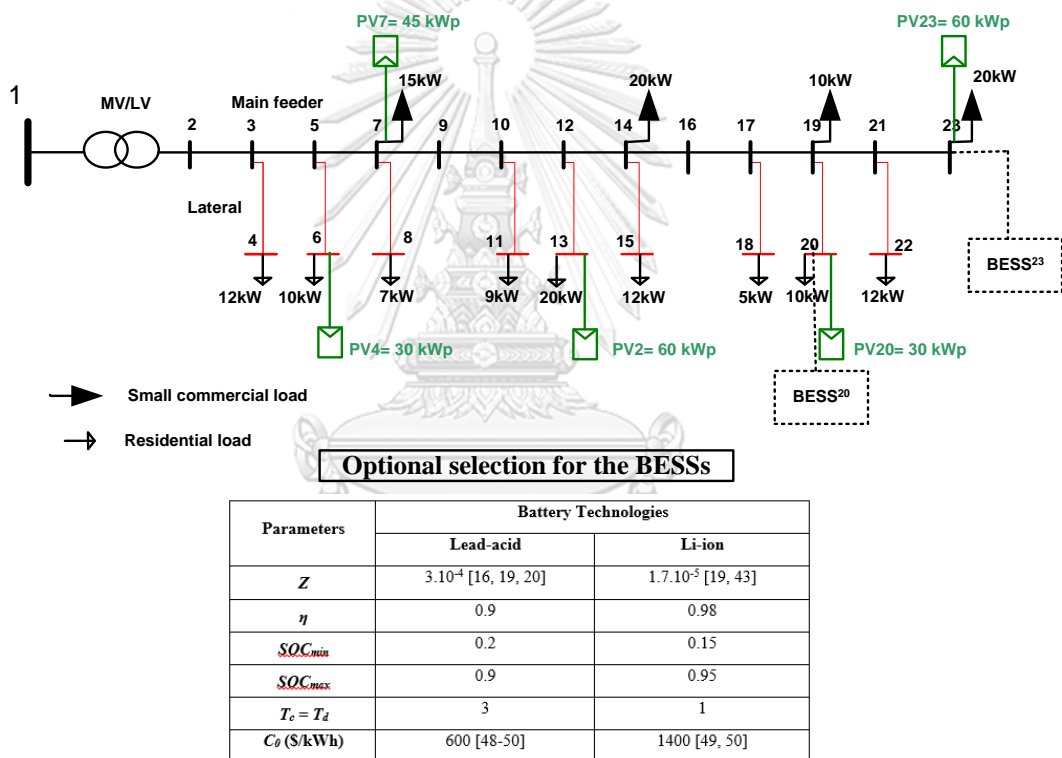


Figure 6.12 Case study for one-month cost evaluation of the BESSs

By running simulation on the basis of one day, battery capacities that decrease during their operation are updated after each day until thirty days are completed. As a result, total costs of the BESSs in one month which the BESSs are responsible for voltage regulation are \$1917 and \$1300 corresponding to lead-acid and Lithium-ion, respectively. Cost curves of the BESSs are drawn on Figure 6.13 and details are provided in Appendix B for two options.

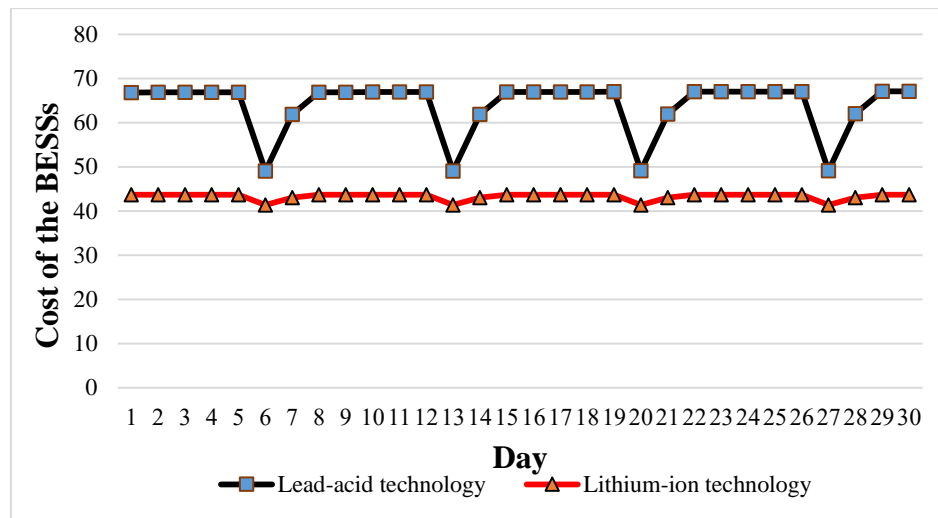


Figure 6.13 Cost of the BESSs according to battery technologies

From the result, it is very interesting that although price of Lithium-ion battery is much higher than Lead-acid battery, its operation cost is considerably lower around 2/3 in comparison with Lead-acid for one month simulation. This is because Lithium-ion has dominant characteristics with high efficiency, high charge/discharge rates and, especially, slow aging process exhibited through its aging coefficient of $1.7 \cdot 10^{-5}$. In addition, because of this slow aging process, the cost curve of lithium-ion BESSs is flatter and lower than the one of Lead-acid BESSs. The drops in each cost curve are simulated for Saturday and Sunday where undervoltage occurs less seriously compared with the working days, resulting in lower cost of the BESSs. In general, the trend of cost curves increase very slightly due to capacity degradation during BESS operation.

Although technical characteristics as well as prices of battery technologies, the inputs of those simulations, are assumed values based on practical data [19, 43, 48-50], they do not correct for all cases. Because prices of the battery varies largely upon various suppliers and dimension of battery project. Therefore, cost evaluation of the BESSs should be done for each specific case with real data and the proposed method keep fully its own effectiveness and usefulness.

CHAPTER 7

CONCLUSION

This chapter gives a summary of the dissertation. The main contributions of the proposed methods and some conclusions based on the simulation results are summarized. Then, some suggestions for improvement of the proposed methods are also presented in this chapter.

7.1 Dissertation summary and conclusion

The dissertation proposes necessary strategies which utilize BESSs to manage voltage problem caused by high penetration of PV rooftops in the LV network to minimize their cost. Initially, cost minimization of a BESS which its location is pre-specified in the network was formulated in the optimization problem, including BESS aging degradation cost and some additional costs specified in the objective function. The constraints are operating conditions of the BESS and voltage requirement of the network. Then, two important strategies for cost minimization of BESSs applied in general cases were developed based on this formulation. The strategies cover siting and sizing of BESSs for long-term planning and then scheduling of the BESSs for operation planning. Effectiveness and usefulness of each formulation were demonstrated on MEA simplified networks with real load and PV generation data recorded by MEA and Chulalongkorn University, respectively. The simulations used Matlab 2016a and Matpower 6.0 as computational tool and fmincon as the solver for optimization problems. Contributions of each formulation and conclusions from simulated results are summarized as follows:

The basis formulation was simulated for a simple system which only one BESS is responsible for voltage management and its location is pre-specified in the network. The derived results are the minimum cost of the BESS, operating parameters of the BESS and effectiveness of voltage regulation. Although there are some limitations in the assumption of the BESS, the formulation is used as a quantitative tool to investigate the effect of the influential factors on the voltage regulation cost. For example, BESS locations were illustrated. The results confirm that installation site of the BESS is a very

important factor which strongly influences the regulation effectiveness and cost of the BESS. Therefore, in order to minimize the cost, BESS siting is an indispensable strategy.

Next, the proposed method for siting and sizing BESSs which is very necessary and useful for utility in long-term planning was demonstrated in various networks, from very simple to more complex ones. The results did reflect the theoretical analysis correctly more precisely by quantitative measurement. The proposed method was also used to measure the effect of dispersion of loads and PV rooftops on siting and sizing of BESSs. It was noted that with the same penetration level of PV rooftops, PV rooftops gathered near the end of the main feeder cause voltage violation worse than those gathered near the source, in turn requiring a larger size and more voltage regulation cost. The results prove that PV rooftops should not be more concentrative at the end of the main feeder.

Lastly, for scheduling the BESSs which directly influences the operation cost of the BESSs. The proposed method was successfully simulated to return optimal schedule of each BESS based on forecasted load and generation data. Simultaneously, cost of the BESSs was also evaluated. Moreover, Lead-acid and Lithium-ion technologies were run for a typical month to compare their regulation costs. The result exhibited that despite the higher price of Lithium-ion battery in comparison with Lead-acid battery, voltage regulation cost of Lithium-ion BESS is lower due to its much slower aging degradation and other better characteristics. Although simulated results only represented for the specific cases, they should be considered for battery selection of BESS.

In general, the price of BESS is still high. It may not be economical now in comparison with other traditional solutions for voltage management. However, since BESS is a multi-benefit solution, it will be more economical if other advantages of BESS are simultaneously made of good use in power system such as energy arbitrage, network support, balancing service, carbon savings and so forth. This requires an effective policy for the change in the market and regulatory structure that has been successful with solar power generation. The proposed methods will be really useful when the price of BESS is getting cheaper.

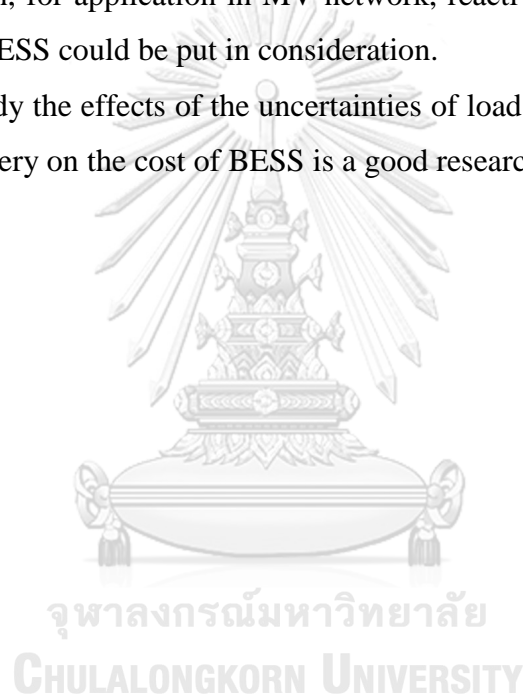
7.2 Recommendation for research development

Some improvement and development of this research are recommended as follows:

Since BESS is a multi-benefit solution, cost evaluation of other applications of BESS can be also investigated and formulated in a multi-objective problem. For example, voltage regulation in conjunction with energy arbitrage and so forth are investigated in the same problem. On the other hand, application of the proposed method in an unbalance power system is also a development.

In addition, for application in MV network, reactive power compensation by converter-based BESS could be put in consideration.

Lastly, study the effects of the uncertainties of load and PV generation as well as the price of battery on the cost of BESS is a good research direction.



REFERENCES

- [1] REN21, "Renewables 2017 Global Status Report," REN21 Secretariat, c/o UNEP, 1 Rue Miollis Building VII, 75015 Paris, France 2017, Available: http://www.ren21.net/wp-content/uploads/2017/06/17-8399_GSR_2017_Full_Report_0621_Opt.pdf, Accessed on: 1/4/2018.
- [2] E. Tourneboeuf, "Learning lessons from the European Experience with large scale solar," 2013, Available: http://www.aie.org.au/aie/documents/solar_scholarship_report.pdf.
- [3] R. Passey, T. Spooner, I. MacGill, M. Watt, and K. Syngellakis, "The potential impacts of grid-connected distributed generation and how to address them: A review of technical and non-technical factors," *Energy Policy*, vol. 39, no. 10, pp. 6280-6290, 2011.
- [4] IEA, "High Penetration of PV in Local Distribution Grids," Report IEA PVPS T14-02:2014, 2014, Available: http://iea-pvps.org/index.php?id=295&eID=dam_frontend_push&docID=2210, Accessed on: 8/8/2017.
- [5] T. Van Dao, H. T. N. Nguyen, S. Chaitusaney, and R. Chatthaworn, "Local reactive power control of PV plants for voltage fluctuation mitigation," in *Electrical Engineering/Electronics, Computer, Telecommunications and Information Technology (ECTI-CON), 2014 11th International Conference on*, 2014, pp. 1-6: IEEE.
- [6] R. Tonkoski, L. A. Lopes, and T. H. El-Fouly, "Coordinated active power curtailment of grid connected PV inverters for overvoltage prevention," *IEEE Transactions on Sustainable Energy*, vol. 2, no. 2, pp. 139-147, 2011.
- [7] A. Einfalt, F. Zeilinger, R. Schwalbe, B. Bletterie, and S. Kadam, "Controlling active low voltage distribution grids with minimum efforts on costs and engineering," in *Industrial Electronics Society, IECON 2013-39th Annual Conference of the IEEE*, 2013, pp. 7456-7461: IEEE.
- [8] S. Weckx, C. Gonzalez, and J. Driesen, "Combined central and local active and reactive power control of PV inverters," *IEEE Transactions on Sustainable Energy*, vol. 5, no. 3, pp. 776-784, 2014.

- [9] M. Oshiro *et al.*, "Optimal voltage control in distribution systems using PV generators," *International Journal of Electrical Power & Energy Systems*, vol. 33, no. 3, pp. 485-492, 2011.
- [10] S. Hashemi, J. Østergaard, and G. Yang, "A scenario-based approach for energy storage capacity determination in LV grids with high PV penetration," *IEEE Transactions on Smart Grid*, vol. 5, no. 3, pp. 1514-1522, 2014.
- [11] H. Sugihara, K. Yokoyama, O. Saeki, K. Tsuji, and T. Funaki, "Economic and efficient voltage management using customer-owned energy storage systems in a distribution network with high penetration of photovoltaic systems," *IEEE Transactions on Power Systems*, vol. 28, no. 1, pp. 102-111, 2013.
- [12] H. Silva, R. Castro, and M. Almeida, "A Battery Based Solution to Overvoltage Problems in Low Voltage Distribution Networks with Micro Generation," *International Journal on Electrical Engineering and Informatics*, vol. 6, no. 1, p. 53, 2014.
- [13] M. Kabir, Y. Mishra, G. Ledwich, Z. Y. Dong, and K. P. Wong, "Coordinated control of grid-connected photovoltaic reactive power and battery energy storage systems to improve the voltage profile of a residential distribution feeder," *IEEE Transactions on industrial Informatics*, vol. 10, no. 2, pp. 967-977, 2014.
- [14] L. Wang, D. H. Liang, A. F. Crossland, P. C. Taylor, D. Jones, and N. S. Wade, "Coordination of multiple energy storage units in a low-voltage distribution network," *IEEE Transactions on Smart Grid*, vol. 6, no. 6, pp. 2906-2918, 2015.
- [15] IRENA, "Battery storage for renewables: market status and technology outlook," *International Renewable Energy Agency (IRENA)*, Abu Dhabi, 2015.
- [16] B. Ansari, D. Shi, R. Sharma, and M. G. Simoes, "Economic analysis, optimal sizing and management of energy storage for PV grid integration," in *Transmission and Distribution Conference and Exposition (T&D), 2016 IEEE/PES*, 2016, pp. 1-5: IEEE.
- [17] G. Lorenzi and C. A. S. Silva, "Comparing demand response and battery storage to optimize self-consumption in PV systems," *Applied Energy*, vol. 180, pp. 524-535, 2016.

- [18] G. Merei, J. Moshövel, D. Magnor, and D. U. Sauer, "Optimization of self-consumption and techno-economic analysis of PV-battery systems in commercial applications," *Applied Energy*, vol. 168, pp. 171-178, 2016.
- [19] Y. Riffonneau, S. Bacha, F. Barruel, and S. Ploix, "Optimal power flow management for grid connected PV systems with batteries," *IEEE Transactions on Sustainable Energy*, vol. 2, no. 3, pp. 309-320, 2011.
- [20] Y. Ru, J. Kleissl, and S. Martinez, "Storage size determination for grid-connected photovoltaic systems," *IEEE Transactions on Sustainable Energy*, vol. 4, no. 1, pp. 68-81, 2013.
- [21] T. Aziz and N. Ketjoy, "PV Penetration Limits in Low Voltage Networks and Voltage Variations," *IEEE Access*, vol. 5, pp. 16784-16792, 2017.
- [22] B.-I. Crăciun, T. Kerekes, D. Séra, and R. Teodorescu, "Overview of recent grid codes for PV power integration," in *Optimization of Electrical and Electronic Equipment (OPTIM), 2012 13th International Conference on*, 2012, pp. 959-965: IEEE.
- [23] IEEE, "IEEE Application Guide for IEEE Std 1547™, IEEE Standard for Interconnecting Distributed Resources with Electric Power Systems," vol. IEEE Std 1547.2™-2008, 2008.
- [24] FNN, "VDE-AR-N 4015:2011-08 Power generation systems connected to the low-voltage distribution network - Technical minimum requirements for the connection to and parallel operation with low-voltage distribution networks," 2011.
- [25] PEA, "Interconnecting Distributed Resources with Electric Power Systems Grid Code," *PEA grid code*, 2015.
- [26] MEA, "Interconnecting Distributed Resources with Electric Power Systems Grid Code," *MEA grid code*, 2015.
- [27] S. Hashemi and J. Østergaard, "Methods and strategies for overvoltage prevention in low voltage distribution systems with PV," *IET Renewable Power Generation*, vol. 11, no. 2, pp. 205-214, 2016.
- [28] ABB, "ABB LV Power Converter Solutions PCS 100 EES, 100kVA to 20MVA, Energy Storage System," Available: <http://www04.abb.com/global/seitp/seitp202.nsf/e308f3e92d9a8fc5c1257c9f0>

0349c99/52e36c88df14683248257c14001a16d3/\$FILE/PCS100+ESS+++2UCD301111_d.pdf, Accessed on: 9/8/2017.

- [29] ABB, "PCS100 ESS Grid Connect Interface for Energy Storage Systems 100kVA to 10MVA," ed, 2011.
- [30] IEC, "Electrical Energy Storage," 2013, Available: <http://www.iec.ch/whitepaper/pdf/iecWP-energystorage-LR-en.pdf>, Accessed on: 9/8/2017.
- [31] X. Hu, C. Zou, C. Zhang, and Y. Li, "Technological Developments in Batteries: A Survey of Principal Roles, Types, and Management Needs," *IEEE Power and Energy Magazine*, vol. 15, no. 5, pp. 20-31, 2017.
- [32] blog.iec61850.com. (7/8/2017). *News in IEC 61850 and related Standarts*. Available: <http://blog.iec61850.com/2017/08/iec-61850-90-9-models-for-electrical.html>
- [33] IEC-TR61850-90-7, "Communication networks and systems for power utility automation – Part 90-7: Object models for power converters in distributed energy resources (DER) systems," 2013.
- [34] IEC61850-7-4, "Communication networks and systems for power utility automation – Part 7-4: Basic communication structure – Compatible logical node classes and data object classes," 2010.
- [35] IEC61850-7-420, "Communication networks and systems for power utility automation – Part 7-420: Basic communication structure – Distributed energy resources logical nodes," 2009.
- [36] M. Team, "A guide to understanding battery specifications," *Academia. edu*, 2008.
- [37] Electropaedia. (9/8/2017). *Battery Performance Characteristics*. Available: <http://www.mpoweruk.com/performance.htm#offset>
- [38] F. Feng, R. Lu, and C. Zhu, "A combined state of charge estimation method for lithium-ion batteries used in a wide ambient temperature range," *Energies*, vol. 7, no. 5, pp. 3004-3032, 2014.
- [39] Electropaedia. (9/8/2017). *Battery Life (and Death)*. Available: <http://www.mpoweruk.com/life.htm#dod>

- [40] C. Lin, A. Tang, and W. Wang, "A review of SOH estimation methods in Lithium-ion batteries for electric vehicle applications," *Energy Procedia*, vol. 75, pp. 1920-1925, 2015.
- [41] H. Bindner, T. Cronin, P. Lundsager, J. F. Manwell, U. Abdulwahid, and I. Baring-Gould, "Lifetime modelling of lead acid batteries," 8755034411, 2005.
- [42] J. Xiao, Z. Zhang, L. Bai, and H. Liang, "Determination of the optimal installation site and capacity of battery energy storage system in distribution network integrated with distributed generation," *IET Generation, Transmission & Distribution*, vol. 10, no. 3, pp. 601-607, 2016.
- [43] E. Lemaire-Potteau, F. Mattera, A. Delaille, and P. Malbranche, "Assessment of storage ageing in different types of PV systems: technical and economical aspects," in *23rd European Photovoltaic Solar Energy Conference (Valencia, Spain, 2008)*, 2008, pp. 2765-2769.
- [44] POWERTHRU, "LEAD ACID BATTERY working – LIFETIME STUDY," Available: <http://www.powerthru.com/documents/The%20Truth%20About%20Batteries%20-%20POWERTHRU%20White%20Paper.pdf>, Accessed on: 9/8/2017.
- [45] (2016). *Data of The Electrical Networks*.
- [46] (2015). *MEA - Load Profile 2015*.
- [47] (2013). *Statistical Record of Solar Radiation*.
- [48] Made-in-china.com. *Rechargeable Battery*. Available: https://www.made-in-china.com/products-search/hot-china-products/Rechargeable_Battery.html
- [49] BATTERYUNIVERSITY. *BU-1006: Cost of Mobile and Renewable Power*. Available: http://batteryuniversity.com/learn/article/bu_1006_cost_of_mobile_power
- [50] WHOLESALESOLAR. *All brands of Deep Cycle Batteries for Solar & Renewable Energy Applications*. Available: <https://www.wholesalesolar.com/deep-cycle-solar-batteries>

APPENDIX



จุฬาลงกรณ์มหาวิทยาลัย
CHULALONGKORN UNIVERSITY

APPENDIX A

Newton Raphson method for load flow calculation

Newton Raphson method is utilized popularly in power system for load flow calculation. In comparison with other methods, this method exhibits more advantages. Due to its quadratic convergence, Newton's method is mathematically superior to the Gauss-Seidel method and is less prone to divergence with ill-conditioned problems. For large power systems, the Newton-Raphson method is found to be more efficient and practical. The number of iteration required to obtain a solution is independent of the system size, but more functional evaluations are required at each iteration.

Load flow calculation based on Newton Raphson method is presented as follows.

Since in the power flow problem real power and voltage magnitude are specified for the voltage control bus, the power flow equation is formulated in polar form. For the typical bus of the power system, the current entering bus i is given by (A.1). This equation can be written in term of bus admittance matrix as

$$I_i = \sum_{j=1}^n Y_{ij} V_j \quad (\text{A.1})$$

In the above equation, j includes bus i . Expressing this equation in polar form, we have

$$I_i = \sum_{j=1}^n |Y_{ij}| |V_j| \angle \theta_{ij} + \delta_j \quad (\text{A.2})$$

The complex number at bus i is

$$P_i - jQ_i = V_i^* I_i \quad (\text{A.3})$$

Substituting from (A.2) for I_i in (A.3),

$$P_i - jQ_i = |V_i| \angle (-\delta_i) \sum_{j=1}^n |Y_{ij}| |V_j| \angle \theta_{ij} + \delta_j \quad (\text{A.4})$$

Separating the real and imaginary part,

$$P_i = \sum_{j=1}^n |V_i| |V_j| |Y_{ij}| \cos(\theta_{ij} - \delta_i + \delta_j) \quad (\text{A.5})$$

$$Q_i = \sum_{j=1}^n |V_i||V_j||Y_{ij}| \sin(\theta_{ij} - \delta_i + \delta_j) \quad (\text{A.6})$$

Equation (A.5) and (A.6) constitute a set of nonlinear algebraic equations in terms of the independent variables, voltage magnitude in per unit, and phase angle in radians. We have two equations for each load bus, given by (A.5) and (A.6), and one equation for each voltage controlled bus, given by (A.5). Expanding (A.5) and (A.6) in Taylor's series about the initial estimate and neglecting all higher order terms results in the following set of linear equations.

$$\begin{bmatrix} \Delta P_2^{(k)} \\ \vdots \\ \Delta P_n^{(k)} \\ \Delta Q_2^{(k)} \\ \vdots \\ \Delta Q_n^{(k)} \end{bmatrix} = \begin{bmatrix} \frac{\partial P_2^{(k)}}{\partial \delta_2} & \cdots & \frac{\partial P_2^{(k)}}{\partial \delta_n} & \frac{\partial P_2^{(k)}}{\partial |V_2|} & \cdots & \frac{\partial P_2^{(k)}}{\partial |V_n|} \\ \vdots & \ddots & \vdots & \vdots & \ddots & \vdots \\ \frac{\partial P_n^{(k)}}{\partial \delta_2} & \cdots & \frac{\partial P_n^{(k)}}{\partial \delta_n} & \frac{\partial P_n^{(k)}}{\partial |V_2|} & \cdots & \frac{\partial P_n^{(k)}}{\partial |V_n|} \\ \frac{\partial Q_2^{(k)}}{\partial \delta_2} & \cdots & \frac{\partial Q_2^{(k)}}{\partial \delta_n} & \frac{\partial Q_2^{(k)}}{\partial |V_2|} & \cdots & \frac{\partial Q_2^{(k)}}{\partial |V_n|} \\ \vdots & \ddots & \vdots & \vdots & \ddots & \vdots \\ \frac{\partial Q_n^{(k)}}{\partial \delta_2} & \cdots & \frac{\partial Q_n^{(k)}}{\partial \delta_n} & \frac{\partial Q_n^{(k)}}{\partial |V_2|} & \cdots & \frac{\partial Q_n^{(k)}}{\partial |V_n|} \end{bmatrix} \begin{bmatrix} \Delta \delta_2^{(k)} \\ \vdots \\ \Delta \delta_n^{(k)} \\ \Delta |V_2^{(k)}| \\ \vdots \\ \Delta |V_n^{(k)}| \end{bmatrix}$$

In the above equation, bus 1 is assumed to be the slack bus. The Jacobian matrix given the linearized relationship between small changes in voltage angle $\Delta \delta_i^{(k)}$ and voltage magnitude $\Delta |V_i^{(k)}|$ with the small changes in real and reactive power $\Delta P_i^{(k)}$ and $\Delta Q_i^{(k)}$. Element of Jacobian matrix are the partial derivatives of (A.5) and (A.6), evaluated at $\Delta \delta_i^{(k)}$ and $\Delta |V_i^{(k)}|$. In short term, it can be written as

$$\begin{bmatrix} \Delta P \\ \Delta Q \end{bmatrix} = \begin{bmatrix} J_1 & J_2 \\ J_3 & J_4 \end{bmatrix} \begin{bmatrix} \Delta \delta \\ \Delta |V| \end{bmatrix} \quad (\text{A.7})$$

For voltage-controlled buses, the voltages magnitudes are known. Therefore, if m buses of the system are voltage-controlled buses, m equations involving ΔQ and ΔV and the corresponding columns of the Jacobian matrix are eliminated. Accordingly, there are $n - 1$ real power constraints and $n - 1 - m$ reactive constraints, and the Jacobian matrix is of order $(2n - 2 - m) \times (2n - 2 - m)$. J_1 is of the order $(n - 1) \times (n - 1)$, J_2 is of the order $(n - 1) \times (n - 1 - m)$, J_3 is of the order $(n - 1 - m) \times (n - 1)$, and J_4 is of the order $(n - 1 - m) \times (n - 1 - m)$.

The diagonal and the off-diagonal elements of J_1 are

$$\frac{\partial P_i}{\partial \delta_i} = \sum_{j \neq i} |V_i| |V_j| |Y_{ij}| \sin(\theta_{ij} - \delta_i + \delta_j) \quad (\text{A.8})$$

$$\frac{\partial P_i}{\partial \delta_j} = -|V_i| |V_j| |Y_{ij}| \sin(\theta_{ij} - \delta_i + \delta_j) \quad j \neq i \quad (\text{A.9})$$

The diagonal and the off diagonal element of J_2 are

$$\frac{\partial P_i}{\partial |V_i|} = 2|V_i| |Y_{ij}| \cos \theta_{ij} + \sum_{j \neq i} |V_j| |Y_{ij}| \cos(\theta_{ij} - \delta_i + \delta_j) \quad (\text{A.10})$$

$$\frac{\partial P_i}{\partial |V_j|} = |V_i| |Y_{ij}| \cos(\theta_{ij} - \delta_i + \delta_j) \quad j \neq i \quad (\text{A.11})$$

The diagonal and the off-diagonal elements of J_3 are

$$\frac{\partial Q_i}{\partial \delta_i} = \sum_{j \neq i} |V_i| |V_j| |Y_{ij}| \cos(\theta_{ij} - \delta_i + \delta_j) \quad (\text{A.12})$$

$$\frac{\partial Q_i}{\partial \delta_j} = -|V_i| |V_j| |Y_{ij}| \cos(\theta_{ij} - \delta_i + \delta_j) \quad j \neq i \quad (\text{A.13})$$

The diagonal and the off-diagonal element J_4 are

$$\frac{\partial Q_i}{\partial |V_i|} = -2|V_i| |Y_{ij}| \sin \theta_{ij} - \sum_{j \neq i} |V_j| |Y_{ij}| \sin(\theta_{ij} - \delta_i + \delta_j) \quad (\text{A.14})$$

$$\frac{\partial Q_i}{\partial |V_j|} = -|V_i| |Y_{ij}| \sin(\theta_{ij} - \delta_i + \delta_j) \quad j \neq i \quad (\text{A.15})$$

The terms $\Delta P_i^{(k)}$ and $\Delta Q_i^{(k)}$ are the difference between the schedule and calculated values, known as the power residuals, given by

$$\Delta P_i^{(k)} = P_i^{\text{sch}} - P_i^{(k)} \quad (\text{A.16})$$

$$\Delta Q_i^{(k)} = Q_i^{\text{sch}} - Q_i^{(k)} \quad (\text{A.17})$$

The new estimates for bus voltages are

$$\delta_i^{(k+1)} = \delta_i^{(k)} + \Delta \delta_i^{(k)} \quad (\text{A.18})$$

$$|V_i^{(k+1)}| = |V_i^{(k)}| + \Delta |V_i^{(k)}| \quad (\text{A.19})$$

The procedure for power flow solution by the Newton-Raphson method is as follow:

For load buses, where P_i^{sch} and Q_i^{sch} are specified, voltage magnitudes and phase angle are set equal to the slack bus value, or 1.0 or A.0, i.e., $|V_i^{(0)}| = 1.0$ and $\delta_i^{(0)} = A$. For voltage-regulated buses, where $|V_i|$ and P_i^{sch} are specified, phase angles are set equal to the slack bus angle, or 0, i.e., $\delta_i^{(0)} = A$.

For load buses, $P_i^{(k)}$ and $Q_i^{(k)}$ are calculated from (A.5) and (A.6) and $\Delta P_i^{(k)}$ and $\Delta Q_i^{(k)}$ are calculated from (A.16) and (A.17).

For the voltage-controlled buses, $P_i^{(k)}$ and $\Delta P_i^{(k)}$ are calculated from (A.5) and (A.16), respectively.

The elements of Jacobian matrix (J_1, J_2, J_3 and J_4) are calculated from (A.8)-(A.15).

The linear simultaneous equation (A.7) is solved directly by optimally ordered triangular factorization and Gaussian elimination.

The new voltage magnitudes and phase angles are computed from (A.18) and (A.19).

The process is continued until the residuals $\Delta P_i^{(k)}$ and $\Delta Q_i^{(k)}$ are less than the specified accuracy, i.e.,

$$|\Delta P_i^{(k)}| \leq \varepsilon \quad (A.20)$$

$$|\Delta Q_i^{(k)}| \leq \varepsilon$$

APPENDIX B

Matlab simulation result

Table B.1 Cost evaluation of the BESSs with different battery technologies

Simulated Month		Cost of the BESSs (\$)	
Order	Typical day	Lead-acid technology	Lithium-ion technology
1	Working day	66.829	43.720
2	Working day	66.848	43.720
3	Working day	66.856	43.720
4	Working day	66.865	43.720
5	Working day	66.873	43.720
6	Saturday	49.035	41.363
7	Sunday	61.859	43.056
8	Working day	66.895	43.721
9	Working day	66.903	43.721
10	Working day	66.912	43.721
11	Working day	66.920	43.721
12	Working day	66.929	43.721
13	Saturday	49.071	41.363
14	Sunday	61.909	43.057
15	Working day	66.951	43.721
16	Working day	66.959	43.721
17	Working day	66.968	43.721
18	Working day	66.976	43.721
19	Working day	66.985	43.721
20	Saturday	49.108	41.363
21	Sunday	61.959	43.057
22	Working day	67.007	43.721
23	Working day	67.015	43.721
24	Working day	67.024	43.722
25	Working day	67.032	43.722

Simulated Month		Cost of the BESSs (\$)	
Order	Typical day	Lead-acid technology	Lithium-ion technology
26	Working day	67.041	43.722
27	Saturday	49.144	41.364
28	Sunday	62.010	43.057
29	Working day	67.063	43.722
30	Working day	67.071	43.722
Total		1917.015	1299.543



VITA

Nguyen Thi Anh was born in Hanoi, Vietnam on October, 27th, 1983. She received the Eng. and M.Sc. degrees in electric power systems at Hanoi University of Science and Technology (HUST), Vietnam in 2006 and 2010, respectively. She is currently pursuing the Ph.D. degree in electrical engineering at Chulalongkorn University, Thailand.

Her research interests include protection in power system, integration of distributed energy resources to the power system.

